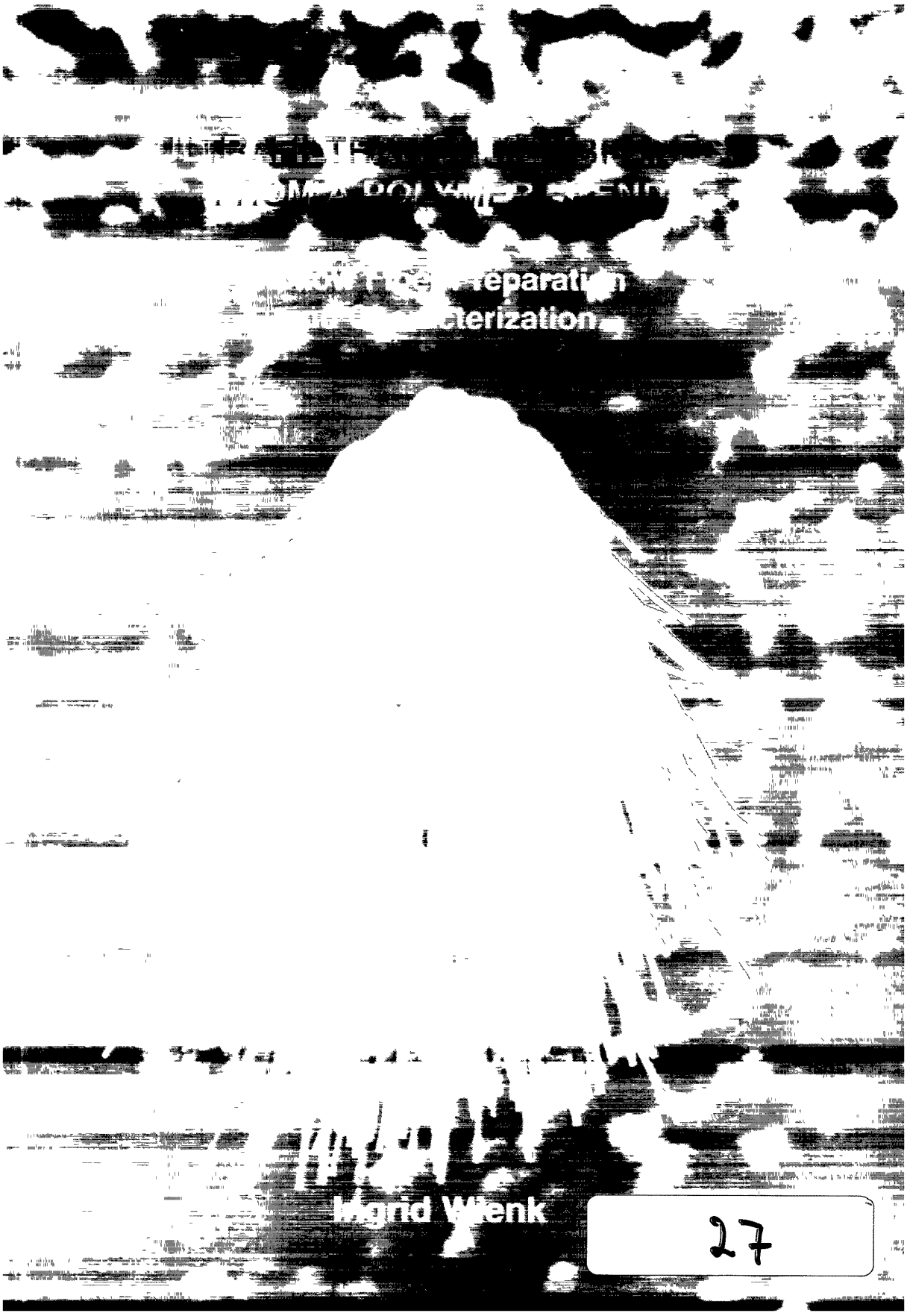

27

# ULTRAFILTRATION MEMBRANES FROM A POLYMER BLEND

## Hollow Fiber Preparation and Characterization

**Proefschrift**

ter verkrijging van
de graad van doctor aan de Universiteit Twente,
op gezag van de rector magnificus,
prof. dr. Th.J.A. Popma,
volgens besluit van het College van Dekanen
in het openbaar te verdedigen
op vrijdag 14 mei 1993 te 15.00 uur

door

**Ingrid Maria Wienk**
geboren 1 maart 1965
te *Oldenzaal*

Dit proefschrift is goedgekeurd door de promotor prof. dr. C.A. Smolders, de co-promotor prof. dr. ing. H. Strathmann en de assistent promotor dr. ir. Th. van den Boomgaard.

**Acknowledgement**

This thesis is the result of a project financially supported by the Dutch Ministry of Economic Affairs, in the framework of the Dutch research program on membranes (IOP-m) and X-flow BV.

## Voorwoord

Membraantechnologen zijn experts op het gebied van specifieke scheidingsprocessen. Ook de membraanvorming is veelal gebaseerd op ontmeng verschijnselen. Echter voor het vergaren van nieuwe kennis over membranen is het noodzakelijk een aantal mensen samen te brengen. Dit proefschrift getuigt dan ook van mijn samenwerking met Herman Teunis, Betty Folkers, Zandrie Borneman, Erik Meuleman en Frank Olde Scholtenhuis. Kees Smolders en Thonie van den Boomgaard waren belangrijke drijvende krachten voor mijn onderzoek. Maar er zijn meer mensen bij mijn werk betrokken geweest. Want, zoals het gebruik van twee polymeren een beter membraan oplevert, zo ontstaan de beste theorieën door uitwisseling van ideeën van verschillende mensen. Dit heb ik gemerkt tijdens de talrijke discussies met mijn kamergenoot Remko Boom. Ook de wetenschappelijke gedachten wisselingen met Erik Roesink, Dick Koenhen, Marcel Mulder en Wim Briels waren altijd verhelderend. Daarnaast waren het enthousiasme en de goede sfeer in de vakgroep membraantechnologie als de milde procescondities bij membraanfiltratie: een aangename omgeving resulteert in optimale opbrengst.

Niet-membraantechnologen stellen altijd de praktische vraag: wat kun je nu met zo'n membraan? De bijdrage van mijn ouders en vrienden aan dit proefschrift bestaat daaruit dat zij juist niet naar de technische details hebben gevraagd.

En dan is er natuurlijk Petrus, de membraantechnoloog wiens belangstelling voor het onderzoek werd overschaduwd door zijn belangstelling voor de onderzoekster.

Iedereen BEDANKT

Ingrid

CIP DATA KONINKLIJKE BIBLIOTHEEK, DEN HAAG

Wienk, Ingrid Maria

Ultrafiltration membranes from a polymer blend: hollow fiber preparation and characterization / Ingrid Maria Wienk. - [S.l. : s.n.]. - Ill.
Thesis Enschede. - With ref.
ISBN 90-9006058-8
Subject headings: ultrafiltration membranes.


Cover: Frans Wienk
Printed by Copy Print 2000, Enschede

*Elke vrouw die de gelijke wil zijn van de man heeft gebrek aan ambitie.*
(Veronica Hamel, filmactrice)

CONTENTS

*Chapter 3 has been published in J. Mem. Sci., 78 (1993) 93*
*The appendix has been published in J. Mem. Sci., 73 (1992) 277*

# 1

# An Introduction to Ultrafiltration Membranes

I.M. Wienk, Th. van den Boomgaard, C.A. Smolders

## 1.1 Membrane separation

A general definition of a membrane was given by Lakshminarayanaiah[1] in 1984. He refers to a membrane as "a phase that acts as a barrier to prevent mass movement but allows restricted and/or regulated passage of one or more species through it". The term 'ultrafiltration' is generally credited to Bechold[2] (1907) who was one of the first to develop methods for controlling the pore size of nitrocellulose membranes. Bechold et al.[3] were also able to measure the pore diameters by a controlled displacement of a liquid in the pores.

Ultrafiltration membranes are porous filters with pore sizes in the region of a few to a few hundred nanometers. This makes ultrafiltration membranes suitable for the separation of large molecules and colloids from low molecular weight species. In figure 1 the separation region of ultrafiltration is shown together with some other pressure driven membrane processes microfiltration, nanofiltration and reverse osmosis.

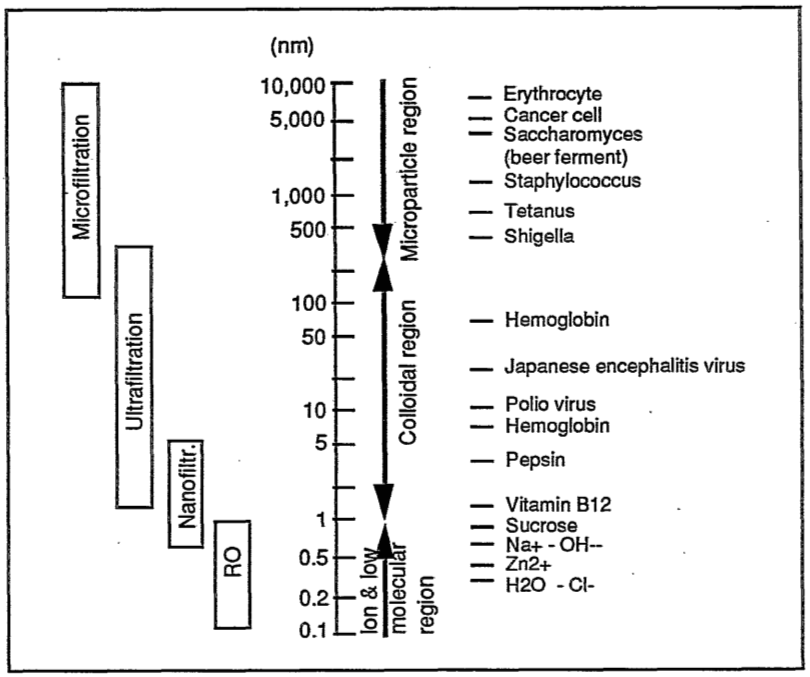


*Figure 1. Separation regions of four membrane processes: microfiltration, ultrafiltration, nanofiltration and reverse osmosis (RO). After Kesting*[4].

Until 1960 the use of ultrafiltration membranes was restricted to lab-scale applications in molecular biology. A review of these applications has already been given by Ferry[5]. Two stepwise developments with the character of breakthroughs were necessary before ultrafiltration could become a competitive technique for large scale applications. The first improvement concerned the permeability of the membranes. In 1962 Loeb and Sourirajan[6] were able to prepare membranes with an asymmetric pore structure consisting of a thin, selective toplayer and a porous sublayer. Because the resistance against transport of these membranes is mainly determined by the toplayer, which in fact is very thin in asymmetric membranes, a significant increase of the permeability could be realised. Secondly, the development of modules and filtration systems was indispensable to scale-up the filtration processes. This latter development took place in a federal research and development program in the USA during the sixties (OSW-program).

The selectivity of ultrafiltration membranes is based on the difference in size of the components to be separated. The driving force for the transport of the components that are small enough to pass the membrane is a hydrodynamic pressure difference between the feed side and the permeate side of the

membrane. In table 1 an overview on separation processes is given classified according to the physical or chemical property that underlies the separation mechanism.

*Table 1. Separation processes based on physical or chemical properties of the components to be separated*[7].

| property | separation process |
|---|---|
| size | filtration, microfiltration, ultrafiltration, dialysis, gas separation, gel permeation, chromatography |
| vapor pressure | distillation, membrane distillation |
| freezing point | crystallization |
| affinity | extraction, adsorption, absorption, reverse osmosis, gas separation, pervaporation, affinity chromatography |
| charge | ion exchange, electrodialysis, electrophoresis |
| density | centrifugation |
| chemical nature | complexation, liquid membranes |

A comparison of the techniques is difficult and the most suitable one in a specific case is of course strongly dependent on the separation to be performed. A few benefits of the use of membranes in general and of ultrafiltration membranes in particular can be mentioned:

- separation takes place without phase change which implies that the energy consumption is low
- separation can be carried out under mild process conditions which makes it a suitable technique in biotechnology and food industry
- no additives are required
- membrane processes can easily be combined with other separation processes
- membrane properties are variable and can be adjusted.

There is also a number of drawbacks:

- the selectivity is generally low
- there is a restricted upper solute concentration limit
- concentration polarization and membrane fouling cause serious problems
- low membrane lifetime still is reason for concern.

For a number of applications the economical benefits of ultrafiltration processes were clearly illustrated by Bemberis and Neely[8].

## 1.2 Applications of ultrafiltration membranes

Since the introduction of ultrafiltration membranes on an industrial scale in the seventies the number of applications as well as the size of installations have grown enormously. An estimation of the world wide sales of total membrane industry was published by Strathmann[9] in 1990. For ultrafiltration the sales per year for water treatment is 60 million US $, for food industry 44 million US $, in medical devices 130 million US $ and 15 million US $ in the chemical industry.

In the last decades many articles on the application of ultrafiltration in various systems appeared in literature. A number of applications is collected by Cheryan in his Ultrafiltration Handbook[10]. Without having the intention to give a complete overview here, a number of industrial applications of ultrafiltration membranes is summarized in table 2.

*Table 2. Applications of ultrafiltration membranes*

| |
|---|
| Environmental problems[11]: |
| Recovery of electrophoretic paints from rinsing water |
| Treatment of emulsified oily wastes |
| Concentration of latex emulsions prior to drying |
| Recovery of sizing agents in the textile industry |
| Treatment of various aqueous effluents in the printing and metallurgical industry[12] |
| Dairy and food industry: |
| Recovery of proteins from cheese whey[13] |
| Concentration of milk proteins for cheese production[14] |
| Fractionation of animal blood |
| Concentration of soy protein isolates |
| Gelatine manufacture |
| Downstream separations in biotechnology |
| Pharmaceutical industry |

The growth rate of the membrane industry is 12-15% per year. This is mainly caused by the expansion in the field of biotechnology and an increase in the governmental concern for the environment resulting in strict regulations for industrial waste streams.

The overview of applications might give the impression that ultrafiltration technology is a state-of-the-art technique, however this is not the case. New sophisticated separation processes ask for tailor-made membranes concerning

pore structure and membrane material. For instance for non-aqueous applications, new chemically resistant membranes must be developed from more resistant polymers or inorganic materials. Another problem is fouling of the membranes, especially for the separation of biological systems. Adsorption of biologic material at the membrane material causes severe decrease of permeability (as an example see figure 2) and requires regular and thorough cleaning of the membranes. For these applications the development of membrane materials more resistant to fouling is very important.

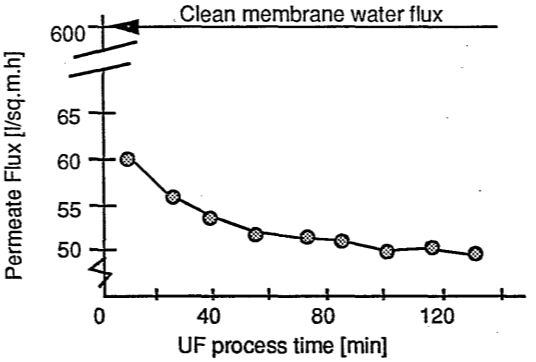


*Figure 2. An example of the time dependent flux decline during whole milk ultrafiltration compared to the water flux of the clean membrane*[15].

## 1.3 Preparation of porous polymeric membranes

The porous structure of ultrafiltration membranes can be symmetric or asymmetric. A symmetric pore structure means a constant pore size (or pore size distribution) over the whole cross section of the membrane film. The cross section of asymmetric membranes shows a pore size gradient with small pores at the top and larger pores in the sublayer. The pore size gradient can be gradual, but there also can be a relatively dense toplayer with a thickness of 0.1 - 0.5 μm supported by a more porous sublayer. A special group of asymmetric membranes are the composite membranes, in these membranes the toplayer and sublayer originate from different materials. Four preparation methods for porous polymeric membranes are introduced here. For further reading and more preparation techniques one is referred to Mulder[7].

### *1.3.1 Stretching*

In this technique, homogeneous films are extruded from partially crystalline polymers (e.g. polypropylene, polyethylene). Stretching of these films

perpendicular to the direction of extrusion will separate the crystalline parts resulting in a porous structure. The porosities of these membranes can be as high as 90 %.

### *1.3.2 Track-etching*

Cylindrically shaped pores with a narrow pore size distribution can be obtained by track-etching. A thin polymeric (e.g. polycarbonate) film is subjected to a high energy particle radiation (metal ions) perpendicular to the film. This treatment creates tracks of a damaged polymer matrix. When the film is afterwards immersed in an acid or alkaline bath the polymeric material is etched away at the weak spots and cylindrical pores are formed. The pore size of these membranes is determined by the etching time while the porosity depends on the radiation time. Usually the porosity is very low.

### *1.3.3 Sintering*

Sintering is used for the preparation of ceramic membranes. With this technique a symmetric pore structure is obtained. For polymers sintering of particles at elevated temperatures is a suitable preparation technique for chemically and thermally resistant membranes because it is not necessary to dissolve the polymer. Membranes of polytetrafluoroethylene are prepared in this way. Ultrafiltration membranes can not be obtained with this technique since generally the pore sizes obtained in this way are larger than 0.1 μm.

### *1.3.4 Phase inversion*

Most commercially available membranes are obtained by phase inversion. It is a very versatile technique allowing the preparation of very different kinds of membrane morphologies. The morphology depends on the change of the thermodynamic parameters of the system and the kinetics of the process. The polymer is dissolved in a solvent and the solution is extruded in the desired configuration. Next, the polymer is precipitated by phase transition either by a change in temperature or by a change in composition of the solution.

*Thermally induced precipitation*[16]

For thermally induced phase separation the polymer solution is prepared at an elevated temperature and then cooled down. If evaporation of the solvent occurs an increase of the polymer concentration in the toplayer will occur and an asymmetric membrane structure will be obtained.

*Diffusion induced precipitation*

In this method the polymer precipitates because the composition of the polymer solution changes in such a way that the polymer becomes insoluble. This can be realised in three ways:

- *precipitation by solvent evaporation*[17]. This method normally results in dense homogeneous membranes. Porous membranes can be obtained with this technique if the polymer is dissolved in a mixture of a volatile solvent and a non-volatile liquid that is a non-solvent for the polymer.
- *precipitation from the vapor phase*[18]. A polymer solution is contacted with vapor of a non-solvent. The vapor diffuses into the polymer solution resulting in precipitation of the polymer and the formation of a symmetric porous membrane.
- *immersion precipitation of a polymer solution in a bath of non-solvent*[19]. In this case the polymer precipitates as a result of two processes: the diffusion of solvent into the coagulation bath and the diffusion of non-solvent into the polymer solution.

## 1.4 Membrane materials

### *1.4.1 Chemical and thermal stability*

The choice of the material is a very important factor determining the applicability of the membrane. Sometimes the separation process demands a material with high chemical and/or thermal resistance. But even if the conditions during the separation process are mild, the resistance of the material has to be high to be able to sufficiently clean the membranes. Cleaning often occurs at elevated temperatures or with strong acidic or alkaline solutions. A few examples of chemically and thermally stable polymers used for ultrafiltration membranes are polyimide, polyetherimide, polysulfone, poly(ether sulfone), polyacrylonitrile and polyamide[7].

An alternative for stable polymers is the use of inorganic materials which are generally chemically very stable and which can be applied to extremely high temperatures. The use of inorganic membranes however is beyond the scope of this introduction. An overview of inorganic membranes is given by Bhave[20].

### *1.4.2 Hydrophilicity*

The main drawback of ultrafiltration membranes is their susceptibility to fouling. Adsorption of components from the solution at the membrane surface leads to a sharp decrease of the permeability. In bioseparations the most adsorbing species are proteins. Since the adsorption of proteins is less extensive and less strong at hydrophilic surfaces[21] a lot of research is aimed to increase the hydrophilic character of the membranes. There are several approaches to render the membranes more hydrophilic and they are briefly described in this paragraph.

*Hydrophilic polymers and copolymers*
The easiest way to obtain hydrophilic membranes is to use a hydrophilic polymer (e.g. cellulose or polyamides). Unfortunately, the thermal and chemical resistance of these polymers is very poor. An alternative way is to chemically introduce hydrophilic groups to the polymer before membrane preparation. Examples are the sulfonation of polysulfone or polyether-etherketone. With this technique $SO_3H$-groups are substituted at the aromatic ring of the polymer. A combination of hydrophilicity and stability can be obtained by the use of copolymers such as ethylene-vinylalcohol and ethylene-vinylacetate.

*Polymer blends*
Instead of using a copolymer a polymer blend can be used to combine the properties of two polymers. The choice of polymers is limited though since only few polymers are miscible with each other[22]. A hydrophilic polymer that is often used as an additive in membrane preparation is poly(vinyl pyrrolidone) (PVP). It forms homogeneous blends with a number of polymers such as polysulfone, poly(ether sulfone)[23], polyimide and polyetherimide[24]. Other examples are blends from cellulose with other polymers such as polyacrylonitrile, polyvinylbutyrate and vinyl acetate-vinylchloride copolymer[25]. The two polymers can be dissolved together in a common solvent and membranes can be made by the phase inversion process.

*Surface modification techniques*
Change of the intrinsic hydrophobic nature of a polymer into a more hydrophilic one can also be realised *after* membrane formation. The surface of the membrane can be modified by chemical modification, grafting, plasma treatment, in-situ polymerization or adsorption coating. As a side effect of these treatments modification of the membrane structure may occur. Three modification techniques are briefly presented here:

- *chemical reaction*. With this technique hydrophilic groups such as carbonyl-, amino-, hydroxyl-groups or ionic groups such as carboxylic, sulfonic and quaternary ammonium groups can be introduced at the surface[26].
- *plasma treatment*. Generally a plasma is created by an electrical glow discharge of a gas. The plasma consists of electrons, ions, photons and neutral atoms or molecules. It is very reactive and different types of reactions can occur with a given chemical surface: deposition of a polymer layer, crosslinking, etching, degradation and introduction of specific groups (functionalization). Introduction of specific groups can be achieved by using $NH_3$, $N_2$ or CO as discharge gas. This technique is often applied to

dense membranes (pervaporation and gas separation) but also on micro- and ultrafiltration membranes[27].

- *adsorption coating*. The membrane surface can easily be coated by physical adsorption of surfactants or polymers[28]. Both ionic and nonionic surfactants as well as polymers such as methylcellulose, polyvinylalcohol and poly(vinyl pyrrolidone) have been applied. The solutes adsorb at the surface but also in the pore walls thereby increasing the hydrophilicity but decreasing the permeability of the membrane. A disadvantage of this technique is that the solutes will desorb during the filtration process unless they are chemically fixed.

## 1.5 Membrane configurations

Membranes can be made in two different configurations: flat or tubular. There are three categories of tubular membranes based on the difference in dimensions:

- hollow fiber membranes (diameter <1 mm)
- capillary membranes (diameter 1-5 mm)
- tubular membranes (diameter >5 mm)

Membranes made by the phase inversion technique are prepared by bringing the polymer solution in the desired configuration followed by precipitation of the polymer. For flat sheet membranes the polymer solution is cast on a glass plate (laboratory scale) or on a non-woven support (industrial scale). For tubular membranes a polymer solution is cast at the inner surface of a supporting tubular material. The capillary membranes and the hollow fibers are self supporting and are made by extrusion of a polymer solution through a spinneret.

For industrial applications the membranes are packed in units called modules. Flat membranes can be placed in a module either by stacking the sheets (plate and frame module) or winding a membrane sheet around a central collection pipe (spiral wound). For these modules the membranes are separated by spacers causing a low surface-to-volume ratio. Different modules and their capital and operating costs are listed in table 3.

*Table 3. A comparison of principal module designs* [29]

| Module type | Membrane surface Module volume [$m^2m^{-3}$] | Capital cost | Operating cost | Flow control | Ease of in-place cleaning |
|---|---|---|---|---|---|
| Tubular | 25-300 | High | High | Good | Good |
| Plate and frame | 400-600 | High | Low | Fair | Poor |
| Spiral wound | 800-1000 | Very low | Low | Poor | Poor |
| Capillary | 600-1200 | Low | Low | Good | Fair |
| Hollow fiber | 2000-30000 | Low | Low | Good | Fair |

For hollow fibers the packing density of the module depends on the dimension of the fibers and can be very high. Another advantage of hollow fibers is their self-supporting capability. Hollow fibers of microfiltration membranes can be in-place-cleaned by back-flushing[24]. For this cleaning technique the pressure difference over the membrane is reversed for a short time. When the permeate flows back through the membrane it lifts the deposited layer from the membrane surface. Part of the permeate is lost because it is flushed back but the increase of the flow due to the removal of the deposit more than compensates for this loss.

## 1.6 Characterization of porous membranes

Two different types of characterization methods for porous membranes can be distinguished[30,31]:

- characterizing *structure-related* parameters. This includes the determination of the pore size distribution, the thickness of the toplayer and the surface porosity.
- characterizing *permeation-related* parameters. This includes the determination of the separation parameters by using model solutes, the flux of pure water and the flux reduction after e.g. protein adsorption.

The characterization of structure related parameters can serve as a feed-back in membrane preparation studies. It is often difficult to relate the structure parameters to the permeation parameters of the membrane. The reason for this is that the determination of structure related parameters is based on pore models that are large simplifications of the actual morphology. Nevertheless, a combination of techniques can be used as a first estimate in determining the possible fields of application for the membrane. A number of characterization techniques is listed in table 4[31].

*Table 4. Overview of characterization techniques for porous membranes*[31]

| Method | Characteristic | Remarks |
|---|---|---|
| electron microscopy<br>scanning-<br>transmission-<br>field emission- | pore size distribution of<br>cross section<br>toplayer thickness<br>surface porosity | dry sample |
| solvent flux<br>measurements | hydraulic pore radius<br>pure solvent permeability | wetted sample |
| solute rejections<br>measurements | membrane rejection<br>'cut-off values' | wetted sample |
| gas-liquid displacement<br>technique | pore size distribution<br>of active pores | sample changes from<br>wet to dry |
| liquid-liquid<br>displacement technique | pore size distribution<br>of active pores | wetted sample |
| mercury porosimetry | pore size distribution | dry sample |
| thermoporometry | pore size distribution<br>pore shape | wetted sample |
| permporometry | pore size distribution<br>of active pores | sample changes from<br>dry to wet to dry |
| gas adsorption-<br>desorption<br>measurements | pore size distribution<br>specific surface area<br>(BET area) | dry sample |

## 1.7 Structure of the thesis

The aim of the research described in this thesis is the development of hollow fiber ultrafiltration membranes with a high flux and low fouling tendency. The effort for the preparation of the hollow fibers is based on knowledge of the membrane formation mechanism and characterization of the membrane structure and properties.

It is anticipated that hydrophilic, low fouling membranes can be prepared from a blend of polymers. Poly(ether sulfone) (PES), the membrane forming

polymer, is chosen because of its good chemical and thermal stability[32]. Poly(vinyl pyrrolidone) (PVP)[33] is a water-soluble polymer which forms homogeneous blends with PES. A common solvent for the two polymers is N-methylpyrrolidone (NMP). NMP is also very well miscible with the precipitation liquid, water which on the other hand is a non-solvent for PES. The chemical structures of the materials are shown in figure 3.

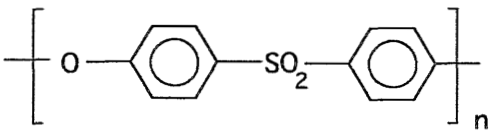


poly(ether sulfone) (PES)

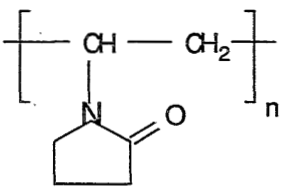


poly(vinyl pyrrolidone) (PVP)

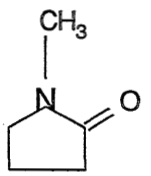


N-methylpyrrolidone (NMP)

*Figure 3. Structure formulae of the materials used in this thesis.*

The membranes are prepared according to the diffusion induced phase inversion mechanism. The same quaternary system PES/PVP/NMP/water has been investigated by Boom et al.[23]. They thoroughly studied the role of PVP as a macromolecular additive on membrane formation by immersion precipitation. The experimental work described in this thesis is partly based on the theory of these authors. The work of Roesink[24] is also related to the research described here. He developed a hollow fiber *micro*-filtration membrane from a blend of poly-etherimide (PEI) and PVP.

In *chapter* 2 the dry-wet spinning of hollow fiber ultrafiltration membranes is discussed. Relations between a number of spinning conditions and the morphologies of the membranes are shown. An adapted version of the spinning set-up is used with a fixed airgap length and variable humidity conditions to be able to discriminate between the phase inversion parameters and the mechanical forces exerted on the fibers during spinning.

In *chapter* 3 a new spinning technique is applied for the preparation of ultrafiltration membranes. A new type of spinneret having three concentric

orifices is used to spin hollow fibers according to the dual bath method. It is shown that the presence of PVP is an important condition in order to obtain porous membranes with this technique.

In *chapter 4* the post-treatment of the membrane fibers is presented. The presence of the hydrophilic PVP in the membrane causes swelling of the membrane structure in water resulting in a low permeability. To increase the water flux of the membranes a post-treatment as used by Roesink[22] is applied. Also the effects of washing and drying the membranes on the performance is determined. A new method to obtain hydrophilic ultrafiltration membranes is introduced.

In *chapter 5* the characterization of hollow fiber ultrafiltration membranes is discussed. The characterization of the membranes involves the hydrophilic nature of the membranes, the morphological structure, the pore size distribution and the performance. The membrane structure is studied by means of several microscopic techniques. The pore size distribution is found using the liquid displacement method. Performance of the membranes is determined by measuring the water flux through the membranes and the retention for a protein solution. Flux reduction during filtration of a protein solution as well as the adsorption behavior of the membranes is studied.

In *chapter 6* a new mechanism is proposed for the formation of the toplayer of ultrafiltration membranes. There is substantial evidence that the toplayer of polymeric ultrafiltration membranes consists of polymer spheres. The formation of this nodular structure can not be explained by conventional membrane formation mechanisms.

In the *appendix to this thesis* a study on the effect of the concentration and the molecular weight of PVP on the structure of the membranes is presented. The study is focused on the appearance of large holes (macrovoids) in the membrane and the structure of the toplayer.

## 1.8 Literature

1. N. Lakshminarayanaiah, Equations of membrane biophysics., Academic Press, New York, 1984
2. H. Bechold, Kolloidstudien mit der Filtrationsmethode, Z. Phys. Chem. Sto. Verw., 60 (1907) 257
3. H. Bechold, M. Schlesinger, K. Silbereisen, Porenweite von Ultrafiltern, Koll. Z., 55 (1931) 172

4. R.E. Kesting, Synthetic polymeric membranes, McGraw Hill, New York, 1985
5. J.D. Ferry, Ultrafilter membranes and ultrafiltration, Chem. Rev., **18** (1936) 373
6. S. Loeb, S. Sourirajan, Seawater demineralization by means of an osmotic membrane, Adv. Chem. Ser., **38** (1963) 117
7. M. Mulder, Basic principles of membrane technology, Kluwer Academic Publishers, Dordrecht 1991
8. I. Bemberis, K. Neely, Ultrafiltration as a competitive unit process, AIChE Symp. Ser., **82** (250) (1986) 65
9. H. Strathmann, Economic assessment of membrane processes, In: Separation and purification technology, N.N. Li, J.M. Calo (ed.), Marcel Dekker Inc., New York, 1992
10. M. Cheryan, Ultrafiltration handbook, Technomic, Lancaster, 1986
11. *a)* M.C. Porter, Handbook of industrial membrane technology, Noyes Publ., Park Ridge, 1990
    *b)* R.G. Gutman, Membrane filtration, Adam Hilger, Bristol, 1987
12. K. Marquardt, Abwasseraufbereitung in der metallverarbeitenden Industrie, Metalloberfläche, **43** (1989) 4
13. R. de Boer, J. Hiddink, Membrane processes in the dairy industry, Desalination, **35** (1980) 169
14. *a)* Koch Int., Production of edible quarg and other types of fresh cheese by means of ultrafiltration, North Eur. Dairy J., **3** (1987) 75
    *b)* J.C. Watters, R. Rezvani, Reduction of the lactose content of skim milk by continuous countercurrent cascade ultrafiltration, Sep. Sci. Techn., **24** (5&6) (1989) 369
15. P.S. Tong, D.M. Barbano, M.A. Rudan, Characterization of porteinaceous membrane foulants and flux decline during the early stages of whole milk ultrafiltration, J. Dairy Sci., **71** (1988) 604
16. D.R. Lloyd, J.W. Barlow, Microporous membrane formation via thermally induced phase separation, AIChE. Symp. Ser., **84** (261) (1988) 28
17. R.E. Kesting, Concerning the microstructure of dry-RO membranes, J. Appl. Pol. Sci., **17** (1973) 1771
18. *a)* R. Zsigmondy, W. Bachman, Uber neu filter, Z. Anorg. Allgem. Chem., **103** (1918) 119
    *b)* H. Strathmann, K. Koch, P. Amar, R.W. Baker, The formation mechanism of asymmetric membranes, Desalination, **16** (1975) 179
19. *a)* S. Manjikian, S. Loeb, J.W. Mc. Cutchan, Proc. First. Symp. Water Des., (1965) 165
    *b)* M.A. Frommer, D. Lancet, The mechanism of membrane formation: membrane structures and their relation to preparation conditions, In: Reverse osmosis membrane research, H.K. Lonsdale, H.E. Podall (ed.), Plenum Press, New York, 1972, p. 85
    *c)* D.M. Koenhen, M.H.V. Mulder, C.A. Smolders, Phase separation phenomena during the formation of asymmetric membranes, J. Appl. Pol. Sci., **21** (1977) 199
    *d)* M. Guillotin, C. Lemoyne, C. Noel, L. Monnerie, Physicochemical processes occurring during the formation of cellulose diacetate membranes, Desalination, **21** (1977) 165
    *e)* J. G. Wijmans, J.P.B. Baaij, C.A. Smolders, The mechanism of microporous or skinned membranes produced by immersion precipitation, J. Mem. Sci., **14** (1983) 263
    *f)* A.J. Reuvers, J.W.A. van de Berg, C.A. Smolders, Formation of membranes by means of

immersion precipitation. I. A model to describe mass transfer during immersion precipitation, J. Mem. Sci., 34 (1987) 45
*g)* A.J. Reuvers, C.A. Smolders, Formation of membranes by means of immersion precipitation. II. The mechanism of formation of membranes prepared from the system cellulose acetate-acetone-water, J. Mem. Sci., 34 (1987) 67

20. R.R. Bhave, Inorganic membranes: Synthesis, characteristics and applications, Van Nostrand Reinhold, New York, 1991
21. W. Norde, Adsorption of proteins from solutions at the solid-liquid interface, Adv. Coll. Int. Sci., 25 (1986) 267
22. D.R. Paul, S. Newman, Polymer blends, Academic Press, New York, 1978
23. *a)* R.M. Boom, Th. van den Boomgaard, C.A. Smolders, Equilibrium thermodynamics of a quaternary membrane forming system with two polymers. I. Theory, submitted for publication to Macromolecules
*b)* R.M. Boom, H.W. Reinders, H.H.W. Rolevink, U. Cordilia, Th. van den Boomgaard, C.A. Smolders, Equilibrium thermodynamics of a quaternary membrane forming system with two polymers. II. Experimental, submitted for publication to Macromolecules
*c)* R.M. Boom, Th. van den Boomgaard, C.A. Smolders, Mass transfer and thermodynamics during immersion precipitation for a two polymer system: Evaluation with the system PES-PVP-NMP-water, submitted for publication to J. Mem. Sci.
*d)* R.M. Boom, S. Zanic, Th. van den Boomgaard, C.A. Smolders, Membranes from PES and PVP: Membrane morphology and its relation to the formation mechanism, submitted for publication to J. Mem. Sci.
*e)* R.M. Boom, H.H.W. Rolevink, Th. van den Boomgaard, C.A. Smolders, Membranes prepared from PES and PS: Comparison with the PES-PVP system, submitted for publication to J. Mem. Sci.
*f)* R.M. Boom, Th. van den Boomgaard, C.A. Smolders, Metastable demixing phenomena by thermal quench experiments. I. Theory, submitted for publication to J. Appl. Pol. Sci.
*g)* R.M. Boom, S. Rekveld, U. Cordilia, Th. van den Boomgaard, C.A. Smolders, Metastable demixing phenomena by thermal quench experiments. II. The systems PES-NMP-water and PES-NMP-PVP-water, submitted for publication to J. Appl. Polym. Sci.
24. H.D.W. Roesink, Microfiltration: membrane development and module design, PhD Thesis, University of Twente, Enschede, 1989
25. D.D. Grinshpan, T.A. Savitskaya, S.E. Makarevich, F.N. Koputskii, Kinetic stability and viscosity of cellulose-synthetic polymer blends in a common solvent, Acta Polym. 37 (1986) 670
26. F.F. Stengaard, Characterization and performance of new types of ultrafiltration membranes with chemically modified surfaces, Desalination, 70 (1988) 207
27. *a)* J. Wolff, H. Steinhauser, G. Ellinghorst, Tailoring of ultrafiltration membranes by plasma treatment and their application for the desalination and concentration of water soluble organic substances, J. Mem. Sci., 36 (1988) 207
*b)* M. Krakelle, R.J. Zdrahala, Membranes for biomedical applications: utilization of plasma polymerization for dimensionally stable hydrophilic membranes, J. Mem. Sci., 41

(1989) 305

28. *a)* A.G. Fane, C.J.D. Fell, K.J. Kim, The effect of surfactant pretreatment on the ultrafiltration of proteins, Desalination, **53** (1985) 37
*b)* K.J. Kim, A.G. Fane, C.J.D. Fell, The effect of Langmuir-Blodgett layer pretreatment on the performance of ultrafiltration membranes, J. Mem. Sci., **43** (1989) 187
*c)* L.E.S. Brink, D.J. Romijn, Reducing the protein fouling of polysulfone surfaces and polysulfone ultrafiltration membranes: optimization of the type of presorbed layer, Desalination, **78** (1990) 209
*d)* V. Chen, A.G. Fane, C.J.D. Fell, The use of anionic surfactants for reducing fouling of ultrafiltration membranes: their effects and optimization, J. Mem. Sci., **67** (1992) 249
29. E.M. Stitt, Membrane separation, In: Solid-liquid separations, 3rd edition, L. Svarovsky (ed.), London 1990, p. 629
30. G. Trägardh, Characterization of ultrafiltration membranes: proceedings from an international workshop, Örenäs slott, Sweden, 1987
31. F.P. Cuperus, C.A. Smolders, Characterization of UF membranes: membrane characteristics and characterization techniques, Adv. Coll. Int. Sci., **34** (1991) 135
32. J.B. Rose, Discovery and development of the "Victrex" polyarylethersulphones, In: High performance polymers: their origin and development, R.B. Seymour, G.S. Kirshenbaum (ed.) Elsevier, New York, 1986, p.169
33. P. Molyneux, Water soluble synthetic polymers: properties and behavior, Vol I, CRC Press Inc., Boca Rabon, Florida 1982 p.146

2

# Spinning of Hollow Fiber Ultrafiltration Membranes from a Polymer Blend

I.M. Wienk, F.H.A. Olde Scholtenhuis, Th. van den Boomgaard, C.A. Smolders

## Summary

In this study the dry-wet spinning technique is used for the preparation of hollow fiber membranes. In the polymer solution a blend of two polymers, poly(ether sulfone) and poly(vinyl pyrrolidone), is used. The morphological structure of the membranes obtained is related to rheological characteristics and phase behavior of the polymer solution during spinning. At the bore side pore structure is determined by the solvent/non-solvent ratio of the internal bore liquid. For the outer surface pore structure is mainly dependent on the conditions in the airgap. The typical performance of the membranes lies in the ultrafiltration region.

## 2.1 Introduction

The spinning of hollow fibers is very often applied as a preparation technique for ultrafiltration membranes. Even so the number of fundamental contributions to this subject is limited[1-6]. Much knowledge about the spinning of porous hollow fiber membranes has been described in patents. In the spinning process both phase separation and rheological phenomena will have an influence on the shape and morphology of the membrane fibers.

In this study membranes are made from a blend of two polymers. Poly(ether sulfone) (PES) is used as membrane forming polymer. The thermal stability is very high (190°C for continuous use) which makes the membranes resistant to steam sterilization. PES is also stable with respect to thermal oxidation[7], and resistant against the attack of mineral acids, alkali and salt solutions. Moreover the resistance of PES to detergents and hydrocarbons is good[8].

The hydrophilic polymer poly(vinyl pyrrolidone) (PVP) is used as an additive in the polymer solution. The introduction of this polymer will give the membranes a hydrophilic character. It is known[9] that hydrophilic materials are less susceptible to adsorption of proteins, which for membranes is a very attractive behavior. Roesink et al.[10] used PVP together with poly-etherimide (PEI) in preparing microfiltration membranes. They measured a reduced bovine serum albumin (BSA) adsorption for membranes containing PVP. PVP is a well known additive in membrane forming systems[1-5,11-14]. The effects of this additive are an increase in viscosity of the polymer solution, a suppression of macrovoid formation and an increase in permeability of the membranes. For this last reason PVP is often called a pore former. The general idea is that PVP leaches out in the washing procedure thereby leaving holes in the membrane matrix. Only a few people gave a description of the effects of PVP in relation to the membrane formation process. In our laboratory Roesink[5] studied the effect of PVP in combination with PEI to spin hollow fiber microfiltration membranes. Boom et al.[15-19] thoroughly investigated the quaternary system PES/PVP/NMP/water. Their ideas are discussed in the theoretical section. The role of PVP on the suppression of macrovoid formation is described in the appendix to this thesis[20].

The membranes described here are made using the dry-wet spinning technique. This means that after extrusion the polymer solution passes through an airgap before it enters into a coagulation bath. Together with the polymer solution a liquid containing a certain amount of non-solvent is pumped through the bore of the spinning fiber. A number of spinning parameters have been varied. Special attention is paid to the conditions in the airgap. Here the amount of water vapor diffusing into the polymer solution can be varied either by changing the humidity of the airgap or by varying the residence time of the nascent membrane in the airgap. The morphological structures of the membranes have been studied using electron microscopy. Furthermore the water flux and the retention for BSA have been measured. The influence of the spinning parameters on the morphology and the performance of the membranes is discussed in the light of existing theories about membrane formation.

## 2.2 Theory

### *2.2.1 Phase separation in a ternary system[21].*

Before we start with the theory of membrane formation in this paragraph some aspects of phase separation are introduced. For reasons of simplicity this is done for a ternary system. Consider a system of a monodispers, non-crystalline polymer, a solvent and a non-solvent for the polymer. The

compositions of such a system can be described by a ternary phase diagram. In figure 1 a schematic representation is given. The binodal and spinodal curves and the tie-lines in the diagram are determined by equilibrium thermodynamics and they are valid for constant pressure and temperature. The binodal curve is the border of the demixing gap which can be divided into two parts: a metastable region between the binodal and the spinodal curve and an instable region within the spinodal curve. A composition (x) in the demixing gap will demix into two liquid phases, a polymer rich phase (y) and a polymer lean phase (z). In the phase diagram the compositions of the two phases lie at the points were the tie-line through composition x crosses the binodal curve. The ratio of the volumes of the two phases is proportional to the distances according to the lever rule:

$$\frac{\text{volume of polymer rich phase}}{\text{volume of polymer lean phase}} = \frac{\text{length xz}}{\text{length xy}}$$

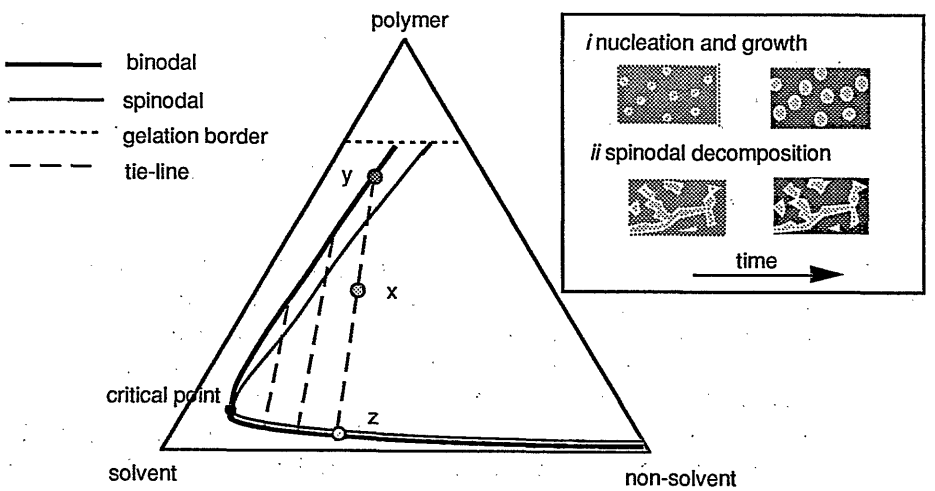


*Figure 1. Schematic drawing of a ternary phase diagram. In the square phase separation according to i) nucleation and nucleus growth and ii) spinodal decomposition are depicted.*

In the metastable region the phase separation will take place by nucleation and nucleus growth. If the polymer concentration is above the critical point (see figure 1) the polymer lean phase will nucleate and the polymer rich phase will be continuous. At low polymer concentration (below the critical point in figure 1) the polymer rich phase will nucleate and a latex is formed. In the metastable region an activation energy for nucleation has to be

overcome before nuclei are stable and are able to grow further. The activation energy is supplied by supersaturation of the system and can locally be high by fluctuations due to Brownian movement. At a large supersaturation (further away from the binodal curve) the number of stable nuclei will be high.

A composition in the spinodal region is highly unstable. Any concentration fluctuation present will grow and lead to phase separation of the system. Spinodal decomposition was investigated by Cahn[22] and applied for polymer systems by van Aartsen and co-workers[23]. Phase separation in the spinodal region can be described by a superposition of cosine functions. They are random in orientation, phase and amplitude. The wavelength is fixed at chosen conditions and it depends on the kind of system and the supersaturation. The wavelength is small at high supersaturation and for a small radius of gyration of the polymer. Unless the volume fractions of the two phases differ too much, spinodal demixing will lead to a structure in which both phases are continuous (co-continuous structures, also shown in figure 1).

In some polymer systems crystallization or aggregate formation of the polymer molecules may occur. As this is not the case in the system of study these phenomena will not be discussed here. At high polymer concentrations gelation or vitrification of the solution takes place. Once the polymer rich phase is getting a certain rigidity profound changes in morphology are not possible anymore.

The location of the binodal curve in the ternary phase diagram can be found by cloud-point measurements or by measuring the light scattering of the polymer solutions for varying compositions or it can be calculated if the thermodynamic interaction parameters of the system are known. Tompa[24] and Altena et al.[25] calculated phase diagrams for ternary polymeric systems. For the quaternary system PES, PVP, NMP and water this has been done by Boom et al.[15,16]. The theoretical considerations and theories of Boom et al. are of great importance for the experiments described in this chapter since the system of investigation is exactly the same.

### *2.2.2 Membrane formation by diffusion induced phase separation.*

Phase separation of a polymer solution can be induced by:

- quenching the solution to a lower temperature
- immersion of the solution in a bath of non-solvent
- contacting the polymer solution with a vapor of the non-solvent
- evaporation of the solvent.

For membrane formation immersion precipitation is the most important procedure and therefore it is the subject of this section. Phase separation processes by evaporation or contact with a non-solvent vapor are closely related to the immersion precipitation process because they are also diffusion induced. In paragraph 2.2.4 the processes that play a role during spinning are discussed.

Upon immersion of a film of a polymer solution in a non-solvent or coagulation bath the non-solvent will diffuse into the polymer solution whereas the solvent diffuses into the bath. The diffusion coefficient of the polymer is much lower and therefore the mobility of these polymeric molecules will reach only for smaller distances.

Fundamental studies on membrane formation by immersion precipitation in ternary systems of polymer, solvent and non-solvent have been carried out by Cohen et al.[26] Reuvers et al.[27], Tsay et al.[28] and Radovanovic et al.[29]. They developed mass transfer models to describe the diffusion processes for especially the first moments of immersion. Such a kinetic model results in a composition path in the ternary phase diagram. This path represents either the change in composition of a small volume in time or the compositions at all loci in the film at a certain moment. Combined with the equilibrium thermodynamics of the system it can be determined when and where the composition path will cross the binodal curve. So it is possible to predict at what time after immersion phase separation will start and what the composition profile of the polymer solution will be at that moment.

Based on the calculated composition paths and supported by experimental data Reuvers et al.[27] divided membrane formation processes into two groups: instantaneous demixing systems and systems that give delay of demixing. If for a given system at a very short moment after immersion the composition path crosses the binodal the process is called instantaneous demixing. For systems that have a delay time of demixing the composition path will not cross the binodal curve until that (delay) time has passed. Instantaneously demixing systems usually lead to the formation of porous structures whereas delay of demixing results in membranes with a dense toplayer. Therefore in order to obtain ultrafiltration membranes the membrane forming system should be chosen in such a way that it will give instantaneous demixing.

For many membrane forming systems phase separation will take place in the metastable region. The critical point usually is at rather low polymer concentrations. The choice for higher polymer concentrations implies that nucleation of a polymer lean phase will occur. Nucleation takes place at a

certain place in the film, which by diffusion shifts deeper into the demixing gap. Mostly it is assumed that in diffusion induced demixing processes nucleation of the polymer lean phase will take place before the composition of the polymer solution is able to reach the instable region.

The metastable demixing phenomena of a ternary system consisting of one polymer, a solvent and a non-solvent were measured by Boom et al.[19]. Light scattering measurements have been used to study polymer solutions that were brought into the metastable region by a temperature quench. From the experiments they concluded that at the moment the demixing starts all nuclei are already present in the polymer solution. Also the number of nuclei was found to be independent of the value of the supercooling (or supersaturation). Boom et al. give two possible nucleation mechanisms: *i)* heterogeneous nucleation on a substrate with extremely good interaction with the nucleating phase or *ii)* nucleation due to large amplitude concentration fluctuations in the polymer solution (which indeed are always present).

The mass transfer model is valid only for homogeneous polymer solutions (i.e. the trajects outside the demixing gap). As soon as the polymer solution demixes the mass exchange with the immersion bath will be different for the two phases. More information then is available now is necessary on how the compositions and the volumes of the two phases change in time to be able to expand the mass transfer model for the inhomogeneous region.

It is important to notice that the thermodynamic data of the binodal and spinodal curves are based on equilibrium conditions. If the kinetics of the process are very rapid the equilibrium thermodynamics will not give adequate information on the compositions in the demixing system at the time and place of inspection. This will be important especially in the formation of toplayers of ultrafiltration membranes because here the diffusion rates of solvent and non-solvent are usually very high. The polymer being a macromolecular component with a relatively small diffusion coefficient is not able to respond to the fast diffusion processes of solvent and non-solvent. How this will result in a nodular structure which is a typical structure for the toplayers of ultrafiltration membranes is dealt with in the chapter 6 and the appendix to this thesis[20].

Despite its restrictions the mass transfer model is suitable to explain qualitatively the effects of system variables, such as concentration, temperature and interaction between the components, on the structure of the ultimate membrane. The system parameters that are important for the spinning experiments and their influence on the membrane structure are discussed in

paragraph 2.2.4. First the role of the hydrophilic macromolecular additive PVP is presented.

*2.2.3 Influence of PVP on the membrane formation process*

When PVP is added to the polymer solution the structure of the membranes changes drastically as was mentioned in the introduction. Roesink[5] was able to find an explanation for the high interconnectivity of the pores in microfiltration membranes containing PEI and PVP. PVP is very well miscible with the other components PEI, NMP and water. It was suggested that during phase separation by nucleation and growth of a polymer lean phase PVP will diffuse towards the polymer lean phase. However since diffusion of macromolecules is slow, PVP will not be able to completely reach the nuclei and it will be trapped in the solidifying polymer rich phase. This leads to an intermediate PVP phase between the nuclei and the polymer (PEI) rich phase. At places in the membrane where two growing nuclei approach each other the material in between the pores will mainly consist of PVP. This layer can easily break up upon drying, which causes the high interconnectivity of the pores. It is not clear in this picture how PEI molecules can move out in the narrow wall between the pores.

For the quaternary system PES/PVP/NMP/water Boom et al.[15-18] followed a different approach of phase separation which will briefly be described here. The interaction between PVP and PES is very good and the diffusion of the two polymers with respect to each other is slow. Therefore Boom regarded the two polymers at the very beginning of the mass exchange process as one constituent, having interactions with NMP and water that are 'intermediate' values of those for PES and PVP. It was found that the demixing gap of such a quasi ternary system is much reduced in magnitude; the system can contain a lot of the non-solvent water (up to 50 volume %) without demixing. In figure 2b the so called virtual binodals belonging to the quasi ternary system are shown for different ratios of PES and PVP. This situation is only valid for a very short time. When the two polymers are regarded as freely moving species the demixing gap is much more expanded and a small amount of water will already cause demixing of the system (figure 2a). The binodal belonging to the quaternary system will be indicated as the equilibrium binodal. This binodal coincides with the cloudpoint curve of the system. Interpolation of cloudpoint data as measured by Boom to the concentration range used in our experiments indicate that this curve is reached when the amount of water in the system is 6-7 weight%.

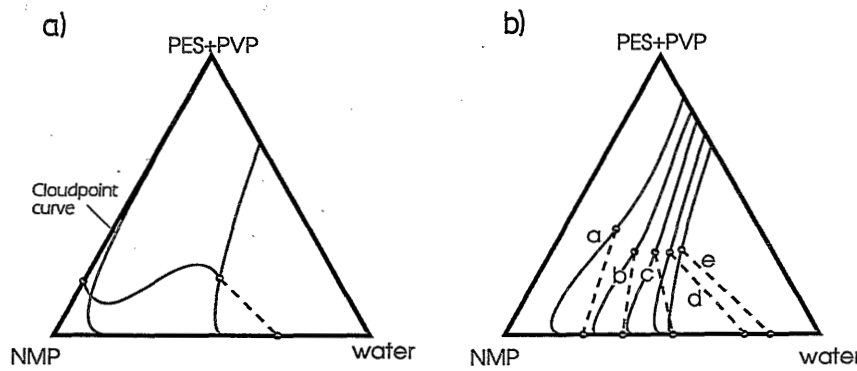


*Figure 2. Cross sections through quaternary phase diagrams at a constant ratio between the concentrations of PES and PVP. Figures are from the work of Boom et al.[16] a) Cloud point curve (equilibrium binodal) and virtual binodal for a system with an equal amount of PES and PVP. Also in this figure an initial composition path for the immersion of a solution containing 20 vol% polymer (PES and PVP) in water. b) calculated virtual binodals for the system PES-PVP-NMP-water, valid as long as no movement between the two polymers is possible. Ratios of PVP to PES are a: 0, b: 0.25, c: 0.5, d: 0.75, e: 1.0. Dashed lines are tie-lines. (For more data concerning these figures one is referred to Boom et al.[16])*

Boom defines two time scales for diffusion. One is a short time scale for the diffusion of solvent and non-solvent. On this scale the interdiffusion between the two polymers is negligible. The system is quasi ternary and the virtual binodals are valid. On the other hand there is a long time scale for the diffusion of the two polymers with respect to each other. For the first moments (fractions of seconds) after immersion the phenomena taking place on a short time scale are the most important events. But as the diffusion processes proceed further the long time scale becomes more important.

With this model the effect of PVP as pore former can be explained. A composition path for immersion in the pure non-solvent as calculated by Boom et al.[16] is shown in figure 2a. For the calculations of this composition path the diffusion of solvent and non-solvent are considered and the virtual binodals are used. However immediately after immersion the cloudpoint line is reached and the diffusion of the two polymers with respect to each other will start (although this diffusion takes place on the long time scale). Thus when the equilibrium binodal (cloud point line) is considered the composition path will lie inside the demixing gap indicating the occurance of instantaneous demixing. As said before instantaneously demixing systems lead to the formation of porous structures.

Boom et al.[15] calculated the equilibrium compositions of the two phases arising from phase separation of these quaternary systems. The calculations indicate that one phase consists of PES, NMP and water while the other consists of PVP, NMP and water. It seems that the two polymers have a driving force to separate completely. Thus the demixing process of the system is mainly determined by the diffusion of the two polymers with respect to each other. The incubation time for nucleation is zero (as was indicated by light transmission measurements performed by Boom et al.[19]) thus demixing starts as soon as the equilibrium binodal is passed. However because the diffusional exchange of the solvent and the non-solvent with the coagulation medium is much faster than the demixing process there still can be a large supersaturation of the polymer solution.

According to this mechanism the composition paths might lie even in the instable region. Therefore Boom et al.[17,18] suppose that for these systems spinodal decomposition occurs which can be an explanation for the high interconnectivity of the pores in membranes containing PVP. In this case the interconnected pores are in fact a continuous polymer lean phase intertwined by a continuous polymer rich phase which forms the membrane matrix.

So far only the diffusion processes until the beginning of phase separation have been considered. When the cloudpoint composition of the polymer solution is reached a polymer (PES) rich and a polymer lean (PVP rich) phase will arise. Because of the shift of the virtual binodal towards the equilibrium binodal it is difficult to say whether phase separation will take place by nucleation or by spinodal demixing. The compositions of the two phases will change towards the equilibrium compositions. Meanwhile the diffusional exchange with the coagulation medium continues. In practice the equilibrium compositions might not be reached. The growth in concentration of PES in the polymer rich phase will profoundly increase the viscosity of this phase thereby hindering further diffusional processes. At a certain point vitrification of the polymer rich phase occurs which is generally considered as the end of the structure formation process. The polymer lean phase is still fluid and represents the pores of the membrane. The solvent and PVP present in this phase can be removed by rinsing the membrane with water. When the polymer (PES) rich phase is vitrified it may contain a certain amount of solvent, non-solvent and PVP. The solvent and non-solvent can be removed by intensively rinsing but the PVP, being a high molecular weight component, is partially trapped in the PES matrix.

### *2.2.4 Membrane formation by spinning of hollow fibers*

In the dry-wet spinning technique there are three stages of diffusion induced phase separation:

- vapor penetration of non-solvent at the outer surface in the airgap
- immersion precipitation at the outer surface, once the nascent membrane has passed the airgap and enters the water bath
- immersion precipitation from the inside (through diffusional exchange with a bore liquid)

Besides this the polymer casting solution can also undergo a temperature quench if the temperature of the coagulation medium is lower than the extrusion temperature of the polymer solution.

In the airgap between spinneret and coagulation bath a vapor of the non-solvent water is supplied. The water diffuses into the spinning jet of polymer solution. Out-diffusion (evaporation) of solvent can be neglected because the temperature in the airgap is far below the boiling temperature of the solvent. If the initial composition of the polymer solution is already close to the cloudpoint composition, the indiffusion of water vapor can induce phase separation in the airgap. Since the indiffusion of water from the vapor phase is not very fast and the outdiffusion of solvent is nil the difference between the short and long time scale for demixing is not so profound. The supersaturation will therefore not be large. An increase of the water vapor concentration in the airgap will result in an increased driving force and a higher water concentration in the outer layer of the polymer solution. Upon phase separation of this polymer solution the volume of the polymer lean phase will be larger. This is schematically drawn in figure 3.

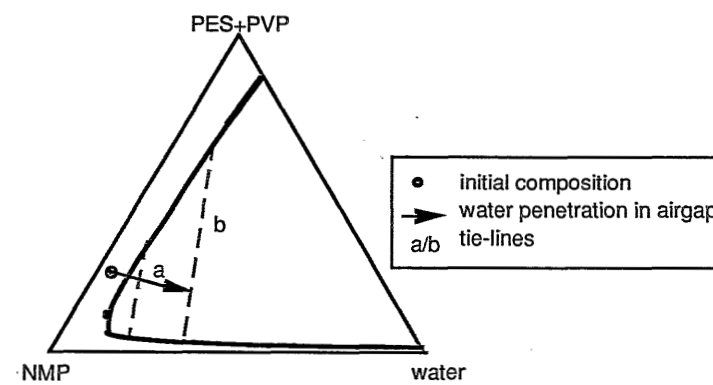


*Figure 3. A schematic drawing of the effect of water penetration in the airgap on the polymer concentration in the top layer of the solution. When the humidity in the airgap is higher more water will penetrate into the polymer solution (for the same residence time in the airgap). In this situation tie-line b will be reached and upon phase separation the volume of the polymer lean phase will be larger.*

Vitrification of the polymer rich phase in the airgap is not likely to occur because the residence time is too short for the solvent to diffuse to the polymer lean phase and the solvent can not diffuse out of the solution. The gelation will therefore take place during immersion in the coagulation bath. In this bath non-solvent diffuses into the polymer casting solution while solvent diffuses out. In the system of study the coagulation strength of the non-solvent is high. The strength is high because of a high interaction of the non-solvent with the solvent and a low interaction between non-solvent and the polymer (PES). The diffusion processes of solvent and non-solvent will be fast due to their high mutual interaction. In this situation the existence of the short time scale (for solvent and non-solvent) and the long time scale (for the two polymers) becomes important and may result in a high supersaturation of the polymer solution.

In the toplayer of the nascent membrane where demixing already starts in the airgap the diffusion processes in the water bath rapidly lead to vitrification of the polymer (PES) rich phase. The pore volume of this layer is determined by two processes: *i)* the amount of water that diffuses into the solution during its contact time with the vapor and *ii)* the amount of solvent that diffuses into the coagulation bath. Below the toplayer the phase separation starts in the coagulation bath. Here the large supersaturation can lead to spinodal demixing of the polymer solution and thus the formation of a co-continuous membrane structure. The polymer concentration in the sublayer will not be increased as much as in the toplayer because of less outdiffusion of solvent. The pores in the sublayer will therefore be larger the more remote they are from the surface.

At the bore side the coagulation strength of the bore liquid, starting from the pure non-solvent, generally is reduced by the addition of solvent. Diffusion processes of solvent and non-solvent are slower then, since the driving forces (concentration gradients) are lower. Especially the out-diffusion of solvent is retarded. The result is a relatively low polymer concentration during phase separation and a high porosity. Normally such coagulation media would give a delay time for demixing. However in this case the polymer solution will demix instantaneously because the presence of PVP causes a shift of the virtual binodal towards the equilibrium binodal.

In the spinning process the diffusion processes are combined with a temperature effect. The extrusion temperature of the polymer solution is often higher than the temperature of the coagulation medium. The temperature can affect the phase separation process in two ways. Reducing the temperature may *i)* induce demixing of the polymer solution and *ii)*

reduces the diffusion coefficients of the components. The growth of the nuclei therefore is slowed down and gelation of the polymer rich phase is promoted. The general effect is that at a lower temperature the velocity of the phase separation process is slowed down whereas the vitrification point is reached at a lower polymer concentration.

Besides phase separation rheological phenomena may influence the structure of the membrane in the spinning process. Aptel et al.[1] have spun fibers from a solution containing polysulfone, PVP and DMAc with the skin on the inside. The bore liquid used was water, causing fast precipitation of the polymer. They found that the performance of the membranes depends on the extrusion rates of the polymer solution and on the bore liquid. According to Aptel shear forces in the spinneret cause orientation of polymer molecules. If gelation of the solution due to contact with the bore liquid is faster than the relaxation time of the polymer solution the stretched polymer chains are frozen in and the permeability of the membrane is lower. Roesink[5] mentioned that the shear forces will lead to a die-swell of the polymer solution after it leaves the spinneret. Any effect on the performance of the membranes was not reported. The diameter of the hollow fiber depends on the take-off rate and on the extrusion rate of the polymer solution as was published by Cabasso et al.[3]. Espenan et al.[2] found that the diameter of the fiber decreases when the airgap becomes longer or when the flow rate of the polymer solution decreases. The diameter of the bore increased if the flow rate of the bore liquid was enhanced. An empirical relation was found between the wall thickness and the permeability but it was not based on a physical model.

## 2.3 Materials and Methods

### *2.3.1 Materials*

Poly(ether sulfone) (PES) was purchased from ICI (Victrex 5200P. $M_w$ 44,000 g/mole). Later on spinning experiments with a controlled humidity in the airgap were performed using PES from BASF (Ultrason E6010P). The weight average molecular weight of this polymer was somewhat lower (43,000 g/mole). Two types of poly(vinyl pyrrolidone) (PVP) from Janssen Chimica were used, K90 ($M_w$ 507,000 g/mole) and K30 ($M_w$ 18,000 g/mole). The weight average molecular weights of the polymers were determined using GPC. The polymers were used as received. The water content of the polymers was measured in a Buchi oven and was 1.5 wt % for PES and 6 wt% for PVP. The solvent 1-Methyl-2-pyrrolidone (NMP) was purchased from Merck (synthetic grade). The non-solvent was water.

### 2.3.2 The spinning set-up

Two spinning apparatuses have been used in this study. In the first set-up the humidity in the airgap was dependent on the temperature of the water bath. The fibers were transported on rollers, automatically cut into pieces and stored in water. In the second set-up the conditions in the airgap were controlled externally and the fibers were not transported but collected at the bottom of the coagulation bath.

*First spinning set-up*

The first set-up is shown in figure 4. The polymer solution was contained in a thermostated vessel. With a gear pump it was extruded through a tube-in-orifice spinneret. For the bore liquid also a gear pump was used and it was pumped through the inner orifice of the spinneret. The dimensions of the spinneret ere 0.8 mm for the outer diameter of the inner orifice and 1.5 mm for the diameter of the outer orifice. The thickness of the needle wall was 0.1 mm. The airgap is the space between the spinneret and the coagulation bath. The humidity and temperature of the airgap were determined by the temperature of the water bath below the airgap. Once the fiber was coagulated in the water bath it could be transported by rollers. The fibers were cut automatically in pieces of about 30 cm. The fibers were collected in a rinsing bath. By cutting the fibers into shorter lengths the bore liquid could be flushed out more readily.

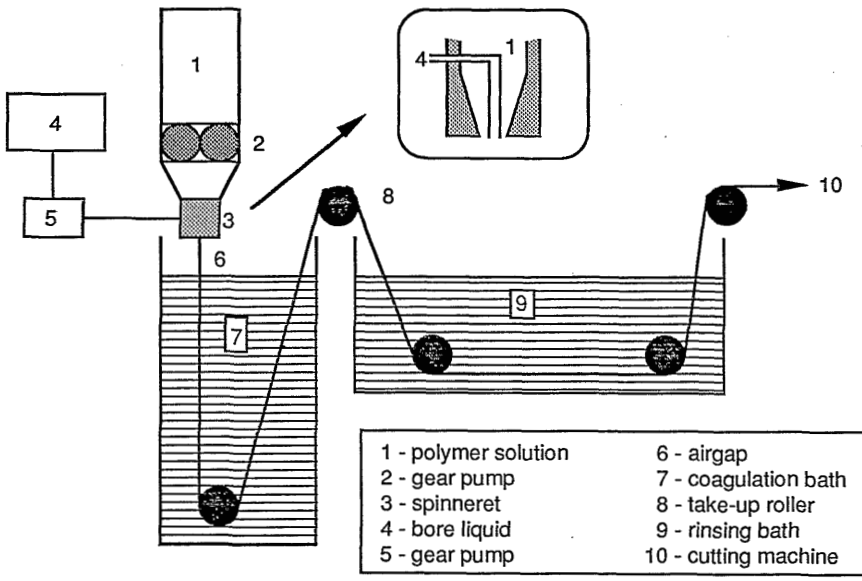


*Figure 4. Spinning set-up with transport of the fibers to a rinsing bath. Conditions of the airgap are dependent on the water bath below the airgap.*

*Second spinning set-up*
To be able to control the humidity and temperature of the airgap irrespective of the conditions of the coagulation bath in the second set-up a casing was placed between the spinneret and the water bath. In the casing the airgap was 5 cm long. A nitrogen stream as saturated with water of 60 °C and mixed with a heated but dry nitrogen stream. The mixed gas was lead to the space around the fiber and then slowly flows upwards with a linear velocity of 2.75 cm/s. The temperature in the isolated casing was 50 °C. A schematic representation of this set-up is shown in figure 5.

The humidity of the saturated nitrogen stream can be calculated using the Antoine equation for saturated vapor pressures:

$$\log P_i^0 = A + \frac{B}{(C+T)} \qquad (1)$$

with $P^0_i$ the partial vapor pressure at saturation (in mm Hg) and temperature T (in °C). The Antoine constants for water are[30]:

A = 8.071
B =-1730.630
C = 233.426

The humidity of the airgap is found by taking the volume average of the dry and saturated nitrogen stream. It can be varied between the partial pressure of the coagulation bath below the airgap (water bath of 20 °C, $P^0_{H_2O}$ = 0.023 Bar) and the temperature in the airgap which is 50 °C ($P^0_{H_2O}$ = 0.123 Bar). If the partial pressure would become higher water vapor would condense on the wall of the casing and on the fiber.

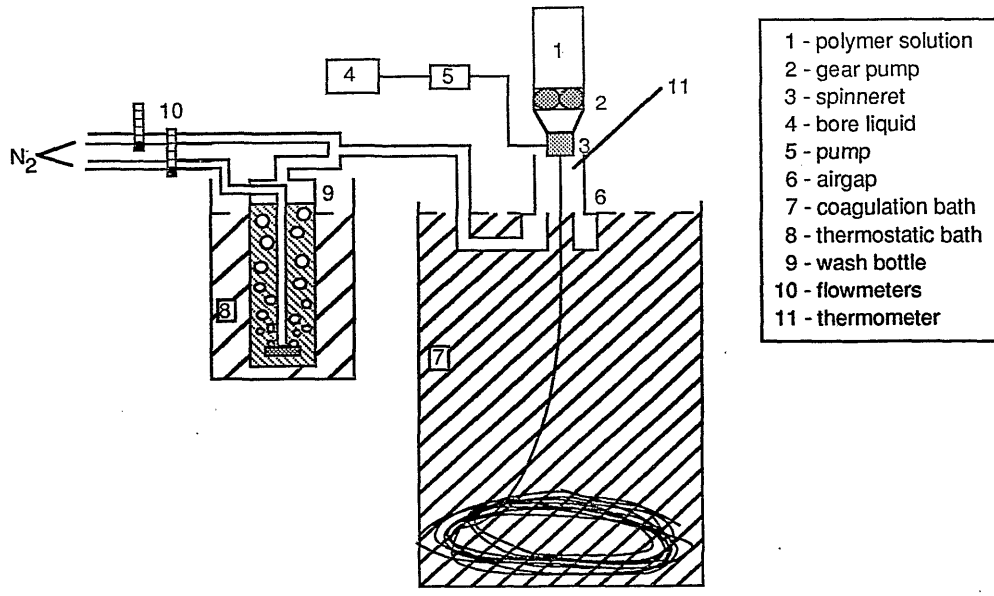


*Figure 5. Spinning set-up with controlled humidity in the airgap. Fibers are collected at the bottom of the coagulation bath.*

### *2.3.3 The spinning process and post-treatment*

Clear polymer solutions were obtained by dissolving PES and PVP in NMP and adding water to a known amount. All polymer casting solutions contained 20 wt% PES and 5 wt% water. The concentration and molecular weight of the PVP was varied. The viscosity of the polymer solutions was measured using a rotary viscometer (Brabender). Unless mentioned otherwise the bore liquid contained 78 wt% NMP and 3 wt% PVP in water.

The polymer solutions and bore liquids were filtered by a metal filter (25 μm) and were degassed before use. Temperature of the bore liquids was 25 °C. After spinning and coagulation the fibers were rinsed with water of 50 °C for two days. Following earlier work in our laboratory (Roesink[5]), excess PVP could be removed after contacting the fibers with a 4000 ppm sodium hypochlorite solution for 48 hours. After rinsing for one more day the fibers were put in a water bath containing 10 wt% glycerol for one day and finally they were dried at room temperature.

### *2.3.4 Characterization methods*

Membrane morphology was studied using a scanning electron microscope (JEOL, JSM T220A). Water for flux measurements was prefiltered by reverse osmosis. BSA retentions were measured using a 0.1 wt% BSA solution. BSA

($M_w$ 65,000 g/mole) was purchased from Sigma Chemical company and dissolved in a phosphate buffer solution of pH 7.4, containing 0.1M NaCl. Flux and retention measurements were carried out in a cross-flow filtration setup. The applied pressure difference was 2 bars and after 30 minutes conditioning time the water flux was practically constant. BSA concentrations were determined spectrophotometrically at 280 nm. The retention (R) was calculated according to the formula:

$$R=1-C_p/C_f \ (*100\%) \qquad (2)$$

in which $C_p$ and $C_f$ represent the BSA concentration in the permeate and in the feed respectively.

## 2.4 Results and Discussion

Hollow fiber ultrafiltration membranes have been spun using the dry wet spinning technique. Firstly the structures at the bore side that were obtained by varying the solvent/non-solvent ratio of the bore liquid are considered. After this the attention is focused on preparing hollow fiber membranes with the selective toplayer at the outside. The influence of the humidity in the airgap on the performance of the membranes is discussed. The humidity has been varied by changing the temperature of the water bath below the airgap (section 2.4.2) or by applying a nitrogen stream with a certain water vapor concentration (section 2.4.3).

### *2.4.1 The composition of the internal coagulation bath*

Internal coagulation baths have been varied from 10 to 80 wt% NMP in water. In this series a range of membrane structures can be found. In most experiments 3 wt% PVP K90 was added to the bore liquid to enhance its viscosity. This was necessary to obtain a round shape of the bore.

At low NMP content of the internal coagulation liquid a skin was formed at the bore side of the fiber. Pore sizes in the skin layer increase with increasing NMP content in the bore liquid. For two compositions of the bore liquid the flux for water and for a BSA solution are shown in table 1. A photograph of the toplayer is shown in figure 6a.

*Table 1. Flux and BSA retention of hollow fiber ultrafiltration membranes for two compositions of the bore liquid. The selective toplayer is at the bore side of the fibers. The polymer solution contained 20 wt% PES, 7.5 wt% PVP K90 and 5 wt% water in NMP. Deviations from mean values of three experiments are given between brackets.*

| bore liquid wt%/wt% | water flux [l.m$^{-2}$h$^{-1}$bar$^{-1}$] | flux for BSA solution [l.m$^{-2}$h$^{-1}$bar$^{-1}$] | BSA retention [%] |
|---|---|---|---|
| 10 NMP/90 water | 376 (±6) | 132 (±3) | 99 (±1) |
| 20 NMP/80 water | 480 (±5) | 150 (±8) | 98 (±1) |

At medium NMP concentrations in the bore liquid, between 40 and 70 wt%, a very rough surface was found at the bore side of the fibers. The PVP content of the polymer casting solution was very high in this case (13 wt%, K90). A photograph of the cross section is shown in figure 6b. The structure seems to originate from macrovoids that coalesced and disrupted the skin. These results are not in agreement with the general opinion that PVP prevents macrovoid formation[14,20]. However the formation of such a structure can be explained with the theory of Boom et al.[17]. Due to a high solvent concentration in the bore liquid the concentration gradient of solvent is small. Thus the diffusion processes for the short time scale (solvent and non-solvent) are slow and the diffusion of PVP with respect to PES (long time scale) is important. As PVP forms the polymer (PES) lean phase, the polymer rich phase contains more PES. The interaction of the polymer (PES) rich phase with the coagulation medium causes the formation of the macrovoids since this phase does not contain enough PVP to prevent macrovoid formation.

If the internal coagulation bath contains about 80 wt% of NMP, diffusion processes of solvent and non-solvent are so slow that the separation of PES and PVP can almost go to completion. The PVP phase then contains most of the non-solvent water and this phase grows out to very large, more or less spherical pores. The interaction of the PES phase with the coagulation medium is such that there is a delay time for demixing. After this delay time the PES phase also demixes. This results in small pores in the membrane matrix near the surface as can be seen in figure 6c. This composition of the internal bore liquid can be used if the toplayer of the membrane is chosen to be at the outer surface. Higher concentrations in the bore liquid would lead to dissolution of the polymer casting solution in the coagulation medium.

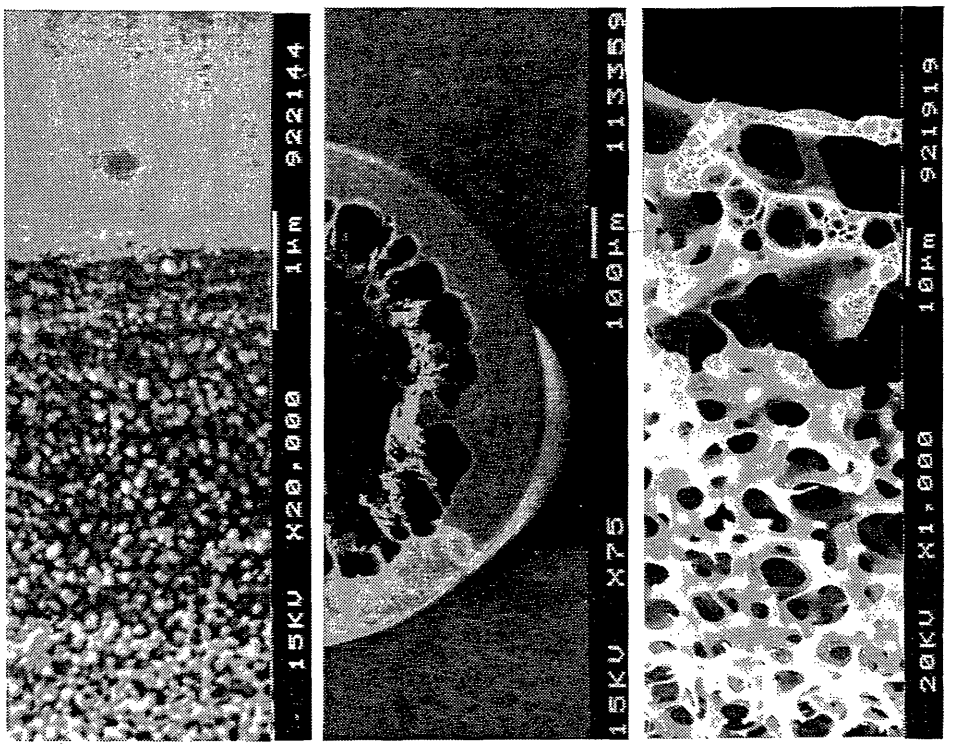


a) b) c)

*Figure 6. SEM pictures of cross sections of hollow fibers to show the morphologies at the bore side due to different amounts of NMP in the bore liquid: a) 20 wt% , b) 70 wt% and c) 80 wt% NMP in water. In a) and c) the bore side is at the upper part of the pictures.*

### *2.4.2 Dry-wet spinning technique*

Fibers were spun using the spinning set-up as depicted in figure 4 (uncontrolled conditions in the airgap). The spinning solution contained 20 wt% PES, 5 wt% PVP K30, 5 wt% PVP K90 and 5 wt% water. The length of the airgap has been varied for two temperatures of the water bath. The humidity and temperature of the airgap are related to the temperature of the water bath underneath. The residence time of the nascent membrane in the airgap depends on the length of the airgap and the spinning velocity. Airgap residence times are roughly between 1/10 and 1/2 second (see figure 7). The spinning velocity is not an independent variable because in the airgap stretching of the casting solution occurs due to gravity force. The influence of the gravity force on the nascent fiber is more profound as the length of the airgap is larger and as the viscosity of the polymer solution is lower. In table 2 it is shown that if the length of the airgap is larger, the take-up speed of the

fiber has to be higher to transport the fiber over the rollers. Also the ultimate diameter of the fiber decreases when the length of the airgap increases. Besides gravity force also die-swell and shear forces during extrusion are effective on the polymer solution.

At 44°C the effects of fiber stretching were stronger. Compared to 22 °C the take-up speed increased even more going from an airgap length of 1 cm to 5 cm. Also for the same length of the airgap the dimensions of the fibers were smaller at 44°C. The reason for this is that the viscosity of the polymer casting solution is lower at a higher temperature hence gravity force has more impact. The polymer casting solution which is kept at 50°C in the container will cool down rapidly until it reaches the temperature of the airgap.

*Table 2. Spinning conditions and diameters of the fibers. The composition of the polymer casting solution was 20 wt% PES, 5 wt% PVP K30, 5 wt% PVP K90 and 5 wt% water in NMP. The polymer solution was kept at 50 °C. The bore liquid consisted of 78% NMP and 3 wt% PVP in water. The temperature of the bore liquid was 25 °C, its flow rate was 2.6 ml/min. The viscosity at zero shear force is 75,800 cpoise at 22 °C and 25,400 cpoise at 44 °C.*

| Temperature water bath [°C] | length airgap [cm] | extrusion rate [ml/min] | take-up speed [m/min] | external diameter [mm] | internal diameter [mm] |
|---|---|---|---|---|---|
| 22 | 1 | 4.5 | 4.2 | 1.40 | 0.88 |
| 22 | 3 | 4.5 | 5.6 | 1.21 | 0.75 |
| 22 | 5 | 5.3 | 7.4 | 1.16 | 0.74 |
| 44 | 1 | 4.5 | 4.1 | 1.40 | 0.88 |
| 44 | 3 | 4.5 | 5.9 | 1.17 | 0.74 |
| 44 | 5 | 5.3 | 7.8 | 1.10 | 0.65 |

After post-treatment of the membrane fibers water flux and retention for BSA have been measured. In figure 7 water flux and retention are plotted versus the residence time which is the ratio of the length of the airgap and the take-up speed. If the residence time in the airgap went up water flux decreased while retention increased. At a higher temperature of the water bath membranes were made with a higher water flux and a lower retention for BSA both being more dependent on the residence time in the airgap than at 22 °C.

These results are not consistent with the theory of membrane formation by phase separation as discussed in the theoretical section. According to this

theory a longer contact time with water vapor will allow more water to diffuse into the polymer solution while outdiffusion of non-solvent is not possible. A more open porous structure would be expected, resulting in a high water flux through the membrane. The observed low water flux at longer residence time leads to the conclusion that gravity force on the nascent fiber and fiber stretching influence the membrane formation in such a way that it hinders the generation and growth of pores. A physical model to explain these phenomena is not easy to derive since apart from gravity force also shear forces in the spinneret and the die-swell on leaving the spinneret influence the rheological behavior of the polymer solution.

If the temperature of the water bath is higher more water vapor is present in the airgap and growth of nuclei is faster due to higher diffusion coefficients. Therefore pore sizes are larger at a higher temperature which corresponds with the experiments.

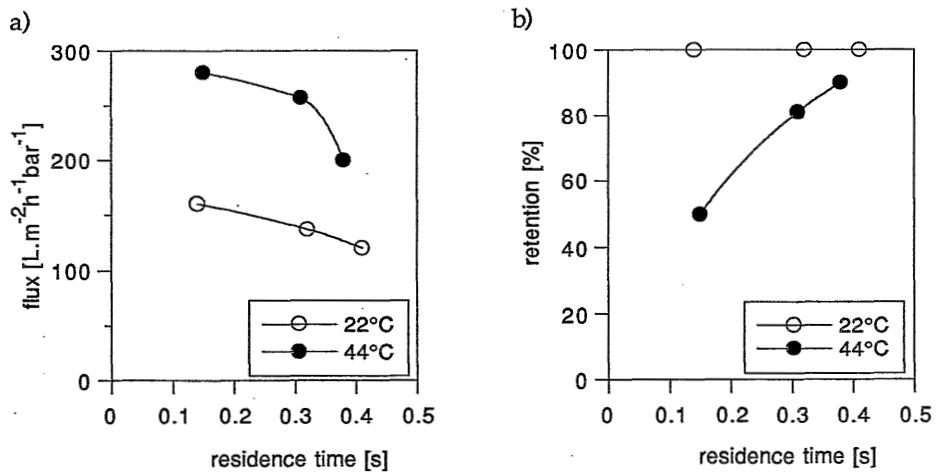


*Figure 7. Performance of the membranes spun with the conditions mentioned in table 2. a) water flux and b) retention for a 0.1 wt% BSA solution. Residence time in the airgap is the ratio of the length of the airgap and the take-up speed. Deviations from mean values are for water fluxes within 10% and for retentions within 2%.*

While performing more experiments than shown here it was found that the reproducibility of the spinning process with this set-up is not very good. The conditions in the airgap are susceptible to environmental changes and transport of the fiber over the rollers may easily cause an extra stretching force on the nascent fiber. To avoid these problems some modifications have been made to the spinning apparatus. The results of these are the subject of the next section.

*2.4.3 Controlled humidity in the airgap*

The spinning set-up as depicted in figure 5 was used to investigate the influence of the humidity in the airgap at constant airgap length on the structure and the performance of the membranes. Three polymer solutions were used containing different amounts of PVP K90: 7.5 wt%, 10 wt% and 12.5 wt%. All solutions contained 20 wt% PES and 5 wt% water. The cloud point composition of the polymer solution lies at a water content of 6-7 wt% (extrapolated from values measured by Boom[15]). The addition of water to the polymer solution will bring its composition closer to the binodal composition. Therefore over the entire wall thickness only a small amount of water from the coagulation medium is necessary to induce demixing. The process conditions can be found in table 3.

In these experiments the airgap had a fixed length (5 cm); in the airgap the humidity was varied in an independent way as described in section 2.3.2. For the three polymer casting solutions the residence time was not the same due to differences in viscosities. This resulted also in different dimensions of the fibers as is shown in table 3. Small deviations in diameters are due to temperature fluctuations (45 °C - 50 °C) in the airgap. For the 12.5 wt% PVP solution the deviation is most profound because the dependency of the viscosity on the temperature is largest for this solution.

*Table 3. Spinning conditions and diameters of the fibers. The polymer spinning solution consisted of 20 wt% PES, 5 wt% water and different amounts of PVP K90 in NMP. Extrusion temperature of the solution was 60°C and the extrusion rate was 2.5 ml/min. The bore liquid consisted of 78% NMP and 3 wt% PVP in water; the temperature was 25 °C, the flow rate was 1.7 ml/min The temperature of the water bath was 20 °C.*

| concentration PVP [wt%] | viscosity* [cpoise] | residence time [s] | external diameter [mm] | internal diameter [mm] |
|---|---|---|---|---|
| 7.5 | 21,100 | 1.0 | 1.40 (5%)** | 0.94 (5%)** |
| 10.0 | 58,600 | 1.5 | 1.55 (8%) | 1.04 (8%) |
| 12.5 | 100,800 | 2.2 | 1.94 (13%) | 1.38 (13%) |

* viscosity at 50 °C extrapolated to shear force zero.

** numbers between brackets are deviations from the mean values.

The performance of the membranes, spun at different humidities in the airgap, is given in figure 8 where fluxes for water and for a BSA solution as well as the retention for BSA are plotted versus the vapor pressure of water in the airgap. The general course of the curves is the same for the three plots. The morphologies of the membranes are studied using SEM. In figure 9 the photographs of the outer surface for the solution containing 12.5 wt% PVP are shown.

The photographs (figure 9) show that pore sizes in the skin of the membranes increase when a higher water vapor pressure was used in the airgap. The same trend was found for the flux measurements. When the humidity in the airgap goes up, the water flux of the membranes increased while the retention for BSA decreased. This result is in accordance with the theory of membrane formation as described in the theoretical section. More penetration of water will lead to a higher water content of the polymer solution. Upon phase separation the volume of the polymer (PES) lean phase is larger, resulting in a higher porosity of the ultimate membrane. It is clear that in *this* experiment for one composition of the polymer solution the gravity forces are constant.

In figure 8 it can be seen that at a high vapor pressure in the airgap the 12.5 wt% PVP solution shows a higher water flux and a lower BSA retention compared to the values of the solutions containing less PVP. According to Boom et al.[16,17] the demixing gap for the short time scale is lying further to the right hand side of the phase diagram when the PVP concentration is higher (see also figure 2b). Thus at high PVP concentration more water diffuses into the polymer solution. Unlike the virtual binodal the cloud point curve is not very dependent on the PVP concentration. The phase separation process starts at the same water content but during phase separation the polymer solution with 12.5 wt% PVP contains more water. Also the residence time in the airgap is longer due to the high viscosity of the 12.5 wt% solution and water vapor has more time to diffuse into the nascent membrane. A third effect is that during phase separation the PVP also diffuses towards the polymer (PES) lean phase. More PVP (at the same PES concentration) would thus result in a larger volume of the polymer lean phase and a larger pore volume in the ultimate membrane.

At low vapor pressure in the airgap the differences of the three polymer solutions are not so profound. Here the water flux for the 12.5 wt% solution is even lower than for the fibers with lower PVP content. The reason for this is that at low vapor pressure the phase separation of the polymer solution will probably not start in the airgap. In the water bath the phase separation and thus pore formation is rapidly followed by vitrification of the polymer

(PES) rich phase. The vitrification point is reached sooner if the viscosity of the initial polymer concentration is higher as is the case for the 12.5 wt% PVP solution.

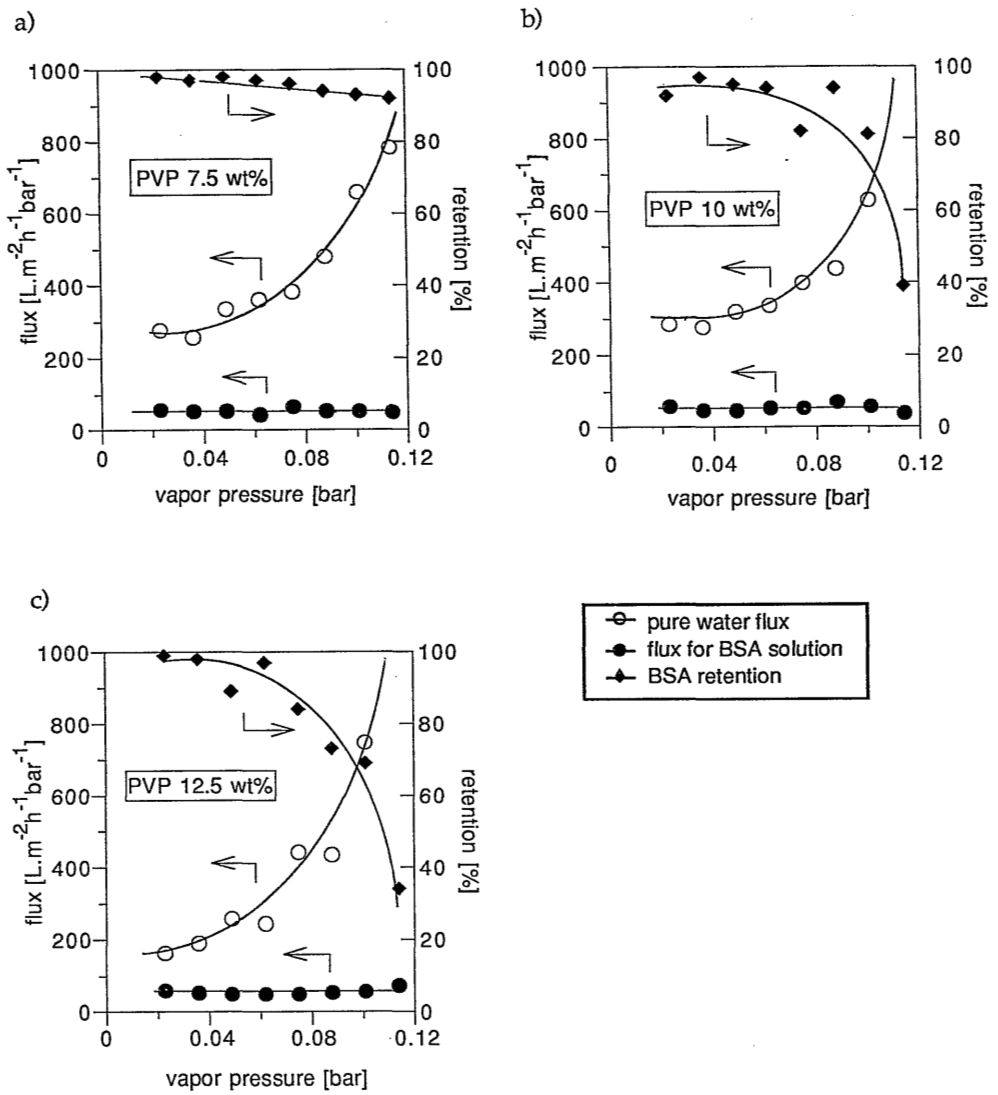


*Figure 8. Performance of the membranes spun with different vapor pressures in the airgap: pure water flux and flux and retention for a 0.1 wt% BSA solution. The spinning conditions were as mentioned in table 2. a) 7.5 wt% PVP, b) 10 wt% PVP and c) 12.5 wt% PVP in the spinning solution. Deviations from mean values were for water fluxes within 10% and for retentions within 2%.*

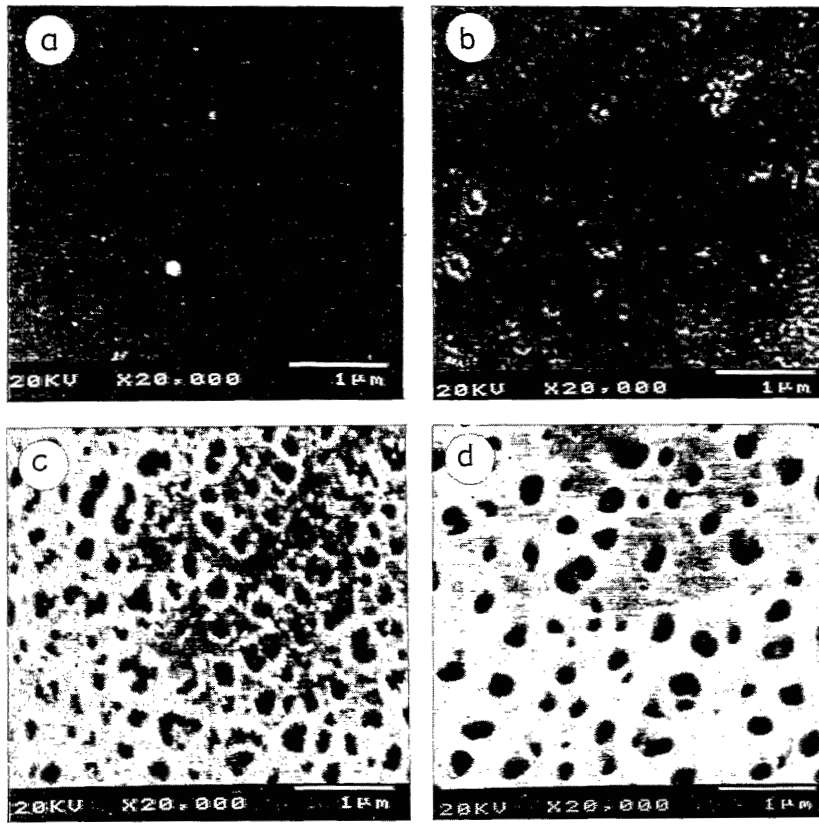


*Figure 9. Morphologies at the outer surface of the membranes, photographs made with SEM. The spinning solution contained 12.5 wt% PVP. Vapor pressure in the airgap was: a) 0.036 bar, b) 0.062 bar, c) 0.101 bar, d) 0.114 bar.*

After the fiber has passed the airgap it enters into the water bath. Here the nascent membrane undergoes a temperature quench from 50 to 20 °C. Since NMP is very well miscible with water the outdiffusion of solvent is fast. In the toplayer these two effects will lead to rapid vitrification of the polymer rich phase. The fast vitrification in the toplayer is nicely illustrated in figure 10. In the cross section the smallest pores are not found at the outer surface but about 10 μm deeper into the membrane. This pore size distribution in the toplayer is a direct result of the concentration profile of water that has diffused into the polymer solution in the airgap. This phenomenon was also found by Roesink[5]. It can be diminished by an increase of the temperature of the water bath but this was not the aim of our research. In this study the fast coagulation in the water bath implies that the membrane structures found at the outer surface are mainly determined by the conditions in the airgap. Further away from the interface (at distances larger than 10 μm) the phase

separation process is slowed down because the toplayer forms a barrier for the diffusion of solvent and nonsolvent. The pore size will therefore be larger the further the pores are situated from the surface. In figure 10 it can be seen that the pore interconnectivity is very good which indicates that the structure is most likely formed by spinodal decomposition of the polymer solution.

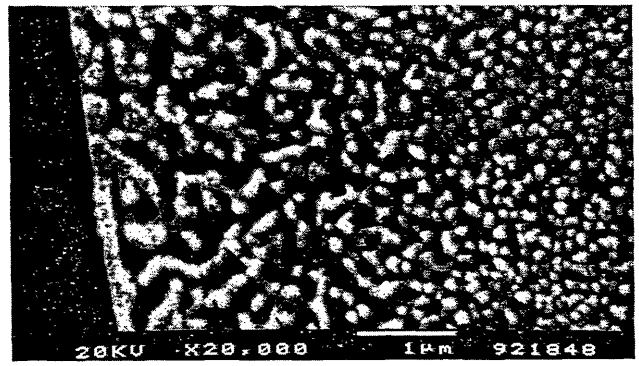


*Figure 10. Cross section of a toplayer showing the transition from the airgap into the water bath. PVP concentration in the polymer solution was 10 wt%, vapor pressure in the airgap was 0.114 bar. The surface pore structure (not visible on this photograph) is comparable to the one shown in figure 9d.*

Two more remarks have to be made on the results presented here. The SEM photographs of figure 6a and 9 show that for low vapor pressures in the airgap a nodular structure in the toplayer is formed. The formation mechanism of this structure is the subject of chapter 6. The second remark concerns the flux for the BSA solution. This flux is almost the same in all cases. The flux decline from water flux to the flux for the BSA solution however is higher as the pores are larger. This is due to pore blocking of the large pores by BSA molecules. The retention measurements are discussed more thoroughly in chapter 5.

## 2.5 Conclusions

Ultrafiltration membranes can be spun from the system PES, PVP, NMP and water. Pore sizes at the bore interface can be controlled by varying the solvent/non-solvent ratio in the bore liquid. To be able to control the pore sizes at the outer surface by applying an airgap a distinction has to be made between effects caused by forces acting on the polymer spinning solution (gravity, shear forces in the spinneret, die-swell) and demixing processes. The forces on the polymer solution can be very important. Only when these have been taken into account, results are in accordance with the theory on phase

separation. The high interconnectivity of the pores in the membranes is a strong indication that demixing started in the spinodal region.

**Acknowledgement**
The authors like to thank H. Teunis for performing part of the spinning experiments.

## 2.6 Literature

1. P. Aptel, N. Abidine, F. Ivaldi, J.P. Lafaille, Polysulfone hollow fibers, effect of spinning conditions on ultrafiltration properties, J. Mem. Sci., **22** (1985) 199
2. J.M. Espenan, P. Aptel, Outer skinned hollow fibers spinning and properties, Membranes and Membrane processes, E. Drioli, M. Nakagaki, Plenum publishing corporation, New York, 1986
3. I. Cabasso, E. Klein, J.K. Smith, Polysulfone hollow fibers. I. Spinning and properties, J. Appl. Polym. Sci., **20** (1976) 2377
4. I. Cabasso, E. Klein, J.K. Smith, Polysulfone hollow fibers. II. Morphology, J. Appl. Polym. Sci., **21** (1977) 165
5. H.D.W. Roesink, Microfiltration, membrane development and module design, Thesis Univ. of Twente, the Netherlands, 1989
6. S. Doi, K. Hamanaka, Pore size control technique in the spinning of polysulfone hollow fiber ultrafiltration membranes, Desalination, **80** (1991) 167
7. C. Hall, Polymer materials: an introduction for technologists and scientists, second edition, MacMillan education, Basingstoke, 1989, p 42
8. D. R. Dreger, The polysulfones, Machine Design, **50** (1978) 114
9. *a)* L.E.S. Brink, D.J. Romijn, Reducing the protein fouling of polysulfone surfaces and polysulfone ultrafiltration membranes: Optimization of the type of presorbed layer, Desalination, **78** (1990) 209
   *b)* G. Capannelli, A. Bottino, V. Gekas, G. Tragardh, Protein fouling behavior of ultrafiltration membranes prepared with varying degrees of hydrophilicity, Proc. Biochem. Int., December (1990) 221
   *c)* A.S. Jonsson, B. Jonsson, The influence of nonionic and ionic surfactants on hydrophobic and hydrophilic ultrafiltration membranes, J. Mem. Sci., **56** (1991) 49
10. H.D.W. Roesink, M.A.M. Beerlage, W. Potman, Th. van den Boomgaard, M.H.V. Mulder, C.A. Smolders, Characterization of new membrane materials by means of fouling experiments: Adsorption of BSA on polyetherimide-polyvinylpyrrolidone membranes, Coll. Surf., **55** (1991) 231
11. L.Y. Lafreniere, F.D.F. Talbot, T. Matsuura, S. Sourirajan, Effect of polyvinylpyrrolidone additive on the performance of polyethersulfone ultrafiltration membranes, Ind. Eng. Chem. Res., **26** (1987) 2385
12. T.A. Tweddle, O. Kutowy, W.L. Thayer, S. Sourirajan, Polysulfone ultrafiltration

membranes, Ind. Eng. Chem. Prod. Res. Dev., 22 (1983) 320

13. X. Xie-qing, Additive reagents for ultrafiltration membranes of polysulfone resin, Maku 8 (1983) 311
14. S.Munari, A. Bottino, G. Capannelli, P. Moretti, P. Petit Bon, Preparation and characterization of polysulfone-polyvinylpyrrolidone based membranes, Desalination, 70 (1988) 265
15. *a)* R.M. Boom, Th. van den Boomgaard, C.A. Smolders, Equilibrium thermodynamics of a quaternary membrane forming system with two polymers. I. Theory, submitted for publication to Macromolecules
    *b)* R.M. Boom, H.W. Reinders, H.H.W. Rolevink, U. Cordilia, Th. van den Boomgaard, C.A. Smolders, Equilibrium thermodynamics of a quaternary membrane forming system with two polymers. II. Experimental, submitted for publication to Macromolecules
16. R.M. Boom, Th. van den Boomgaard, C.A. Smolders, Mass transfer and thermodynamics during immersion precipitation for a two polymer system: Evaluation with the system PES-PVP-NMP-water, submitted for publication to J. Mem. Sci.
17. R.M. Boom, S. Zanic, Th. van den Boomgaard, C.A. Smolders, Membranes from PES and PVP: Membrane morphology and its relation to the formation mechanism, submitted for publication to J. Mem. Sci.
18. R.M. Boom, H.H.W. Rolevink, Th. van den Boomgaard, C.A. Smolders, Membranes prepared from PES and PS: Comparison with the PES-PVP system, submitted for publication to J. Mem. Sci.
19. *a)* R.M. Boom, Th. van den Boomgaard, C.A. Smolders, Metastable demixing phenomena by thermal quench experiments. I. Theory, submitted for publication to J. Appl. Polym. Sci.
    *b)* R.M. Boom, S. Rekveld, U. Cordilia, Th. van den Boomgaard, C.A. Smolders, Metastable demixing phenomena by thermal quench experiments. II. The systems PES-NMP-water and PES-NMP-PVP-water, submitted for publication to J. Appl. Polym. Sci.
20. Appendix to this thesis, also published: R.M. Boom, I.M. Wienk, Th. v.d. Boomgaard, C.A. Smolders, Microstructures in phase inversion membranes, part II. The role of a polymeric additive, J. Mem. Sci., 73 (1992) 277
21. P.W. Atkins, Physical chemistry, fourth edition, Oxford university press, Oxford, 1978, p 187
22. J. W. Cahn, Phase separation by spinodal decomposition in isotropic systems, J. Chem. Phys., 42 (1965) 93
23. *a)* J.J. van Aartsen, Theoretical observations on spinodal decomposition of polymer solutions, Eur. Pol. J., 6 (1970) 919
    *b)* C.A. Smolders, J.J. van Aarsen, A. Steenbergen, Liquid-liquid phase separation in concentrated solutions of non-crystallizable polymers by spinodal decomposition, Koll. Z. u. Z. Pol., 243 (1971) 14
24. H. Tompa, Polymer solutions, Butterworths, London, 1956, p 82
25. F.W. Altena, C.A. Smolders, Calculation of liquid-liquid phase separation in a ternary system of a polymer in a mixture of a solvent and a nonsolvent, Macromolecules, 15 (1982)

1491

26. C. Cohen, G.B. Tanny, S. Prager, Diffusion controlled formation of porous structures in ternary polymer systems, J. Polym. Sci., Polym. Phys. Ed. 17 (1979) 477
27. *a)* A.J. Reuvers, J.W.A. v.d. Berg, C.A. Smolders, Formation of membranes by means of immersion precipitation. I. A model to describe mass transfer during immersion precipitation, J. Mem. Sci., 34 (1987) 45
*b)* A.J. Reuvers, C.A. Smolders, Formation of membranes by means of immersion precipitation. II. The mechanism of formation of membranes prepared from the system cellulose acetate-acetone-water, J. Mem. Sci., 34 (1987) 67
28. C.S. Tsay, A.J. McHugh, Mass transfer modeling of asymmetric membrane formation by phase inversion, J. Pol. Sci. part B: Pol. Phys., 28 (1990) 1327
29. *a)* P. Radovanovic, S.W. Thiel, S.T. Hwang, Formation of asymmetric polysulfone membranes by immersion precipitation. Part I: Modelling mass transport during gelation, J. Mem. Sci., 65 (1992) 213
*b)* P. Radovanovic, S.W. Thiel, S.T. Hwang, Formation of asymmetric polysulfone membranes by immersion precipitation. Part II: The effects of casting solution and gelation bath compositions on membrane structure and skin formation, J. Mem. Sci., 65 (1992) 231
30. J. Gmehling, U. Onken, U. Weidlich, Vapor liquid equilibrium data collection, Vol 1, part 1, Dechema, Frankfurt, 1977

3

# A New Spinning Technique for Hollow Fiber Ultrafiltration Membranes

I.M. Wienk, H.A. Teunis, Th. van den Boomgaard, C.A. Smolders

## Summary

A new spinning technique for hollow fiber membranes with a densified outer toplayer has been developed in our laboratory. This technique makes use of a new type of spinneret having three concentric orifices. Apart from extruding polymer solution and bore liquid as applied in classical spinnerets a third liquid can be pumped through an outer layer. After a certain contact time with the third liquid the nascent hollow fiber membrane meets the coagulation bath. This spinning technique has been applied to produce hollow fiber ultrafiltration membranes. The presence of Poly(vinyl pyrrolidone) in the polymer solution is shown to be essential to induce a porous toplayer. Membranes having a water flux of 275 $L.m^{-2}h^{-1}bar^{-1}$ and BSA retention of 97% have been spun. Although more research has to be done the first results seem to be very promising.

## 3.1 Theoretical introduction

In practical applications of ultrafiltration membranes permeabilities are usually low due to low surface porosities and severe fouling tendencies. Several researchers[1] have stated that fouling can be reduced by applying hydrophilic membranes, showing a significant decrease in adsorption of proteins at the membrane surface. In our laboratory Roesink[2] was able to produce phase inversion microfiltration membranes with a hydrophilic character by adding Poly(vinyl pyrrolidone) (PVP) to the polymer solution. In the present investigation hollow fiber ultrafiltration membranes are made from a solution containing poly(ether sulfone) (PES) and PVP.

Membrane formation by immersion precipitation for systems containing PES and PVP have been studied thoroughly by Boom et al.[3]. He showed that the introduction of PVP to the membrane forming system has a profound influence on the morphology of the membrane: macrovoid formation can be suppressed and pores become very well interconnected. PES and PVP are miscible but upon immersion in a water bath PVP starts to move into the water phase. Based on thermodynamic theories Boom found that demixing of these systems is determined by the phase separation of the two polymers. This implies diffusion of PES and PVP relative to each other which is a slow process compared to solvent and non-solvent exchange. Therefore the composition of the polymer solution will become highly unstable without nucleation of a polymer (PES) lean phase taking place. In these systems spinodal demixing occurs and a co-continuous structure is obtained. According to the theory of Boom the interconnectivity of the pores is a result of spinodal demixing of the polymer solution. A more detailed description of the demixing mechanism of PES-PVP systems according to Boom et al.[3] is given in chapter 2.

Cabasso et al.[4] found that PVP enlarges pore size and that addition of PVP is not suitable in preparing membranes with a dense toplayer, like applied for gas separation or pervaporation. Usually membranes prepared with PVP in the solution have no distinct toplayer but pore sizes increase gradually from one side to the other (as can be seen in figure 3b of this chapter).

It is anticipated that the permeability of PES/PVP ultrafiltration membranes should increase substantially when the structure of these membranes consists of a thin selective toplayer and a very porous sublayer. For gas separation membranes starting with a solution of one polymer, it is known[5] that membranes with thin, dense toplayers can be formed if two successive coagulation baths are used. The non-solvent liquid used as the first coagulation medium has been chosen in such a way that the solvent flux out of the polymer solution is high, while the inflow of this non-solvent is very low. Therefore the polymer concentration at the interface is increased. In the second bath phase separation occurs. Due to the high interfacial polymer concentration a thin gas-tight toplayer is formed.

With the new type of spinneret that has recently been developed in our laboratory the dual bath system can be applied in a continuous spinning process for making ultrafiltration membranes[6]. The triplet spinneret has three concentric orifices, a schematic drawing is shown in figure 1. The polymer solution is pumped through the middle opening. The inner orifice is used for the internal coagulation medium or bore liquid. This medium determines the pore structure at the inner (bore) surface and prevents the

fiber from collapse during spinning. The first external coagulation medium is pumped through the outer opening. The three liquid streams are extruded from the spinneret and after a certain contact time they enter a water bath. In this second external coagulation bath the first coagulation medium is replaced by water and coagulation proceeds quickly.

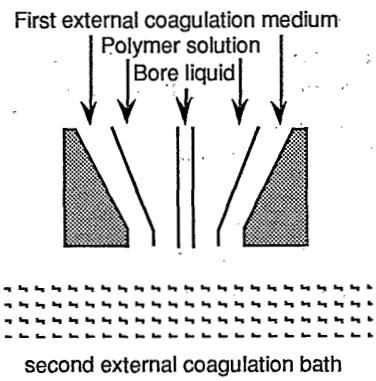


*Figure 1. Triple layer spinneret, schematic drawing. The streams are pumped through the three concentric openings simultaneously. After a certain contact time they enter the second bath where the outer liquid layer is exchanged for a strong non-solvent.*

## 3.2 Materials and methods

### *3.2.1 Materials*

Poly(ether sulfone) (PES) was purchased from ICI (Victrex 5200P). Using GPC the weight average molecular weight was determined at 44,000 g/mole. Two kinds of Poly(vinyl pyrrolidone) (PVP) from Janssen Chimica were used, K90 ($M_w$ 507,000 g/mole) and K30 ($M_w$ 18,000 g/mole). The solvent 1-methyl-2-pyrrolidone (NMP) was purchased from Merck (synthetic grade). Non-solvents were water, 2-propanol, 1-pentanol and dehydrated glycerol. The last three were purchased from Merck (analysis grade).

### *3.2.2 The spinning process*

PES and PVP were dissolved in NMP and water was added. Two different polymer casting solutions were used:

Solution A: PES/PVP(K90)/PVP(K30)/water/NMP 20/5/5/5/65 wt%
Solution B: PES/PVP(K30)/water/NMP 20/10/5/65 wt%

Filtered polymer solutions and liquids used as first coagulation medium were degassed before use. Spinning temperature of the polymer solution was 50 °C, coagulation baths were used at 25 °C. After spinning and coagulation the fibers were rinsed with hot water for two days. Following Roesink[2], excess

PVP was removed by contacting the fibers with a 4,000 ppm sodium hypochlorite solution for 48 hours (see also chapter 4). After rinsing for one more day the fibers were put in a water bath containing 10 wt% glycerol for two days and finally dried at room temperature.

### *3.2.3 Characterization methods*

Membrane morphology was studied using a scanning electron microscope (JEOL, JSM T220A). Water for flux measurements was prefiltered by reverse osmosis. Retentions were measured using either a BSA solution or a PEG solution. BSA ($M_w$ 65,000 g/mole) was purchased from Sigma Chemical company and dissolved in a phosphate buffer solution of pH 7.4, containing 0.1M NaCl. Poly-ethyleneglycol, PEG ($M_w$ 40,000 g/mole) was purchased from Serva. Flux and retention measurements were carried out in a cross-flow filtration setup. Small modules were made containing five fibers with internal diameter of 0.8 mm and external diameter of 1.3 mm and a length of 20 cm. The applied pressure difference was 2 bars and after 30 minutes conditioning time the water flux was almost constant. BSA and PEG concentrations were determined spectrophotometrically.

### *3.2.4 Light transmission measurements for determination of delay times[7]*

For flat membranes delay times were measured using a setup in which a light detector is placed below a coagulation bath and a light source above. The output of the light detector is converted into a recorder signal. The delay time is defined as the time between immersion of the polymer film and the beginning of turbidity in the nascent membrane. The turbidity indicates the onset of precipitation and is detected by a drop in light transmittance through the polymer film.

## 3.3 Results

### *3.3.1 Light transmission*

For polymer solution A, immersed in a number of liquids to be used as the first coagulation bath, delay times have been measured. The coagulation baths are non-solvents for PES but solvents for PVP. The transmittance decrease in time is depicted in figure 2. In all cases delay times were zero, meaning that demixing of the polymer films starts instantaneously after immersion. However the velocity of decrease in transmittance was different for all non-solvents and it increased in the following order:

glycerol < (50 wt% 2-propanol in glycerol) < 1-pentanol < 2-propanol < (20 wt% NMP in water) < water.

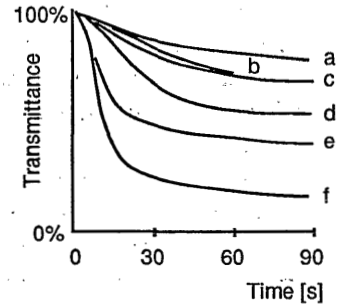


*Figure 2. Transmittance decrease in time for films of polymer solution A immersed in a number of liquids:. a: glycerol, b: 50 wt% 2-propanol in glycerol, c: 1-pentanol, d: 2-propanol, e: 20 wt% NMP in water, f: water.*

### *3.3.2 Spinning of ultrafiltration membranes*

Ultrafiltration membranes have been spun using the triple layer spinneret. For polymer solution A the non-solvents, or mixtures of non-solvents as given in table 1 have been used as a first coagulation medium. Polymer solution, bore liquid and first coagulation medium were pumped through the spinneret. After 0.5 seconds these streams entered a water bath of 20 °C where the first non-solvent was exchanged with water. We tried to use water for both the first and the second bath but in that case the fibers broke during spinning and could not be measured.

Water fluxes and retentions for BSA have been measured for all fibers; values are listed in table 1. For comparison an experiment with a conventional spinneret (tube-in-orifice) is added. In this case the first coagulation medium is air at ambient temperature and a humidity belonging to the water bath of 20 °C underneath ($P^0_{H_2O}$=0.023 bar). After contact with the air the fiber enters into the water bath.

In table 1 it can be seen that the use of 1-pentanol as a first coagulation medium results in a substantially higher flux compared to the flux in case an airgap is used. If glycerol is used water flux is somewhat higher than with an airgap but retention is much lower.

*Table 1. Water flux and BSA retention for hollow fibers spun with different first external coagulation media. Polymer solution A (containing PVP K90 and K30) was used. The contact time of the polymer solution with the first coagulation medium was 0.5 s. In all cases the second external coagulation bath was a water bath of 20 °C. The bore liquid was 80% NMP in water.*

| First external coagulation medium | water flux* [$L.m^{-2}h^{-1}bar^{-1}$] | BSA retention** [%] |
|---|---|---|
| glycerol | 163 | 84 |
| 50 wt% 2-propanol in glycerol | 110 | 63 |
| 1-pentanol | 275 | 97 |
| 2-propanol | 140 | 91 |
| 20 wt% NMP in water | 148 | 94 |
| air*** | 120 | 100 |

* Deviation from mean values for flux measurements is within 10%.

** BSA concentration in the feed solution was 0.1 wt%. Deviation from mean values for retention measurements is within 2%.

*** Spun with normal tube-in-orifice spinneret; instead of a first external coagulation bath the spinning solution passed an airgap before it entered the water bath. In the airgap the humidity depends on the temperature of the water bath underneath (see also chapter 2).

The structure of the toplayer has been studied using SEM. Photographs of two membranes, prepared with 1-pentanol and with air as the first coagulation medium are shown in figure 3. In the case of 1-pentanol the transition from toplayer to porous sublayer is very clear, toplayer thickness is 0.5 μm in this case. Toplayer thickness of the membrane made with the normal tube-in-orifice spinneret is 1 μm and pore sizes in the sublayer are much smaller. The membrane structure in the toplayer consists of polymer spheres. The formation mechanism of this nodular structure is discussed in chapter 6.

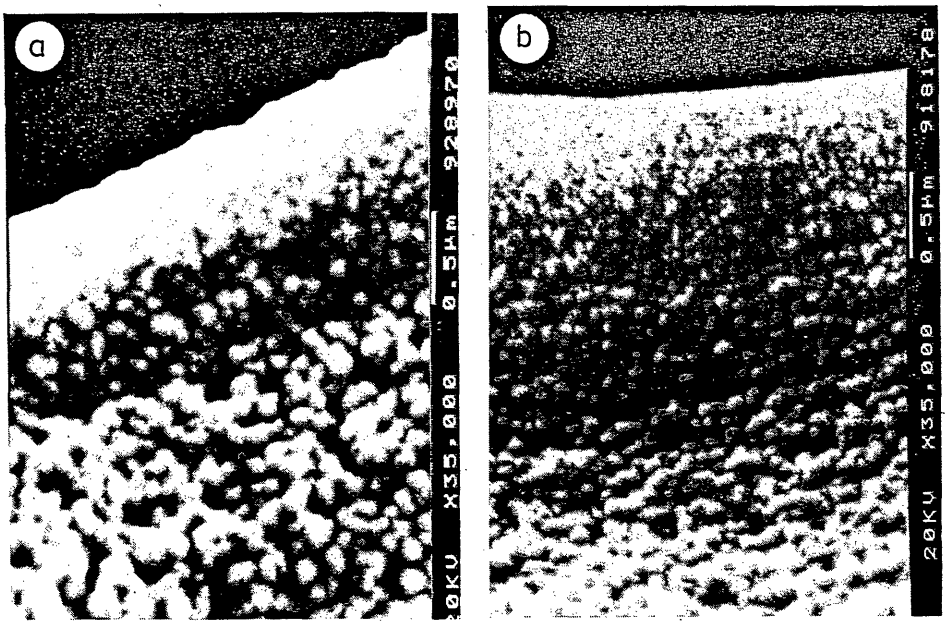


*a)* *b)*

*Figure 3. Toplayer of hollow fiber membranes spun with two different first coagulation media, 1-pentanol (a) and air (b). The second coagulation medium was water.*

In a different set of experiments polymer solution B (containing low molecular weight PVP only) was used also to investigate the influence of the water bath temperature on water flux and retention. The results in table 2 show that water flux is independent of the temperature of the second bath while retention decreases with increasing temperature.

For other ultrafiltration membranes that have a selective toplayer at the inside of the fiber the triple layer spinneret can be used to obtain outer surfaces with large pores. In table 3 pore sizes at the outer surface, as determined from SEM pictures are compared for different coagulation baths.

*Table 2. Influence of the temperature of the water bath, being the second external coagulation bath, on the water flux and the PEG retention. Polymer solution B (containing only PVP K30) was used. The first external coagulation bath was 10 wt% NMP in water, the contact time was 0.5 s. The bore liquid was 80 wt% NMP in water.*

| Temperature of water bath [°C] | water flux* [L.m$^{-2}$h$^{-1}$bar$^{-1}$] | PEG retention** [%] |
|---|---|---|
| 23 | 57 | 99 |
| 43 | 52 | 92 |
| 60 | 66 | 75 |

* Deviation from mean values for flux measurements is within 10%.
** PEG concentration in the feed solution was 0.1 wt%. Deviation from mean values for retention measurements is within 2%.

If the triple layer spinneret is used as in the first two experiments of table 3, pore sizes are considerably larger than in case the normal tube-in-orifice spinneret is used. From the first two experiments of table 3 it can be seen that in this case the temperature of the water bath influences the pore size at the surface. At a higher temperature of this second bath pore size is larger. The three membranes of table 3 are all ultrafiltration membranes with the selective toplayer at the bore side. Therefore water flux of these membranes are almost equal and about 85 L.m$^{-2}$h$^{-1}$bar$^{-1}$.

*Table 3. Water flux and mean pore size at the outer surface of ultrafiltration membranes with the selective toplayer at the inside of the fiber. Polymer solution A (containing PVP K90 and K30) was used. In all cases the nascent membrane entered the second external coagulation bath (water) after 0.5 seconds. The internal coagulation bath was 20 wt% NMP in water.*

| First coagulation medium | temperature of second bath [°C] | pore size [μm] | water flux [L.m$^{-2}$h$^{-1}$bar$^{-1}$] |
|---|---|---|---|
| 80 wt% NMP in water | 25 | 1 | 80 |
| 80 wt% NMP in water | 62 | 5 | 85 |
| air* | 62 | 0.5 | 82 |

* Spun with double orifice spinneret. In the airgap the humidity depends on the temperature of the water bath underneath (see also chapter 2).

### 3.4 Discussion

In the systems investigated here no delay of demixing was found. This is due to the presence of PVP in the polymer solution. Delay times for a PES solution without PVP have been measured by Van 't Hof[5]. They were strongly dependent on the non-solvent used and could be very large, e.g. 1200 seconds for glycerol.

The slopes of loss in transmittance for the different non-solvents as found by us have the same sequence as the delay times measured by van 't Hof[5]. This means that even though in all cases the polymer solution starts to demix immediately the demixing *rate* depends on the non-solvent used.

For gas-separation membranes a certain contact time with the first coagulation medium (with finite delay time) is necessary in order to sufficiently increase the polymer concentration in the toplayer. In the PVP containing systems as discussed here the polymer solutions demix instantaneously when brought in contact with the first coagulation medium. Thus the first coagulation medium affects the membrane formation process in two ways:
- the polymer concentration in the toplayer of the nascent membrane is increased
- in the toplayer immediately pore formation starts.

In the second bath the strong coagulant water is used and the structure in the toplayer is fixed rapidly hindering further growth of pore sizes.

From this it is clear that to obtain small pores in the toplayer which will be generated in the first coagulation medium growth of pores should be slow or has to be stopped rapidly. In order to obtain a selective toplayer either one or both of the following conditions have to be fulfilled:
- the nucleus growth process has to be slow
- the contact time with the first coagulation medium has to be short.

A thin toplayer is obtained if the demixing front does not penetrate deeply into the polymer film during its contact with the first coagulation medium. This also implies a short contact time between polymer solution and coagulation medium.

Below the toplayer demixing will start when the fiber has entered the water bath. In the sublayer the length of the diffusion path between demixing front and coagulation bath is larger and the densified toplayer will form a barrier slowing down the flux of solvent and non-solvent. Thus compared to the interface more solvent is present. Also in the sublayer the polymer concentration is lower as it has not been increased in the first coagulation

medium. Because of the presence of PVP, in the sublayer instantaneous demixing takes place according to the spinodal mechanism as proposed by Boom et al.[3]. According to the theory of spinodal demixing the relatively high solvent concentration in the sublayer will lead to a structure consisting of large interconnected pores.

In the experiments shown in table 1 the contact time in the first liquid layer was 0.5 seconds in all cases. For glycerol with a slow demixing rate a high retention membrane would be expected. However the best result was found for 1-pentanol as the first coagulant. This discrepancy is due to a different effective contact time with the first coagulation medium. In all cases the polymer solution entered the second bath after 0.5 seconds. In the case of glycerol mixing with water is slow due to the high viscosity of glycerol (0.945 Pa.s) and glycerol remains in contact with the fiber for a significantly longer time. The effective residence time was therefore much longer (after 30 seconds it could still be seen that glycerol was removed from the surface of the fiber). During this contact time the nuclei grow and the demixing front penetrates more deeply into the polymer solution resulting in a rather thick toplayer with moderate retention for BSA. On the contrary pentanol is only slightly miscible with water and has a lower density than water. As soon as the polymer solution entered the water bath pentanol was removed from the surface and floated on top of the water bath. The effective residence time of pentanol was therefore little more than 0.5 seconds.

Compared to the conventional spinneret the triple layer spinneret can lead to membranes with better performances. But as shown here, the type of the first coagulation medium and the contact time with this liquid layer are very important parameters that have to be investigated more thoroughly.

As said before the structure of the toplayer has to be fixed rapidly in the second bath. Water is a strong coagulant and therefore very suitable for this purpose. If the temperature of the water bath is increased membranes are obtained with lower retentions. This indicates that at higher temperatures more growth of the nuclei takes place, resulting in larger pores. The water fluxes of these membranes are almost equal and lower than the values shown in table 1. The reason for this is a bad interconnectivity of the pores. These membranes are made from polymer solution B containing only the low molecular weight PVP. The influence of this type of PVP on the demixing process is not profound enough to ensure the formation of a co-continuous structure in the membrane. Experiments presented in the appendix of this thesis[8] as well as the theory of Boom[3] indicate that a minimum amount of PVP with a high enough molecular weight is necessary

for the formation of a co-continuous structure.

With this triple layer spinneret it is also possible to obtain microporous toplayers as shown in table 3. The high solvent content in the first coagulation medium used here causes a low outdiffusion of solvent. Therefore the polymer concentration in the toplayer will remain low. As was mentioned before a low polymer concentration results in a structure with large pores. For ultrafiltration membranes with the selective toplayer at the bore side of the fibers the new spinneret has no positive influence on flux or retention. However there are some other advantages of using a liquid layer over that of an airgap. A liquid bath is not as much influenced by environmental conditions as an airgap. Secondly in the case of an airgap the temperature of the water bath has to be far above room temperature to obtain pore sizes in the micrometer range. From these results the triple orifice spinneret seems to be a promising tool for spinning microfiltration membranes but more research on this subject has to be done.

## 3.5 Conclusions

The experiments described in this chapter indicate that the dual bath system using a triple layer spinneret is a suitable technique for the spinning of hollow fiber ultrafiltration membranes. The addition of PVP to the polymer solution is essential to induce demixing in the first coagulation medium. For a polymer solution without PVP no porous toplayer would be obtained when using these coagulation media. The selection of the type of liquid and the effective contact time of the polymer solution with the first coagulation medium are important parameters. Using 1-pentanol as the first external coagulation bath and water as the second bath, high flux membranes can be prepared showing good retention for BSA. For membranes with the selective toplayer at the bore side of the fiber this spinning technique can be used to produce pore sizes at the outer surface of up to 5 μm.

## 3.6 Literature

1. *a)* L.E.S. Brink, D.J. Romijn, Reducing the protein fouling of polysulfone surfaces and polysulfone ultrafiltration membranes: Optimization of the type of presorbed layer, Desalination, 78 (1990) 209
*b)* G. Capannelli, A. Bottino, V. Gekas, G. Tragardh, Protein fouling behavior of ultrafiltration membranes prepared with varying degrees of hydrophilicity, Proc. Biochem. Int., December (1990) 221
*c)* A.S. Jonsson, B. Jonsson, The influence of nonionic and ionic surfactants on hydrophobic

and hydrophilic ultrafiltration membranes, J. Mem. Sci., 56 (1991) 49

2. H.D.W. Roesink, Microfiltration, membrane development and module design, Thesis Univ. of Twente, the Netherlands, 1989.
3. *a)* R.M. Boom, Th. van den Boomgaard, C.A. Smolders, Equilibrium thermodynamics of a quaternary membrane forming system with two polymers. I. Theory, submitted for publication to Macromolecules
   *b)* R.M. Boom, H.W. Reinders, H.H.W. Rolevink, U. Cordilia, Th. van den Boomgaard, C.A. Smolders, Equilibrium thermodynamics of a quaternary membrane forming system with two polymers. II. Experimental, submitted for publication to Macromolecules
   *c)* R.M. Boom, Th. van den Boomgaard, C.A. Smolders, Mass transfer and thermodynamics during immersion precipitation for a two polymer system: Evaluation with the system PES-PVP-NMP-water, submitted for publication to J. Mem. Sci.
   *d)* R.M. Boom, S. Zanic, Th. van den Boomgaard, C.A. Smolders, Membranes from PES and PVP: Membrane morphology and its relation to the formation mechanism, submitted for publication to J. Mem. Sci.
   *e)* R.M. Boom, H.H.W. Rolevink, Th. van den Boomgaard, C.A. Smolders, Membranes prepared from PES and PS: Comparison with the PES-PVP system, submitted for publication to J. Mem. Sci.
   *f)* R.M. Boom, Th. van den Boomgaard, C.A. Smolders, Metastable demixing phenomena by thermal quench experiments. I. Theory, submitted for publication to J. Appl. Pol. Sci.
   *g)* R.M. Boom, S. Rekveld, U. Cordilia, Th. van den Boomgaard, C.A. Smolders, Metastable demixing phenomena by thermal quench experiments. II. The systems PES-NMP-water and PES-NMP-PVP-water, submitted for publication to J. Appl. Pol. Sci.
4. I. Cabasso, E. Klein, J.K. Smith, Polysulfone hollow fibers. II. Morphology, J. Appl. Pol. Sci, 21 (1977) 165.
5. J.A. van 't Hof, A.J. Reuvers, R.M. Boom, H.M.M. Rolevink, C.A. Smolders, Wet spinning of asymmetric gas separation membranes with high selectivity by a dual-bath coagulation method, J. Mem. Sci., 70 (1992) 17
6. *a)* G.H. Koops, S. Li, Het spinnen van asymmetrische holle vezelmembranen met een dichte niet-poreuze toplaag en een poreuze onderlaag, resp. met zowel een poreuze toplaag als een poreuze onderlaag, Dutch Patent 91.02151
   *b)* S. Li, G.H. Koops, M.H.V. Mulder, Th. van den Boomgaard, C.A. Smolders, Wet spinning of asymmetric hollow fibers with a new type of spinneret, to be published.
7. A.J. Reuvers, C.A. Smolders, Formation of membranes by means of immersion precipitation. Part II. The mechanism of formation of membranes prepared from the system CA/acetone/water, J. Mem. Sci., 34 (1987) 67
8. Appendix to this thesis, also published: R.M. Boom, I.M. Wienk, Th. van den Boomgaard, C.A. Smolders, Microstructures in phase inversion membranes, Part II. The role of a polymeric additive, J. Mem. Sci., 73 (1992) 277

4

# Post Treatment of PES/PVP Membranes for Ultrafiltration

I.M. Wienk, E.E.B. Meuleman, Th. van den Boomgaard, C.A. Smolders

## Summary

The treatment of ultrafiltration membranes after spinning the hollow fibers is investigated. The membranes consist of a blend of polymers poly(ether sulfone) (PES) and poly(vinyl pyrrolidone) (PVP). It is shown that pure water flux and retention for BSA are dependent on the temperature of the rinsing bath. Simply drying the membranes results in collapse of the porous structure. This can be prevented by impregnating the membranes with glycerol before the drying step. During membrane formation PVP is trapped in the PES matrix. Tails of the hydrophilic polymer are present in the pores and swell in water resulting in a low permeability of the membrane. The water flux can be increased by removing part of the PVP polymer using hypochlorite. An alternative way to obtain an ultrafiltration membrane with a hydrophilic character is to incorporate a crosslinked hydrogel in the pores of a microfiltration membrane. Some preliminary results of this method are presented.

## 4.1 Introduction

Hollow fiber ultrafiltration membranes have been spun from a blend of two polymers poly(ether sulfone) (PES) and the water soluble polymer poly(vinyl pyrrolidone) (PVP) as was described in chapters 2 and 3[1]. It has been found that PVP influences the phase separation behavior of the polymer solution to a large extent, hence the ultimate morphology of the membranes[2]. Phase separation involves the diffusion of PVP from a polymer rich phase towards a polymer lean phase that contains no PES[3,4]. The polymer (PES) lean phase will be the pores of the ultimate membrane. Characterization of the composition of the membranes as is presented in chapter 5 shows that a certain part of the polymer remains in the PES matrix. The idea is that the

hydrophilic polymer is trapped in the PES matrix and that polymer tails of PVP are present in the pores of the membrane[4]. The total amount of PVP in the membrane is low but the concentration of this polymer at the surface is not negligible (see chapter 5). The presence of PVP in the pores of the toplayer of the ultrafiltration membranes causes swelling of the porous structure in water resulting in a very low flux. A special treatment after spinning is necessary to increase the permeability of the membranes. A very suitable method to increase the water flux of membranes containing PVP is a chemical treatment with hypochlorite as was also used by Roesink et al.[4,5]. The effect of this treatment on the performance of PES/PVP membranes is shown. Also rinsing of freshly spun membranes with water and the effect of uncontrolled drying on the flux are discussed.

Apart from this study on the post-treatment of ultrafiltration membranes a new method for modifying the pore size of a microfiltration membrane is presented. A crosslinked hydrogel is incorporated into a microfiltration membrane with the aim of decreasing its pore size, thereby making it suitable for ultrafiltration applications.

## 4.2 Theoretical background

### *4.2.1 Drying of porous structures*

It is generally known that the porous structure of ultrafiltration membranes may collapse upon drying. The collapse is the result of capillary forces acting on the membrane matrix. The morphology in the toplayer of ultrafiltration membranes consists of nodular structures as is shown in chapters 5 and 6. Therefore the collapse of pores can be considered as the fusion of these polymeric spheres. A similar process, namely the formation of a dense polymer film by drying of a polymer dispersion, was studied by Brown[6]. Brown stated that the coalescence of the spheres is determined by two counteracting forces. The capillary force resulting from the presence of a liquid between the particles promotes the fusion process whereas the fusion is hindered by the resistance of the spheres to deformation. To obtain a good polymer film the capillary force has to exceed the resisting force for deformation. To prevent the collapse of porous structures the opposite has to be true. The capillary force is equal to the pressure times the pore area, $F_c=P*A$.

The pressure is given by Laplace relation:

$$\Delta P = 2*(\gamma / r)*\cos\theta \qquad (1)$$

in which: $\Delta P$ = pressure difference [Pa]
$\gamma$ = surface tension of the liquid in the pores [N/m]
r = pore radius [m]
$\theta$ = contact angle [ °]

According to Brown the force necessary for deformation of two spheres when pressed together is given by: $F_d=0.12*E*A$. E is the tensile modulus of the polymer material. Collapse of a porous structure will not occur if $F_c < F_d$ thus if:

$$E > (2*\gamma*\cos\theta)/(0.12\ r) \qquad (2)$$

in which E=tensile modulus [$N/m^2$].

### *4.2.2 Hypochlorite treatment to decrease the swelling of membranes containing PVP*

Roesink et al.[5,6] were able to increase the permeability of membranes containing PVP by treating them with hypochlorite. These authors developed hollow fiber microfiltration membranes from the blend poly-etherimide (PEI) and poly(vinyl pyrrolidone) (PVP). The water flux of these membranes did not correspond to the pore structure as was found using a scanning electron microscope. The discrepancy was caused by swelling of the water soluble PVP present in the pores during the water flux measurements. Roesink found that the swelling behavior could be diminished by placing the membranes in a 4000 ppm sodium hypochlorite (NaOCl) solution for 48 hours. After this treatment the water flux was in agreement with the pore size and porosity. The reason for the flux increase was a decrease of PVP concentration in the membranes as could be measured by NMR. Although part of the PVP was removed by the chemical treatment the membranes were still wettable with water. Two possible reasons for the selective removal of PVP by reaction of the membrane material with hypochlorite were proposed:

- chain scission of PVP decreases its molecular weight thereby increasing its mobility and diffusion out of the membrane matrix.
- ring opening of the pyrrolidone ring of PVP changes the specific interaction of this polymer with PEI thereby facilitating the removal of PVP by rinsing with water.

According to Roesink removal of PVP from the membranes by means of hypochlorite treatment was mainly due to ring opening of the pyrrolidone

ring.

*4.2.3 Alternative post treatments to obtain high flux ultrafiltration membranes*

An alternative method to diminish the swelling of the membrane material is crosslinking of PVP. In a three dimensional network the mobility of the PVP molecules is restricted and thereby also their ability to swell in water. PVP can be chemically crosslinked using an inorganic persulfate[7,8] or hydrazine and hydrogen peroxide[9]. Crosslinking is also possible by means of gamma irradiation[10,11], UV radiation[12] or by a heat treatment[4]. Another method to obtain crosslinked PVP is simultaneously polymerizing and crosslinking monomers of PVP N-vinylpyrrolidone[13-15].

The mechanism of chemically crosslinking PVP using potassium persulfate ($K_2S_2O_8$) as a radical initiator is shown in scheme 1[7]. A hydrogen atom is abstracted from the tertiary carbon atom of the PVP molecule. The radical thus formed can form a stable covalent crosslink with a radical of another PVP molecule. Other possible rearrangements of the radical are:
- intramolecular crosslinking, giving rise to ring formation
- chain scission via disproportionation in the neighbourhood of the unpaired electron
- oxidative degradation (if oxygen is present).

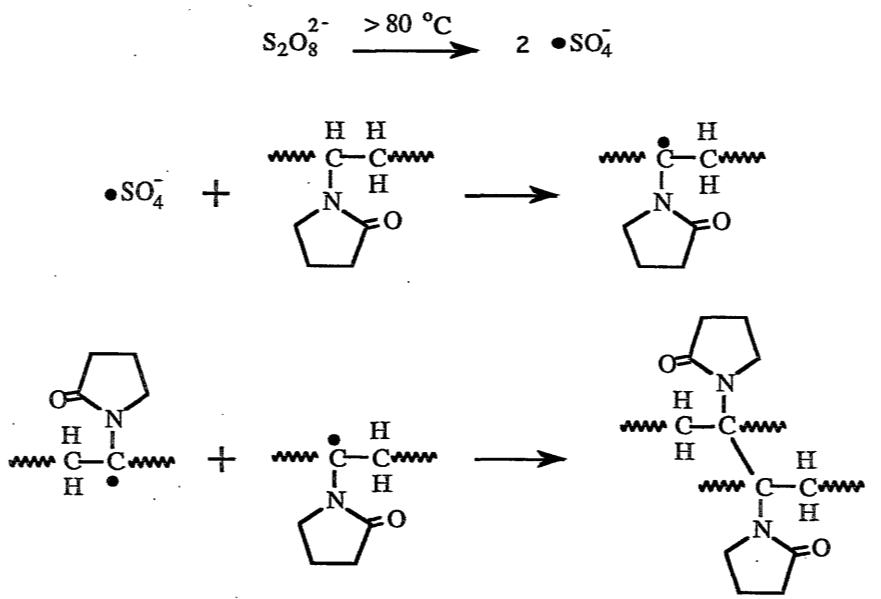

*Scheme 1. Mechanism for the crosslinking reaction of PVP by persulfate ($K_2S_2O_8$) according to Anderson et al.[7].*

Roesink[4] successfully crosslinked PVP in microfiltration membranes by employing a heat treatment at 150°C and atmospheric pressure. This method is not applicable to ultrafiltration membranes because during drying capillary forces will destroy the porous structure. Roesink also tried to chemically crosslink PVP by using persulfate. However for microfiltration membranes this did not lead to a sufficient increase in water flux.

A different approach to deal with the swelling behavior of PVP is adjusting the swelling in such a way that the membrane has the desired pore size when it is in the swollen state. If it is possible to incorporate a PVP hydrogel on the pore walls of a microfiltration membrane, swelling of this gel will decrease the pore size thereby making the membrane suitable for ultrafiltration applications. The swollen PVP gel will improve the hydrophilic character of the membrane surface and if its permeability for water is high the gel might also contribute to the water flux.

From literature[16-18] it is known that the hydrophilicity of hydrophobic membranes can be increased by coating the surface with a water-soluble polymer after which the coating layer is insolubilized by crosslinking. In these situations also a decrease in pore size is observed. Stengaard[16] treated polyvinylidene fluoride (PVDF) ultrafiltration membranes with a solution of hydroxyalkylcellulose containing NaOH. The cellulose was crosslinked during a heat treatment at 150 °C. This surface modification procedure improved the ability of the membrane to be wetted and increased the flux through the membrane when filtering skimmed milk.

In this chapter some preliminary experiments are described with the aim of obtaining a PVP hydrogel in the pores of a microfiltration membrane. The membrane is impregnated with a PVP solution containing persulfate. Crosslinking of PVP takes place at 90°C.

## 4.3 Materials and methods

### *4.3.1 Materials*

Poly(ether sulfone) (PES) was purchased from ICI (Victrex 5200P. $M_w$ 44,000 g/mole). Two different types of poly(vinyl pyrrolidone) (PVP) from Janssen Chimica were used, K90 ($M_w$ 507,000 g/mole) and K30 ($M_w$ 18,000 g/mole). The weight average molecular weights of the polymers were determined using GPC. The solvent 1-Methyl-2-pyrrolidone (NMP) was purchased from Merck (synthetic grade). The non-solvent was water. The structural formulae of these materials are shown in figure 2.

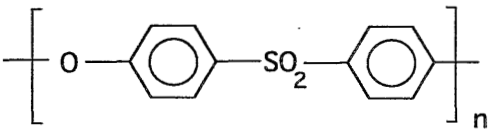


poly(ether sulfone) (PES)

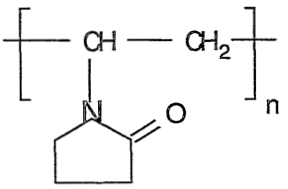


poly(vinyl pyrrolidone) (PVP)

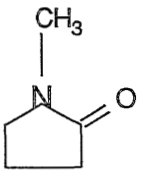


N-methylpyrrolidone (NMP)

*Figure 2. Structure formulae of the materials used for membrane preparation.*

### *4.3.2 Membranes*

To study the influence of temperature of the rinsing bath on the performance of the membranes, polymer solution A was used consisting of 20 wt% PES, 10 wt% PVP(K90) and 5 wt% water in NMP. The effect of drying as well as the hypochlorite treatment were studied using ultrafiltration membranes prepared from polymer solution B consisting of 20 wt% PES, 5 wt% PVP(K90), 5 wt% PVP(K30) and 5 wt% water in NMP. The microfiltration membranes used were kindly supplied by X-flow BV. (X-flow mf02 1.5/2.5). This PES/PVP membrane has the selective toplayer at a bore side of the fiber. Pore sizes are between 0.06 μm and 0.1 μm as determined with a gas-liquid displacement measurement (Coulter porometer).

### *4.3.3 Post treatment of the membranes*

The general procedure applied in this thesis of treating the membranes after the spinning of the fibers is given here. Unless mentioned otherwise fibers were rinsed in a water bath of 50 °C for two days. After this the fibers were placed in a hypochlorite bath containing 4000 ppm NaOCl (Chemproha, technical quality, 15% activity) for 48 hours. The hypochlorite was removed by rinsing the fibers with water for one day at 50 °C. Next the fibers were placed in a glycerol bath containing 10 wt% glycerol (Merck) in water for one day. After this the membrane fibers were dried in air.

*4.3.4 Preparation of a hydrogel in the pores of microfiltration membranes*

PVP (K90) was dissolved in water after which potassium persulfate ($K_2S_2O_8$ Merck pro analyse) was added to obtain a solution containing 5 wt% persulfate and 5, 7.5 or 10 wt% PVP in water. A volume of 200 ml of the PVP/$K_2S_2O_8$ solution was flushed through the bore of a dry membrane fiber at a pressure difference of 0.5 bar. Part of the solution penetrated the porous structure of the membrane. When all the solution had passed the bore excess solution was removed from the bore by applying a gas stream. After this the fibers were placed in an oven circulated with nitrogen gas at 90 °C. The residence time in the oven was 16 hours. Before the fibers were used for the pure water flux measurements they were placed in a water bath for two days.

*4.3.5 PVP content of the membranes*

The PVP concentrations in the films were measured using micro element analysis (MEA). For this method the polymer is completely oxidized at 1800 °C. By gas chromatography of the reaction products the amount of C, H, N and S can be determined. The PVP content is expressed as partial weight percentage of the total polymer content and was calculated as follows:

$$[PVP]\,(wt\%) = \frac{[N]\,(mol\%) * Mw\,(PVP\ monomer)}{[N]\,(mol\%) * Mw\,(PVP\ monomer) + [S]\,(mol\%) * Mw\,(PES\ monomer)} * 100\%$$

Before the membranes were analysed using MEA they were dried in a vacuum oven at 80 °C for 6 weeks. It was assumed that in this drying step all residual solvent was removed.

*4.3.6 Characterization methods*

Membrane morphology was studied using a scanning electron microscope (JEOL, JSM T220A). Water for flux measurements was prefiltered by reverse osmosis. Bovine Serum Albumin (BSA) was used for the retention measurements. BSA (No A2153, fraction V, 96-99% albumin, $M_w$ 65,000 g/mole) was purchased from Sigma Chemical company and dissolved in a phosphate buffer solution of pH 7.4, containing 0.1M NaCl. The BSA solutions were prefiltered using a 0.2 μm filter. Flux and retention measurements were carried out in a cross-flow filtration set-up. The applied pressure difference was 2 bars and after 30 minutes water flux was measured which was practically constant after this conditioning time. BSA concentrations were determined spectrophotometrically at 280 nm.

## 4.4 Results and Discussion

*4.4.1 Washing of the freshly spun membranes with water.*

Hollow fibers were spun using polymer solution A and a triple orifice spinneret giving a toplayer at the outside fiber surface. Demixing of the polymer solution started in the first coagulation medium which was 20 wt% NMP in water. After 0.5 second the nascent membrane entered the second coagulation medium, a water bath, where demixing proceeded. The residence time in this second bath was 30 seconds. Then the fibers were transferred to a rinsing set-up to flush them with water for two days. A more detailed description of the spinning procedure is given in chapter 3[1]. To study the effect of rinsing on the performance of the membranes different temperatures of the second bath and the rinsing bath were used. After that the membranes were treated with hypochlorite and placed in a glycerol bath before they were dried in air. The results of the water flux and retention measurements are shown in figure 3.

It can be seen that a higher temperature of the water bath, either the second bath or the rinsing bath, resulted in a membrane with a higher water flux and a lower retention. This is because at a higher temperature diffusion coefficients are larger and the vitrification of the membrane is retarded. Phase separation will therefore be both faster and longer resulting in a membrane with larger pores. In chapter 6 it is shown that the formation of pores in the toplayer involves disentanglement of polymer chains. The effect of the temperature of the rinsing bath is larger when the temperature of the second bath is higher. If the nascent membrane is contacted with a high temperature water bath the vitrification is not completed in this bath and therefore the influence of the temperature of the rinsing bath is larger.

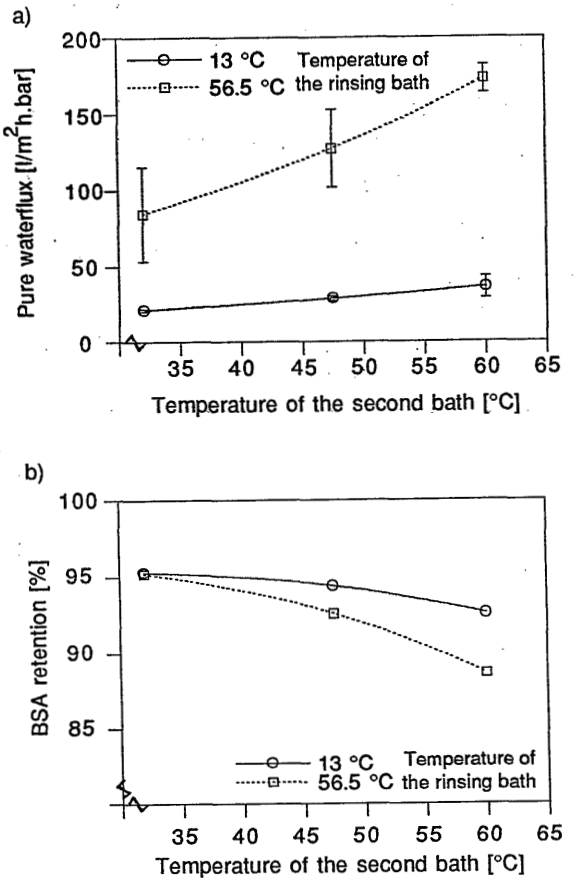


*Figure 3. Performance of membranes plotted as a function of the temperature of the second coagulation bath for two temperatures of the rinsing bath. The first coagulation bath consisted of 20 wt% NMP in water. Contact time of the nascent membranes was 0.5 s with the first bath, 30 seconds with the second (water) bath and 2 days with the rinsing bath. a) pure water flux, b) retention for a BSA solution containing 0.5 g/l BSA.*

As is explained in chapter 2 the high molecular weight additive PVP diffuses from the polymer solution towards the coagulation media. The reason for the presence of part of the PVP polymer in the ultimate membrane is that the vitrification of the membrane is reached before all PVP molecules were able to diffuse out of the polymer matrix. Thus at membrane formation conditions that rapidly lead to vitrification of the membrane the amount of PVP trapped is larger. This was also found experimentally as it is shown in table 1 where the amount of PVP in the membrane is given for membranes

prepared at different temperatures. Since the PVP content was determined after treatment of the membranes with a hypochlorite solution, the amount of PVP was lower than it was after washing.

*Table 1. The amount of PVP expressed as weight percentage of the total polymer content for the membranes of figure 1. In the spinning experiments the temperature of the second coagulation bath and the temperature of the rinsing bath were varied. The first coagulation bath was 20 wt% NMP in water. The PVP content of the polymer solution was 33%. PVP content was determined after treatment of the membranes with the hypochlorite solution.*

| Temp. second bath [°C] | Temp. rinsing bath [°C] | PVP/PVP+PES [%] |
|---|---|---|
| 32 | 13 | 2.7 |
| 47.5 | 13 | 1.8 |
| 60 | 13 | 1.3 |
| 32 | 56.5 | 1.4 |
| 47.5 | 56.5 | 1.2 |
| 60 | 56.5 | 0.7 |

### *4.4.2 Drying of ultrafiltration membranes*

Hollow fiber membranes spun from solution B were dried in air at room temperature from three solutions namely water, hexane and a mixture of 10 wt% glycerol in water. After drying the membranes permeabilities were measured for nitrogen gas, hexane and water. The experiments were performed for untreated membranes and membranes treated with a hypochlorite solution. The results are shown in table 2. Because hexane and water are not miscible an ethanol bath was always used between the flux measurements to remove hexane from the pores.

Although the data in table 2 are not very consistent a few trends can be seen. The membranes dried from air or hexane have very low permeabilities indicating that collapse of the porous structure has occurred. Drying from a glycerol/water bath is therefore the best method. The membranes treated with hypochlorite have a significantly higher permeability which justifies the use of hypochlorite. On the whole the permeability of the membranes for hexane is higher than for water. This is due to swelling of PVP which is lower in hexane than in water.

*Table 2. Permeabilities for nitrogen gas, hexane and water of hollow fiber membranes after different post-treatments. 1: membranes not treated with hypochlorite. 2: membranes treated with 4000 ppm NaOCl for 48 hours. A: drying the water filled membrane in air. B: displacement by a sequence of water, ethanol and hexane, followed by drying in air. C: drying the membrane filled with 10 wt% glycerol in water in air.*

| number | drying liquid | nitrogen gas flux [$*10^3$ l.m$^{-2}$h$^{-1}$bar$^{-1}$] | hexane flux [l.m$^{-2}$h$^{-1}$bar$^{-1}$] | water flux [l.m$^{-2}$h$^{-1}$bar$^{-1}$] |
|---|---|---|---|---|
| *no hypochlorite treatment* | | | | |
| 1A | water | 0 | 0 | 0 |
| 1B | hexane | 35 (18)* | 39 (30) | 2 (1) |
| 1C | glycerol | n.d. | 3 (2) | 22 (4) |
| *hypochlorite treatment* | | | | |
| 2A | water | 4 (1) | 50 (31) | 14 (2) |
| 2B | hexane | 45 (13) | 63 (25) | 13 (1) |
| 2C | glycerol | n.d. | 483 (84) | 217 (20) |

* numbers between brackets are deviations from mean values.
n.d.: not determined.

The collapse phenomena during drying can be quantified using equation 2. PES is a glassy polymer and the tensile modulus $E=3.2*10^9$ N/m$^2$ at room temperature[19]. The surface tension and boiling temperature of the drying liquids used are given in table 3. With these data, and assuming that $\cos\theta = 1$, a critical pore diameter can be calculated. Pores with a diameter smaller than the critical diameter will collapse upon drying the membrane at room temperature and atmospheric pressure.

*Table 3. Surface tension at room temperature (20 °C), boiling temperature of the drying liquids used and the critical pore diameter for collapse of porous structures of PES.*

| liquid | surface tension $\gamma$ [mN/m] | boiling temperature [°C] | critical pore diameter [nm] |
|---|---|---|---|
| water | 73 | 100 | 0.7 |
| glycerol | 63 | 290 (decomposes) | 0.6 |
| hexane | 18 | 68 | 0.2 |

From the critical pore diameters given in table 3 it can be concluded that the porous structure of ultrafiltration membranes having pores larger than 1 nm will not be destroyed by drying. The pore sizes of the PES/PVP membranes are between 10 and 50 nm as was determined with the liquid displacement method (chapter 5). Thus from these calculations no collapse would be expected. However this does not correspond with the measured permeabilities after drying as shown in table 2. Probably the tensile modules of the PES membrane material is lower than the value given in literature. When PES membranes were studied with the atomic force microscope as is shown in chapter 5 it was found that structural changes occurred at a probing force of 20 nN. This force works on half the surface of a nodule with a diameter of 50 nm. The pressure is then $2*10^7$ N/m$^2$ and the critical diameter is 60 nm for water and 15 nm for hexane. Using these data, the low permeability after drying porous structures with initial pore sizes up to 50 nm can be explained. The resistance against deformation of the PES membranes as measured with the atomic force microscope is lower than the literature value which might be due to the loose packing of the molecules or to the presence of residual solvent acting as a plasticizer.

The best liquid for drying ultrafiltration membranes is glycerol or a mixture of glycerol and water. The reason for this is not the surface tension but because glycerol is a non-volatile liquid. It is also very hygroscopic and will therefore withhold some water in the membranes. Correctly speaking membranes are not *dried* from glycerol. It would be better to refer to this state as membranes stored with glycerol in the pores.

### *4.4.3 Hypochlorite treatment*

The effect of the hypochlorite treatment on the performance of membranes containing PVP has been studied extensively by Roesink[4]. The type of membranes studied here are comparable but not identical to the PEI/PVP microfiltration membranes used by Roesink. Therefore a few experiments have been performed to verify whether the hypochlorite treatment affects PES/PVP ultrafiltration membranes in the same manner as the PEI/PVP microfiltration membranes studied by Roesink.

PES/PVP ultrafiltration membranes were treated with a 4000 ppm hypochlorite solution. The residence time of the membrane fibers in the hypochlorite bath was varied. The pure water flux and retention for 1 g/l BSA solution of the membranes were measured and the results are shown in figure 4. It can be seen that the water flux increases when the residence time in the hypochlorite bath is longer while the retention is not affected. These results are consistent with the theory of Roesink explaining that the hypochlorite treatment merely reduces the swelling of PVP in the pores of

the membranes without substantially altering its pore structure.

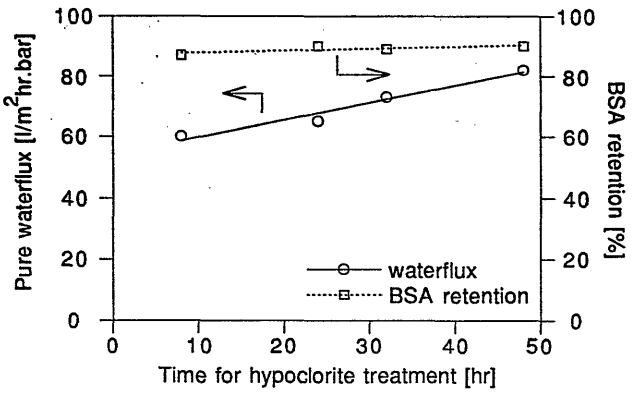


*Figure 4. Pure water flux and retention for a 1 g/l BSA solution of PES/PVP ultrafiltration membranes treated with a 4000 ppm hypochlorite solution for different times.*

The amount of PVP present in the ultrafiltration membranes was determined using MEA. In table 4 it can be seen that due to the hypochlorite treatment the PVP content of the membranes is lowered. The results indicate that PVP can be removed selectively from the membranes due to reaction of the membrane material with hypochlorite. The mechanism of the reaction between PVP and hypochlorite is discussed in the appendix of this chapter. The reaction of PVP with hypochlorite causes chain scission of PVP molecules. The removal of PVP tails present in the pores of the membrane is facilitated due to the decrease of the polymer its molecular weight. The membrane forming polymer PES is fairly resistant to treatment with a hypochlorite solution.

*Table 4. PVP content of the membranes as determined using MEA for membranes treated with a 4000 ppm hypochlorite solution for different times. The hollow fiber membranes have been spun using polymer solution B. PVP concentration of the polymer solution was 33 wt% of the total polymer content.*

| hypochlorite treatment [hr] | PVP/PVP+PES [wt %] |
|---|---|
| 8 | 2.3 |
| 24 | 1.3 |
| 32 | 1.2 |
| 48 | 1.1 |

### *4.4.4 Incorporation of a PVP hydrogel into a microfiltration membrane*

Preliminary experiments were performed to incorporate a PVP hydrogel into a PES/PVP microfiltration membrane. The bore of the hollow fiber microfiltration membrane was flushed with a solution of PVP and persulfate in water and after removal of the liquid in the bore of the fiber, followed by a heat treatment at 90 °C for 16 hours. In the oven the membranes are dried while PVP is crosslinked. The mechanism for crosslinking of PVP using $K_2S_2O_8$ is shown in scheme 1. In the experiments the concentration of PVP in the solution was varied. After crosslinking the fibers were placed in a water bath for two days to verify that swelling of the hydrogel did not destroy the membrane structure. After that the pure water flux of the membranes was determined (water flux 1). The results show (table 5) that a strong decrease of flux is observed after introduction of the hydrogel. The water flux is lower when more PVP is used in the gel forming solution. The dry-wet reversibility of the membranes was studied by drying the fibers after the first water flux measurement followed by a second determination of the water flux (water flux 2 in table 5). It can be seen that after drying the water flux has increased with a factor of two. The water fluxes shown in table 5 were measured after 30 minutes of pure water filtration.

*Table 5. Pure water flux of microfiltration membranes after penetration of a PVP solution and crosslinking of PVP by a heat treatment using persulfate. All solutions contained 5 wt% $K_2S_2O_8$ but different concentrations of PVP. Before water flux 1 was measured fibers were placed in a water bath for two days. After flux measurement 1 the membranes were dried in a vacuum oven overnight. Then water flux 2 was measured. Water fluxes were measured after 30 minutes of filtration.*

| PVP concentration wt% | water flux 1 [$l.m^{-2}h^{-1}bar^{-1}$] | water flux 2 [$l.m^{-2}h^{-1}bar^{-1}$] |
|---|---|---|
| 0.0 | 188 (80)* | 151 (100) |
| 5.0 | 20 (10) | 42 (14) |
| 7.5 | 16 (4) | - |
| 10.0 | 10 (4) | 26 (15) |

* numbers between brackets are deviations from the mean values

For the 10 wt% PVP solution the water flux was also measured during a longer period of time. It was found that the water flux was increased with 20 % after a filtration time of 7 hours. Also the weight increase of the membranes has been measured. After incorporation of the hydrogel the mass per centimeter length compared to the untreated membrane was increased by 37%. Upon water filtration for 7 hours and drying the membranes in a vacuum oven the mass increase (compared to the untreated membrane) was only 5%. Hence almost all of the mass increase disappeared during filtration.

The results of the flux experiments can be explained by the different structure of the membranes. In figure 5 the morphology of the treated membranes before and after filtration is compared with the original membrane structure. For the membranes treated with a 5 wt% PVP solution deposits were found at the bore surface (white structures in figure 5b). After filtration these deposits have disappeared and a porous structure is visible (figure 5c). The structure is caused by $K_2SO_4$ or $K_2S_2O_8$ as could be confirmed using energy dispersive X-ray spectroscopy (EDS). Potassium sulfate is formed after the crosslinking reaction and precipitated due to evaporation of water during heat treatment. Upon filtration with pure water the salt dissolved and was washed away. Figure 5c shows that the PVP hydrogel forms a discontinuous layer at the surface of the membrane. In figure 5c pores are still visible but their number is lower than in the original membrane as shown in figure 5a. Thus the decrease of flux resulted from a decrease of the porosity rather than a decrease of pore size.

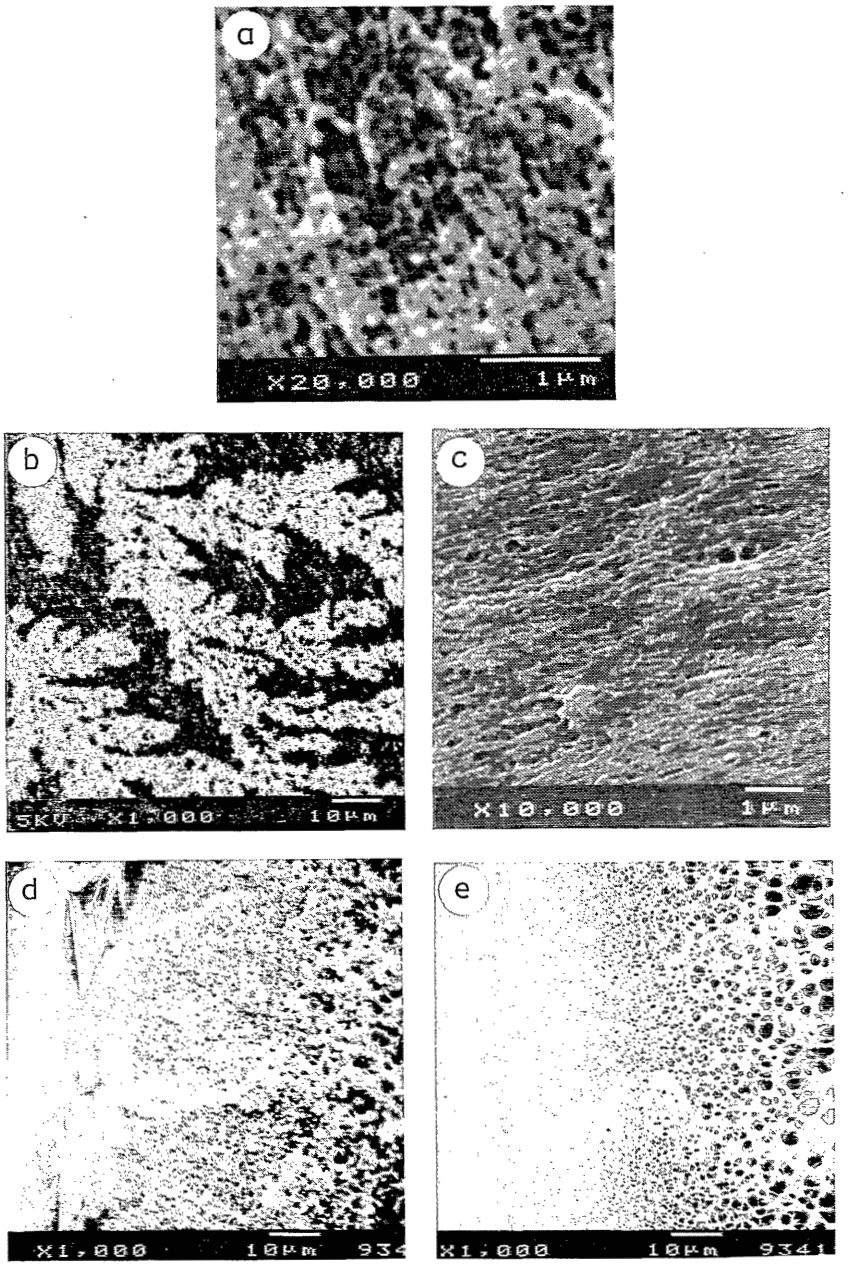


*Figure 5. SEM photographs at the bore side of untreated and treated microfiltration membranes. a) surface view of an untreated membrane; b) surface view of a membrane treated with 5 wt% PVP solution, containing $K_2SO_4$; c) same membrane as shown in figure 5b after filtration of water for 30 minutes; d) view of the cross-section of a membrane treated with 10 wt% PVP solution; e) same membrane as shown in figure 5d after filtration of water for 7 hours.*

In figure 5d it can be seen that after treating the membrane with a 10 wt% PVP solution followed by crosslinking a thick (15 μm) gel layer was formed at the surface of the membrane. Also in the substructure a PVP gel was formed. In this case large $K_2SO_4$ crystals were found at the surface but they are not shown in the picture. Filtration with pure water removes part of the gellayer. After 7 hours only half of the thickness of the gel layer is present as can be seen in figure 5e. The PVP gel in the substructure was removed completely. The removal of the $K_2SO_4$ crystals and part of the PVP gellayer explains the mass decrease of the fibers after filtration.

The formation of a gel layer at the surface of the membrane instead of at the pore wall is possibly caused by the fact that the molecular weight of PVP was too high so the molecules were not able to penetrate the pores. Also part of the PVP might already have been crosslinked in the solution before it had reached the pores of the membrane. Therefore introducing *lower* molecular weight PVP in the pores of the membrane, followed by rinsing the bore with a *second* solution containing persulfate and crosslinking PVP in the oven may result in a better gel-coated pore wall.

### 4.5 Conclusions

The performance of ultrafiltration PES/PVP membranes depends not only on membrane formation conditions but also on the post-treatment of the fibers. The temperature of the rinsing bath affects the pore size and PVP content of the membranes. This might well be caused by processes taking place during nodule formation in the toplayer. The porous structure of the membranes which is susceptible to collapse upon drying can best be preserved by storing the membranes with glycerol in the pores. Swelling of tails of PVP molecules, present in the pores of the membrane and causing a low permeability, can be diminished by treating the membranes with a hypochlorite solution.

Preliminary experiments to incorporate a PVP hydrogel in the pores of a microfiltration membrane in order to decrease the pore size did not succeed. Instead of coating the pore wall with a thin PVP layer a thick gellayer at the surface of the membranes was obtained. The PVP used for these PVP gels possibly had a too high molecular weight.

**Acknowledgement**
The authors like to thank H.A. Teunis and B. Folkers for performing part of the experiments.

## 4.6 Literature


1. Chapter 3 of this thesis, A new spinning technique for hollow fiber ultrafiltration membranes, also published in J. Mem. Sci., 78 (1993) 93
2. Appendix of this thesis, Microstructures in phase inversion membranes. Part 2. The role of a polymeric additive., published in J. Mem. Sci., 73 (1992) 277
3. *a)* R.M. Boom, Th. van den Boomgaard, C.A. Smolders, Equilibrium thermodynamics of a quaternary membrane forming system with two polymers. 1. Theory, submitted for publication to Macromolecules
   *b)* R.M. Boom, H.W. Reinders, H.H.W. Rolevink, U. Cordilia, Th. van den Boomgaard, C.A. Smolders, Equilibrium thermodynamics of a quaternary membrane forming system with two polymers. 2. Experimental, submitted for publication to Macromolecules
4. H.D.W. Roesink, Microfiltration: membrane development and module design, thesis University of Twente, Enschede, 1989
5. H.D.W. Roesink, D.M. Koenhen, M.H.V. Mulder, C.A. Smolders, US Patent 4.798.847
6. G.L. Brown, Formation of films from polymer dispersions, J. Pol. Sci., 22 (1956) 423
7. C.C. Anderson, F. Rodriguez, D.A. Thurston, Crosslinking aqueous poly(vinyl pyrrolidone) solutions by persulfate, J. Apl. Pol. Sci., 23 (1979) 2453
8. C.E. Schildknecht, poly(vinyl pyrrolidone) gels and process of producing the same, US Patent, 2,658,045, 1951
9. General Aniline & Film Corporation, Improvements in or relating to polymeric N-vinyl lactams, Patent 1,022,945, London, 1964
10. J. Rosiak, J. Olejniczak, W. Pekala, Fast reaction of irradiated polymers I. Crosslinking and degradation of polyvinylpyrrolidone, Radiat. Phys. Chem., 36(6) (1990) 747
11. A. Chapiro, C. Legris, Formation de gels de poly-N-vinylpyrrolidone par l'action des rayons gamma sur des solutions aqueuses de poly-N-vinylpyrrolidone, Eur. Pol. J., 21(1) (1985) 49
12. M.H. Kuypers, Method of providing a substrate with a layer comprising a polyvinyl base hydrogel and a biochemically active material, EP 363504, 1990
13. S. Nagaoka, Mechanical properties of composite hydrogels, Pol. J., 21 (1989) 847
14. H.F. Kauffmann, J.W. Breitenbach, N-Vinylpyrrolidon-Popcornpolymere, Ang. Makr. Chem., 45 (1975) 167
15. F. Grosser, Insoluble polymers of vinylpyrrolidone and process for producing the same, US Patent 2,938,017, 1960
16. *a)* F.F. Stengaard, Permeable porous polymeric membrane with hydrophilic character, methods for preparing said membranes and their use, EP 0,257,635, 1987
    *b)* F.F. Stengaard, Hydrophilic membrane for use in ultrafiltration and method of preparation, EP 0,419,396, 1990
17. K. Okita, Hydrophilic porous structures and process for production thereof, US Patent 4,113,912, 1978
18. G.E. Gillberg-LaForce, Modified microporous structures, US 5,049,275, 1990
19. H. Saechtling, Kunststoff Taschenbuch 23. Ausgabe, Carl Hanser Verlag, Munchen, 1986, p 319

Appendix to chapter 4

# Mechanism of the Reaction of Sodium Hypochlorite with Poly(vinyl pyrrolidone)

I.M. Wienk, E.E.B. Meuleman, Z. Borneman, Th. van den Boomgaard, C.A. Smolders

## Summary

Sodium hypochlorite solutions are used to treat membranes prepared from a polymeric blend containing poly(vinyl pyrrolidone) (PVP) in order to increase their water permeability. Sodium hypochlorite affects the membrane material in such a way that PVP is selectively removed from the membrane matrix. The mechanism of the reaction between hypochlorite and PVP is investigated by means of several chemical analysis techniques of the reaction products. Strong indications are found that the reaction involves chain scission of PVP according to a radical mechanism.

## Introduction

Membranes obtained by phase inversion of a polymer solution containing substantial amounts of the macromolecular additive poly(vinyl pyrrolidone) (PVP) usually show a low permeability for water. The low water flux is ascribed to swelling of the hydrophilic PVP present at the interface of the pore walls of the membrane resulting in decreased pore sizes. Roesink et al.[1,2] found that treatment of microfiltration membranes of poly-etherimide (PEI) and PVP with a sodium hypochlorite solution increased the water flux by decreasing the PVP content of the membranes. The positive influence of PVP on the membrane properties, namely giving it a hydrophilic character, is hardly affected by this treatment. In chapter 4 it is shown that upon treating ultrafiltration membranes of poly(ether sulfone) (PES) and PVP with a sodium hypochlorite solution also membranes with a higher flux and a decreased PVP content are obtained.

The reaction of PVP and sodium hypochlorite at pH 11.5 was studied earlier by Roesink[1]. Two possible explanations were given for the selective removal of PVP from the membrane:

- reaction of PVP with sodium hypochlorite causes chain scission of the polymer. This was confirmed by viscosity measurements; reaction with sodium hypochlorite resulted in a decrease of the viscosity of a PVP solution. Since the molecular weight of PVP is decreased it can be washed out of the membrane matrix more easily.
- reaction of PVP with sodium hypochlorite causes ring opening of the pyrrolidone ring of the PVP molecule. The reaction is considered as an oxidation of PVP in alkaline solution. According to Roesink[1] change of the chemical structure of PVP diminishes the interaction of this polymer with PEI and removal of PVP by washing the membrane is facilitated.

The possibility of ring opening of the pyrrolidone group in alkaline solution is reported by other authors[3,4] also but Roesink could not find direct evidence for this mechanism. The experiments that will be presented here will give more clarity on the mechanism of the reaction of PVP with sodium hypochlorite.

## Theory

Sodium hypochlorite (NaOCl) is often used as a bleaching chemical for textile fibers. The effect of hypochlorite on cellulose fibers is therefore studied extensively[5]. Hypochlorite is a non specific oxidizing agent and its activity strongly depends on the pH of the reaction medium. Hypochlorite can attack ether bonds and hydroxyl groups and it is capable of cleaving C-H bonds as well. The oxidizing reactions are fastest at pH between 2 and 7.5 when the chlorite is in the protonated form (HOCl). The general oxidizing reaction can be given by the equation:

$$HOCl + substrate \rightarrow substrate{\cdot}O + HCl \qquad (1)$$

This reaction will cause lowering of the pH of the solution. According to Holst[6] free radicals play an active role in the oxidation with hypochlorite. A free radical chain is set-up as follows:

$$\begin{aligned} &HOCl + OCl^- \rightarrow {\cdot}ClO + Cl^- + {\cdot}OH \\ &{\cdot}OH + OCl^- \rightarrow {\cdot}ClO + OH^- \qquad (2) \\ &{\cdot}ClO + OCl^- + OH^- \rightarrow 2Cl^- + O_2 + {\cdot}OH \end{aligned}$$

According to this scheme the radical ·OH will react with the chain.

However in alkaline solutions sodium hypochlorite in water can be given as:

$$HOCl + OH^- \rightarrow OCl^- + H_2O \qquad (3)$$

and $OCl^-$ is the oxidant.

As said in the introduction reaction of PVP in alkaline media can take place by opening of the pyrrolidone ring to form γ-amino acid units. The mechanism of this reaction is shown in scheme 1. It is analogous to the reaction mechanism for the hydrolysis of lactams in aqueous solutions of potassium hydroxide[3].

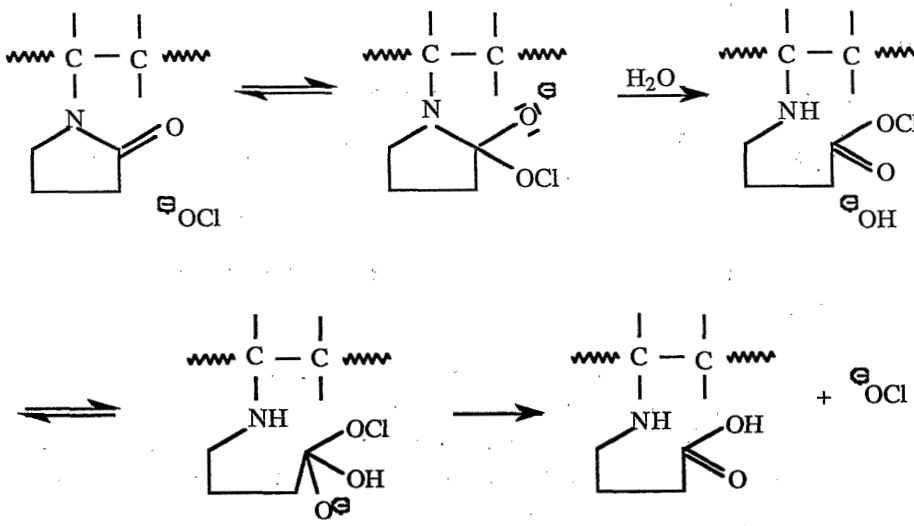


*Scheme 1. Reaction mechanism for the reaction of PVP with hypochlorite in alkaline solution; ring-opening of PVP.*

If radicals are involved in the reaction between hypochlorite and PVP a hydrogen atom can be abstracted from the tertiary carbon atom. Via disproportionation of the radical chain scission can occur. Another possibility is oxidative degradation by which an aldehyde (or carbonyl group) is formed. The reactions described here (and shown in scheme 2) are taken from Anderson et al.[7]. These authors presented the reactions as side reactions that might take place during crosslinking of PVP using persulfate. In the presence of strong acid or alkali opening of the pyrrolidone ring may also take place by means of a radical reaction.

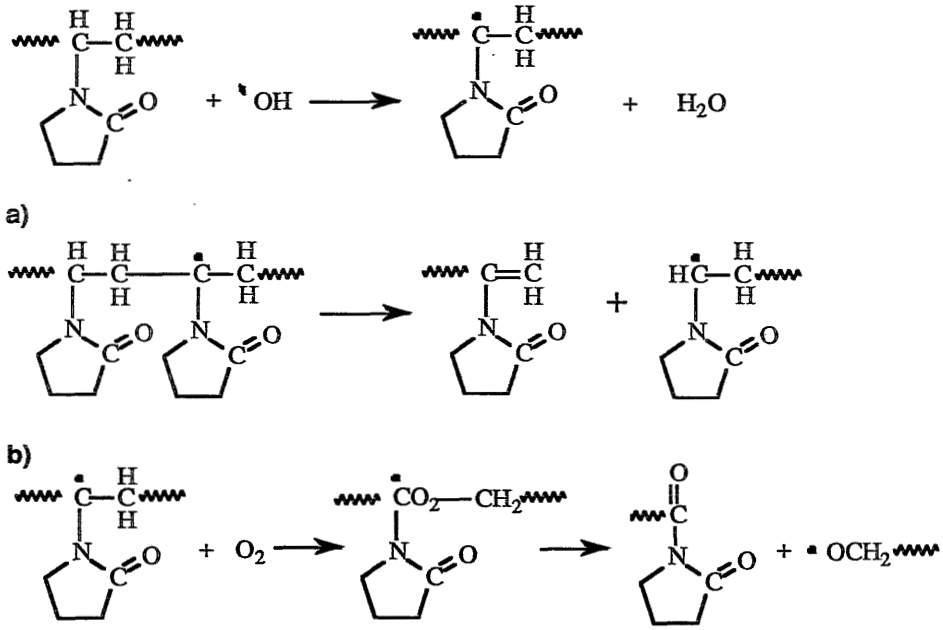

*Scheme 2. Chain scission of PVP via radical reactions: a) disproportionation and b) oxidative degradation.*

It is assumed that the reaction of PVP and hypochlorite takes place according to either one or both of the mechanisms mentioned above. Since the reactions strongly depend on pH, for the experiments that are presented here three reaction media are used at pH 3.9, 6.9 and 11.5. Treatment of membranes containing PVP always takes place at pH 11.5. In these alkaline solutions opening of the pyrrolidone ring is expected to be the main reaction[1,3,4]. Evidence for the reaction mechanism is based on chemical and structural analysis of the reaction products. To prevent any effect of residual hypochlorite this is removed from the reaction mixture by dialysis.

## Experimental

### *Materials*

Poly(vinyl pyrrolidone) (PVP) was purchased from Janssen Chimica, K90. Poly(ether sulfone) (PES) from ICI (Victrex 5200P) was used. Sodium hypochlorite (NaOCl) was purchased from Chemproha (technical quality, 15% activity).

*Reaction*

For the reaction the solution contained 3000 ppm NaOCl. The activity of the chlorite was verified by titration with potassium iodine. The pH of this solution is 11.5. Two solutions were made of lower pH (6.9 and 3.9) by adding hydrochloric acid. 5 g PVP was dissolved in 100 ml hypochlorite solution. Reaction took place for 48 hours at room temperature. Then the low molecular weight components (salts) were removed from the reaction medium by dialysis (dialysis membrane: Tamson 256 k06, pore size 25 Å). The chlorine concentration of the dialysate was tested by adding silver nitrate. After nine days of dialysis no chlorine could be detected anymore. After freeze drying of the solution a white powder was obtained which was used for analysis. A reference sample was obtained by dissolving PVP in water without hypochlorite, dialysis of the solution and freeze drying of the unreacted polymer.

*Analysis of the reaction products*

To obtain $^{13}$C-NMR (Bruker AC250) spectra PVP was dissolved in chloroform ($CDCl_3$). Infra red spectra (IR) were obtained by using an IR apparatus of Nicolet 5SXC.

The number of acidic or alkaline groups of the reaction product can be determined by means of potentiometric titration in non-aqueous solutions.

Micro element analysis (MEA) was used to determine the C/N weight ratio of the reaction product. For this method the powder is completely oxidized at 1800 °C. By gas chromatography of the reaction products the amount of carbon and nitrogen groups can be determined.

GPC measurements were performed using μStyragel columns ($10^5$+$10^4$+$10^3$ Å) and a Guard column (500 Å). Molecular weight was determined by LALLS (Chromatix KMX-6) and by a refractive index detector (Differential Refractometer, Waters 411).

## Results

The reaction of PVP with hypochlorite was performed at three different pH values of the reaction medium. After two days of reaction the pH was again measured. For the three solutions the pH decreased from 11.5 to 11.4, from 6.9 to 1.8 and from 3.9 to 1.4 respectively. Since pH decreases due to the formation of HCl during oxidation this indicates that oxidation has taken place at pH 3.9 and pH 6.9 but at pH 11.5 almost no oxidation has occurred.

In the $^{13}C$-NMR spectra no differences could be found between the reacted and unreacted PVP. If opening of the pyrrolidone ring had occurred a peak of the carboxylic group would appear at a shift of 182.5 ppm. Chain scission would give two peaks of the alkene group at a shift of 94 and 130 ppm. These peaks were not found in the spectra.

By infra red analysis a small peak was found (in the region 1760 - 1780 $cm^{-1}$) that could be ascribed to an ester group or an acid group. The first group could be the result of a crosslinking bond after oxidative degradation of a radical. If the peak represents an acid group it is an indication that ring opening had taken place. This peak was found only in the samples reacted at pH 6.9 and 3.9. The sample of pH 11.5 showed exactly the same spectrum as the reference. If alkene groups would be present in large enough quantities this should result in an additional peak in the IR spectra (in the region 1600-1700 $cm^{-1}$) which was not observed.

Potentiometric titration of the reaction products was performed to verify the presence of carboxylic groups. Both acidic and alkaline groups were found with an acidic strength comparable to propionic acid and sodium propionate respectively. This indicates that the acidic and alkaline groups result from opening of the pyrrolidone unit of PVP. The percentage of the pyrrolidone rings that were opened during reaction of PVP with hypochlorite can be calculated from the number of acidic and alkaline groups. For all three pH values only 1 % ring opening occurred. At pH 11.5 the carboxyl group was present in the alkaline form mainly.

The ratio of nitrogen and carbon atoms of the samples is determined using MEA. The C/N ratio was found to be 5.2 for the reacted as well as the unreacted PVP. The ratio C/N calculated from the molecular structure of PVP is 5.14. With MEA no information on addition of oxygen can be found since it can not be detected with this technique.

Using GPC the molecular weight of PVP before and after reaction was determined. The molecular weight distributions of the three reaction products and the reference are shown in figure 1 together with the weight average molecular weight and the number average molecular weight of the products. From GPC data it can be concluded that the molecular weight of PVP decreases upon reaction with hypochlorite. The chain scission is most effective at pH 11.5 and the reaction also diminishes the polydispersity of the polymer.

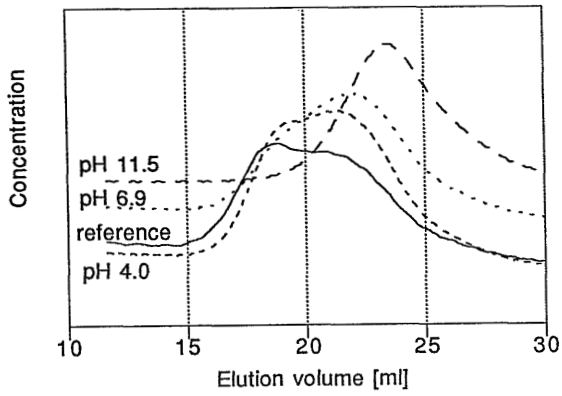


| PVP sample | $M_w$ *$10^3$ g/mole | $M_n$ *$10^3$ g/mole | $M_w$ /$M_n$ |
|---|---|---|---|
| reference | 997 | 242 | 4.12 |
| pH 3.9 | 763 | 182 | 4.19 |
| pH 6.9 | 612 | 156 | 3.92 |
| pH 11.5 | 170 | 141 | 1.21 |

*Figure 1. The results of GPC measurements: distribution curves of the molecular weight of PVP after reaction of the polymer with hypochlorite at three pH values as well as the unreacted polymer are shown. The distribution curve is plotted as concentration versus the elution volume. The elution volume is inversely proportional to the molecular weight of the polymer. Weight average molecular weight and number average molecular weights are shown in the table.*

The GPC technique is applicable only if no structural changes of the molecule have occurred. If during reaction charged groups are introduced the dimension of the molecule might change because of repulsive or attractive forces. To verify the effect of charged groups on the molecular weight distribution as found by GPC two extra measurements were performed. Either acetic acid or tri-ethyl amine was added to the solution in order to diminish if relevant the number of charged groups present in PVP. For all samples the three curves obtained were almost equal. For pH 11.5 the results of these measurements are shown in figure 2.

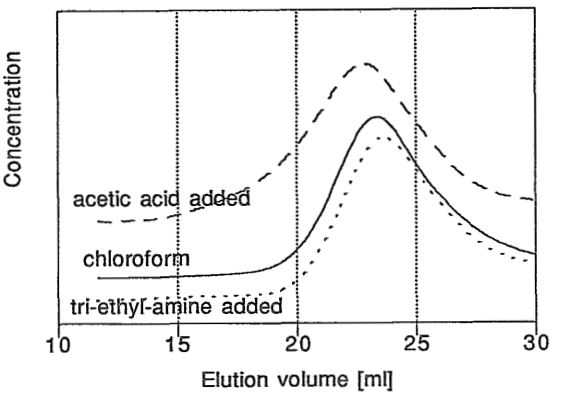


*Figure 2. Checking whether the eventual presence of charged groups in PVP affect the molecular weight distribution curves as measured using GPC.*

Any effect of the dialysis step was investigated by measuring three reference samples: PVP as obtained from the supplier, PVP dissolved in water and dried by freeze drying and PVP dissolved in water, dialysed and dried. For all analysis techniques used not any difference between the three samples could be found.

It has also been investigated whether the hypochlorite reacts with the membrane forming polymer PES. Since PES is not soluble in water it was dispersed in the hypochlorite solution and reaction took place under severe stirring of the solution. The molecular weight distribution of PES after reaction and dialysis was determined using GPC. At pH 6.9 and 11.5 the molecular weight distribution of the reacted polymer was equal to that of the unreacted polymer. However at pH 3.9 a large high molecular weight fraction was found (probably caused by crosslinking) and also the low molecular weight fraction was higher.

## Discussion

The $^{13}$C-NMR spectra do not show structural changes of PVP after reaction of the polymer with hypochlorite. The extra peak found by IR can be ascribed to the carboxyl group indicating that a ring opening reaction had occurred. However at pH 11.5 the peak was not found whereas ring opening was expected to take place most frequent in alkaline solution. Titration of acid and alkaline groups of PVP indicate that only 1% of the pyrrolidone groups had

been opened during reaction. This percentage was the same for all three pH values.

Structural changes of PVP are only small and any charged groups present did not influence the GPC data. Therefore the data found using GPC can be interpreted as caused by a decrease of the molecular weight due to reaction with hypochlorite. The decrease in molecular weight resulting from chain scission of the polymer is strongest at pH 11.5.

Based on the chain scission mechanism of PVP the molecular weight after reaction at pH 11.5 is 170,000 (see figure 1). The number of end-groups of the polymers present is less than 2 for every 1000 monomer groups. The number of carboxylic groups found by titration of the reaction product is 1 for every 100 monomer groups which is apparently too low to be detected with $^{13}$C-NMR. It is therefore reasonable that end groups resulting from chain scission can not be detected by $^{13}$C-NMR or IR.

Another indication that chain scission by a radical mechanism is the main reaction at pH 11.5, is the fact that in the alkaline solution no decrease of pH was observed indicating that no hydrochloric acid was formed during reaction thus no reduction of the hypochlorite had occurred.

## Conclusions

Upon reaction of PVP with sodium hypochlorite structural changes of PVP could not be detected using $^{13}$C-NMR and IR. Titration measurements indicate that 1% of the pyrrolidone rings are opened. Hence only minor structural changes have occurred. On this basis it can be concluded from GPC data, which do show a definite shift in elution volume, that the molecular weight of PVP decreases due to reaction of the polymer with hypochlorite. The decrease in molecular weight is highest at pH 11.5. The decrease in molecular weight of PVP is caused by chain scission according to a radical mechanism.

The membrane forming polymer (PES) is fairly resistant to treatment with a hypochlorite solution, especially at pH 11.5 which is the pH for the after treatment of the membranes.

## Acknowledgement

The authors like to thank J.F.J. Engbersen for the enlightening discussions on this subject.

## Literature

1. H.D.W. Roesink, Microfiltration, membrane development and module design,thesis Twente University, Enschede, 1989
2. H.D.W. Roesink, D.M. Koenhen, M.H.V. Mulder, C.A. Smolders, US Patent 4.798.847
3. M.I. Vinnik, Y.V. Moiseyev, Mechanism of the hydrolysis of lactams in aqueous solutions of potassium hydroxide, Tetrahedron, **19** (1963) 1441
4. P. Molyneux, Water soluble synthetic polymers: properties and behavior, vol I, CRC Press Inc., Boca Rabon, Florida, 1982, p146
5. M. Lewin, Bleaching of cellulosic and synthetic fabrics, In: Handbook of fiber science and technology, vol 2: Chemical processing of fibers and fabrics - functional finishes, M. Lewin, S.B. Sello (ed.), Marcel Dekker, New York, 1985, p.91
6. G. Holst, The chemistry of bleaching and oxidizing agents, Chem. Rev., 54 (1954) 169
7. C.C. Anderson, F. Rodriguez, D.A. Thurston, Crosslinking aqueous poly(vinyl pyrrolidone) solutions by persulfate, J. Appl. Pol. Sci., **23** (1979) 2453

5

# Characterization of PES/PVP Ultrafiltration Membranes

I.M. Wienk, B. Folkers, Th. van den Boomgaard, C.A. Smolders

## Summary

A critical study of a number of characterization techniques for ultrafiltration membranes is presented. The techniques have been applied to lab-made flat and hollow fiber membranes consisting of a blend of two polymers, poly(ether sulfone) (PES) and poly(vinyl pyrrolidone) (PVP). The weight ratio of the two polymers in the membrane has been determined by surface analysis using X-rays (XPS) and by micro element analysis (MEA). Images of the morphology of the membranes were obtained by several microscopic techniques (SEM, TEM, AFM). The pore size distribution could be determined using the liquid displacement method. To study the performance of the membranes the pure water flux and retention and flux for BSA solutions have been measured. The sensibility of membrane permeation for fouling by the adsorption of proteins was found by comparing the pure water flux after contacting the membranes with a BSA solution with the initial water flux.

## 5.1 Introduction

Characterization of ultrafiltration membranes is a difficult and time consuming task. The characterization of membranes can be divided in three parts: chemical composition, morphology and performance. In chapters 2 and 3[1] of this thesis characterization is primarily used to investigate the influence of membrane formation conditions on structure and performance of the membranes. For this purpose some simple characterization methods were chosen by which mutual comparison of the membranes is possible. The morphology was studied by scanning electron microscopy (SEM). Pure water flux and flux and retention of a BSA solution were measured as an indication of membrane performance. In this chapter some critical remarks on these

techniques are made. In addition to this the effect of chemical composition of the membranes are discussed and a more fundamental characterization method (liquid displacement) is presented.

Normally the *chemical composition* of the membrane is the same as that of the polymer used in the casting solution. However the membranes studied in this thesis are prepared from a casting solution containing two polymers: a membrane forming polymer, poly(ether sulfone) (PES) and a hydrophilic polymer additive, poly(vinyl pyrrolidone) (PVP). Since PVP is soluble in the coagulation medium part of this polymer can be leached out during membrane formation as is shown in the previous chapters[1]. The amount of PVP present in the ultimate membrane mainly determines the hydrophilic character of the membrane material and thereby its susceptibility to fouling[2]. Another alteration of the chemical composition at the pore surface may be introduced by a chemical post-treatment of the membranes. This is discussed more thoroughly in chapter 4.

To study the *morphology* of ultrafiltration membranes microscopic techniques, such as SEM, TEM (transmission electron microscopy) and AFM (atomic force microscopy) are used. Interpretation of the photographs obtained with these techniques has to be performed with care as is discussed in this chapter.

The *pore size distribution* of a membrane can be determined using the liquid-displacement technique. The method is based on a pore model consisting of parallel cylindrical pores. Two immiscible liquids A and B with a low interfacial tension are used. Liquid A, the stagnant liquid, is used to fill the pores of the membrane, while liquid B, the displacing liquid, is present at the surface. Liquid A is the liquid that most readily wets the membrane material. In order to displace liquid A in the pores by liquid B a certain pressure has to be applied. This pressure is among others dependent on the size of the pores and it is high for small pores. By increasing the pressure of liquid B the permeability of the membrane increases because successively smaller pores contribute to the permeability. The liquid-displacement method has been introduced by Bechold et al.[3] and Erbe[4] in 1931. Since 1980 Munari and co-workers[5] further developed the measurement technique which finally resulted in a computer controlled set-up. The advantage of this technique over methods such as bubble-pressure, permporometry, thermoporometry and mercury porometry is that the membranes do not have to be dried before or during the measurement[6]. The drying process may alter the porous structure as is shown in chapter 4. Moreover by choosing a pair of liquids with small interfacial tension, the pore sizes can be measured at relatively

low pressures.

*Flux and retention* measurements are simple characterization methods but very much dependent on the process conditions. This is due to a number of effects playing a role during filtration. Even the flux of dilute solutions is dependent on many factors: the transmembrane pressure, the cross-flow velocity, the temperature and the membrane configuration. Also the quality of the 'pure' water is very important when measuring pure water fluxes. For the retention measurements a correct interpretation of the process is hindered due to phenomena like concentration polarization, deposition of a cake or gel layer, adsorption and pore plugging. In literature quite a number of models and empirical relations to describe the influence of these effects on flux decline have been published. An overview of this complex field is given by Van den Berg et al.[7].

Finally a very important characteristic of membranes is their susceptibility to fouling. Especially for ultrafiltration membranes, having applications in food industry and water treatment, a sharp decrease of flux usually occurs due to bio-fouling. The first step in the process of bio-fouling is the adsorption of proteins onto the membrane material[2]. In this chapter the adsorption behavior of proteins on PES/PVP membranes is compared to commercially available polysulfone membranes.

## 5.2 Background of methods and means

### *5.2.1 PVP content of the membranes*

Membranes containing PVP as a polymeric additive have also been investigated by other researchers. Lafreniere et al.[8] added different amounts of PVP ($M_w$ 10,000) to PES casting solutions. The interaction between PVP and PES was found to be strongest at a PVP/PES weight ratio of unity. The authors proposed that the interaction is caused by polar-polar interaction of the N-C=O group of PVP and the O=S=O group of PES or that it is of donor/acceptor nature between N-C=O and an aromatic ring. Even though the effect of PVP on the performance of the membranes was very large, the PVP/PES ratio in the membranes as measured by chemical analysis was only 0.04.

In our laboratory Roesink[9] performed a lot of experiments for PVP/poly(ether imide) (PEI) blends to investigate the behavior of PVP during membrane formation. From these experiments it was concluded that the amount of PVP present in the ultimate membrane depends on the miscibility of the two polymers and on the velocity of the solidification process during membrane formation. For high molecular weight PVP the miscibility was not

very good as two glass transition temperatures were found by a dynamic mechanical measurement of the polymer blend. Upon phase separation diffusion of PVP towards the coagulation medium and the polymer (PES) lean phase occurs until the solidification of the PES rich phase restricts the mobility of the polymers.

Based on thermodynamic calculations Boom et al.[10] found that there only is a driving force for (complete) separation of the two polymers during phase separation of the polymer solution. Equilibrium thermodynamic calculations of the system PES/PVP/NMP/water indicate that from a meta-stable or instable composition two phases arise, one consisting of PES, NMP and water and the other phase consisting of PVP, NMP and water. So the important driving force for separation of a PES/PVP/NMP solution upon immersion in a water bath is the demixing of the two polymers. This also implies that PVP, if present in the ultimate membranes, was trapped there during solidification of the nascent membrane and that the amount might be very low under certain conditions (for instance if the molecular weight of PVP is low).

### *5.2.2 Microscopic techniques*[11]

Most ultrafiltration membranes have an asymmetric morphological structure. In the toplayer the pores are the smallest and pore sizes increase going towards the sublayer. The morphology of the toplayer of the ultrafiltration membranes studied here consists of nodules. In chapter 6 the formation of these kind of structures is discussed. For the characterization of these ultrafiltration membranes the visualization of the nodular structure is the main reason for the application of microscopic techniques. From this point of view the principle of operation and possible draw-backs of several microscopic techniques are briefly discussed in this section.

For scanning electron microscopy (SEM) the membrane is submitted to an electron beam. This causes the emission of secondary and backscattered electrons. The secondary electrons can be detected and the signal can be transformed into a three dimensional image with a resolution of 5 nm and a depth of field of 150 μm. Deviations between the real membrane structure and the microscopic image may result from drying of the specimen, coating the specimen with a gold layer and an inaccuracy caused by the thickness of the electron beam (spot size). The gold layer is sputtered at the surface of the specimen to increase its conductivity and to enhance the emission of electrons. Conductivity is necessary to enable the leaking away of part of the primary electron beam that is not emitted as secondary or backscattered current and which would otherwise damage the specimen. To conduct electricity the gold layer has to have a minimal thickness of 4 nm. Except for

its thickness the gold layer also causes an error due to an uneven distribution of the gold over the surface, the deposition may be different for horizontal faces and vertical ones.

Higher resolution images (in the order of 1 nm) can be obtained with a field emission SEM (FESEM) technique. In this microscope the electrons are emitted from the source by an electric field instead of thermionic emission. Hereby an electron beam with smaller dimensions and increased brightness is obtained. With this technique high magnifications can be reached at low voltages. This causes significantly less beam damage of the specimen and instead of coating with a gold layer a thinner carbon layer can be applied.

Change of the morphology caused by drying the membrane can in principle be avoided by using a cryo-preparation technique combined with a cold-stage SEM. This is a well known technique for studying biological specimens[12]. The object is to rapidly cool the wet specimen in order to prevent the formation of ice crystals. The growth of ice-crystals may alter or damage the structure. Provided the cooling rate is at least $1*10^4$ $Ks^{-1}$, in a sample not thicker than 25-50 μm the ice crystals will be smaller than 10 nm. For biological specimens damage of the morphology occurs if ice crystals larger than 10 nm are formed. Polymers usually have a higher modulus and the water content of membranes is also lower than in biological systems. Therefore it is anticipated that for polymeric systems damage of growing ice crystals is not that disastrous. After cryo-fracture the water is sublimated. Primary drying usually takes place at 173-183 K and a high vacuum by which the bulk of water is removed. Secondary drying takes place at more elevated temperatures at which the non-freezing water associated with hydrophilic surfaces desorbs. Next the sample is coated with a gold layer and under vacuum conditions it is transferred to the cold-stage SEM.

In transmission electron microscopy (TEM) the image is obtained by detecting electrons transmitted through a thin slice of the material. The resolving power is as small as fractions of a nanometer, the depth of field is maximum 2 μm. Fewer electrons are transmitted (resulting in a darker image on the photograph) when the slice is thicker and/or when it is composed of heavier atoms. Often the material is stained to obtain better contrast. After embedding the specimen with a resin thin slices are cut using a microtome. To obtain good slices the hardness of the resin and the polymeric material have to be about equal.

The last technique that will be discussed here is the atomic force microscope (AFM)[13]. A sharp tip is scanned over the surface of a specimen that is placed on top of a piezo driver. The piezo driver is moved in the XY direction and a

voltage is applied that moves the piezo driver over the Z-axis in order to keep the probing force at a constant level. A great benefit of this technique is that the measurements are done at atmospheric pressure and that pretreatment of the specimen is not necessary. This offers the possibility to study membranes submerged in water[14].

### *5.2.3 Liquid-displacement method[3,4]*

For the liquid displacement method the pores of the membrane are filled with a liquid. During the experiment the permeability of the membrane for a second liquid which does not spontaneously displace the first one is measured. Due to the immiscibility of the two liquids a certain pressure has to be applied to fill the pores in the membrane with the second liquid. The pressure difference over a curved interface is given by the Laplace equation (see also figure 1):

$$\Delta P = \gamma\left(\frac{1}{r_1}+\frac{1}{r_2}\right)\cos\theta \qquad (1)$$

in which: $\Delta P$ = pressure difference over the interface [Pa]
$\gamma$ = interfacial tension [N/m]
$r_1, r_2$ = radii of the curved interface between the stagnant liquid and the displacing liquid [m]
$\theta$ = contact angle between the displacing liquid and the pore wall [°]

In a cylindrical pore $r_1$ and $r_2$ are equal. The maximum displacement pressure that can be reached is when $r_1$ and $r_2$ are equal to the pore radius and $\cos\theta$ equals 1. If the applied pressure is higher than this value the interface will move and the pore is filled with the second liquid. For $\cos\theta = 1$ it is necessary that the pore wall is wetted by the stagnant liquid as can be seen in figure 1. By displacing this liquid with the non-wettable liquid a thin layer with thickness *t* will adhere to the pore wall. This means that the pore radius calculated from equation 1 is the real pore radius minus *t*.

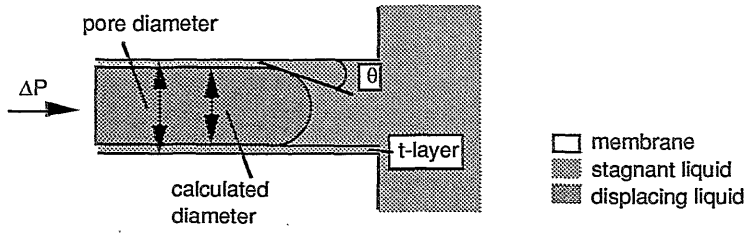


*Figure 1. Curve of the interface between the stagnant liquid and the displacing liquid in a pore.*

The flux through a membrane with a certain pore size distribution is described by the Hagen-Poiseuille equation:

$$J = \frac{\pi . \sum_i (n_i r_i^4)}{8.\eta.\tau.l} * \Delta P \qquad (2)$$

$$\text{with } \frac{\pi . \sum_i (n_i r_i^4)}{8.\eta.\tau.l} = p \text{ (permeability)} \qquad (2')$$

in which: J = flux [m/s]
p = permeability [m/Pa.s]
$\Delta P$ = pressure difference across the membrane [Pa]
$r_i$ = pore radius [m]
$n_i$ = number of pores of radius $r_i$ per unit of cross section [$1/m^2$]
$\eta$ = viscosity of the permeating fluid [Pa.s]
l = membrane thickness (for asymmetric membranes the thickness of the toplayer) [m]
$\tau$ = tortuosity factor [-]

When during a displacement measurement the pressure is increased the flux through liquid exchanged pores increases proportionally. However an extra increase in flux occurs, due to the contribution of pores that just have responded to the displacement liquid. In case the viscosity, the tortuosity and the thickness of the toplayer are known the number of pores with radius $r_i$ can be calculated from the increase in permeability at a certain pressure. The radius $r_i$ belonging to this pressure can be calculated using equation (1).

The permeability of a membrane is determined by its structure and the viscosity of the liquid used. However if the membrane material is susceptible to swelling, the permeability may change in time. The pressure can also influence the permeability in case the compressibility of the structure can not be ignored. The last effect can be corrected for by measuring the permeability of a completely liquid displaced membrane at different pressures.

*5.2.4 Flux and retention measurements*

A simple model to obtain quantitative data on the flux decline during the filtration of a protein solution is derived by Pellegrino and co-workers[15]. In an experiment the fluxes for pure water, a protein solution and pure water again are measured successively. The flux can be described by Darcy's law:

$$J_v=(\Delta P-\Delta\Pi)/\eta(R_m+R_f) \quad (3)$$

with $J_v$ = flux [m/s]
$\Delta P$ = transmembrane pressure [Pa]
$\Delta\Pi$ = osmotic pressure of solutes unable to pass through the membrane [Pa]
$\eta$ = viscosity [Pa.s]
$R_m$ = membrane resistance [$m^{-1}$]
$R_f$ = fouling resistance [$m^{-1}$]

From the experiment the resistances can be calculated. The pure water flux of the clean membrane is used to calculate the membrane resistance. The difference between the water flux of the clean and the fouled membrane (thus the flux of pure water before and after filtration of a protein solution) is due to the resistance caused by fouling ($R_f$). The osmotic pressure, caused by concentration polarization of the proteins, is calculated from the difference between the water flux of the fouled membrane and the flux of the protein solution. In their research Pellegrino and co-workers investigated the influence of several parameters on the flux reduction for three membranes: a hydrophobic polycarbonate membrane that has been surface treated with PVP, and two hydrophilic regenerated cellulose membranes with different pore sizes.

The retention for particles which are smaller than the pores in the membrane can be estimated using an equation derived by Ferry[16] describing steric rejection of non-adsorbing spheres by a capillary:

$$R = 1-C_p/C_f = (\lambda\,(2-\lambda))^2 \quad (4)$$

with: $C_p$ = the solute concentration in the permeate
$C_f$ = the solute concentration in the feed solution
$\lambda$ = the ratio of solute radius and pore radius: $r_{solute}/r_{pore}$

A protein that is often used in model experiments is Bovine Serum Albumin (BSA). BSA is a rather rigid molecule with a molecular weight of 69,000 g/mole and the hydrodynamic dimensions are 14*3.8*3.8 [$nm^3$][17]. In a solution of pH 4.7 the protein molecule together with bound low molecular weight ions has no net charge and therefore it has a very compact structure. This pH is called the iso-electric point of BSA. Because only one type of protein is used for the retention measurements it is impossible to determine the molecular weight cut-off (MWCO) or a pore size distribution of the membranes by these measurements. The retention measurements can only

be used for mutual comparison of membranes prepared in a different way. BSA is also used as a model protein in the adsorption study.

### *5.2.5 Adsorption of BSA*

The adsorption behavior of proteins is a highly complex process due to the specific nature of the protein structure. It will not be discussed in detail here; a fundamental study on protein adsorption has been written by Norde[2] among others. The amount of protein adsorbed on a surface depends on many factors: the adsorption time, the temperature, the type of protein, the salt concentration and pH of the solution, the type of solvent, the presence of other proteins and the type of surface.

The characteristics of a surface in contact with the protein solution are an important factor that is briefly discussed here. In aqueous solutions of proteins the non-polar groups of these molecules are shielded from water by an outer layer of polar groups. In contact with a hydrophobic surface the protein molecule can unfold, resulting in a hydrophobic interaction between the internal groups and the surface. Also at a hydrophilic surface the protein may undergo some structural changes during the adsorption process. In this case the charges of the protein and those at the surface are an important but not the only factor determining the adsorption process. BSA is known to adsorb on both hydrophobic and hydrophilic surfaces, even if the protein and the solid surface are equally charged. This is possible because the adsorption process is mainly taking place through a gain in entropy and this may compensate for unfavourable enthalpy changes involved in the adsorption of a protein on a hydrophilic surface with charges of the same sign[2].

The hydrophobicity of the sorbent surface is important for the *desorption* process, even more so than it is for adsorption. At hydrophilic surfaces, proteins are less tightly bound than at hydrophobic surfaces. For both hydrophilic and hydrophobic surfaces the desorption process is much slower than the adsorption process. Also the activation energy for desorption is higher because the protein has undergone some structural changes in the adsorbed state. An adsorbed protein molecule is more easily removed by displacement through other adsorbing molecules than by dilution of the original solution, in which case all the segments involved in binding the protein to the surface have to be detached simultaneously.

A very rough but indicative method to determine the adsorption of proteins onto membranes is a comparison of the pure water flux before and after the adsorption process. Many researchers found a good correlation between this method and the more fundamental method of measuring the amount of adsorbed proteins by labelling experiments[18-22]. In literature two models can

be found that relate a lower flux after fouling with the adsorbed protein layer. For both models the relative flux reduction is expressed as $1\text{-}RF_w$, with $RF_w$ as the relative permeate flux. $RF_w=J_1/J_0$ in which $J_0$ is the water flux before and $J_1$ the water flux after adsorption of proteins.

Matthiasson[18], Aimar et al.[19] and Nilsson[20] assumed the proteins to form a (multi) layer built on the surface of the membrane thereby increasing the permeability resistance of the system. Equation (3) can than be used to calculate from the relative permeate flux ($RF_w$) the resistance of the adsorbed layer ($R_f$). According to Zeman[21] and Hanemaaijer[23] the proteins rather adsorb on the pore walls thus decreasing the effective pore radius. The thickness of the adsorbed layer ($\Delta r_{pore}$) can be calculated from the Poiseuille relation (equation 2) according to the following equation:

$$\Delta r_{pore} / r_{pore} = 1 - RF_w^{0.25} \qquad (5)$$

The method to study the adsorption behavior of the PES/PVP membranes as is presented in this chapter is comparable to the work done by Roesink et al.[22]. In their case the adsorption behavior of poly(ether imide)/PVP micro-filtration membranes was investigated.

## 5.3 Experimental

### *5.3.1 Materials*

Poly(ether sulfone) (PES) was purchased from ICI (Victrex 5200P. $M_w$ 44,000 g/mole). Four different types of poly(vinyl pyrrolidone) (PVP) from Janssen Chimica were used, K90 ($M_w$ 507,000 g/mole), K60 ($M_w$ 228,000 g/mole), K30 ($M_w$ 18,000 g/mole) and K15 ($M_w$ 10,000 g/mole). The weight average molecular weights of the polymers were determined using GPC. The solvents 1-methyl-2-pyrrolidone (NMP) and di-methyl-formamide (DMF) were purchased from Merck (synthetic grade). The non-solvent was water.

### *5.3.2 Membranes*

For the preparation of dense films PES and PVP were dissolved in DMF and a thin film was cast on a teflon plate. After evaporation of the solvent the films were dried in a vacuum oven at 80 °C for six weeks.

For flat sheet asymmetric membranes PES and PVP were dissolved in NMP. The concentration of PES was always 20 wt%. Thin films were made using a 0.3 mm knife. The films were coagulated in water at room temperature, flushed with water for one day and then dried in air. Some membrane

samples were treated with hypochlorite (see chapter 4). The sheets were kept in a vacuum oven at 80 °C for six weeks. It was assumed that this treatment was sufficient to remove all residual solvent.

PES/PVP hollow fibers were spun as described in chapters 2 and 3[1]. These membranes were all treated with hypochlorite. In this chapter one membrane was used as a standard. This membrane was spun from a polymer solution containing 20 wt% PES, 5 wt% PVP K90, 5 wt% PVP K30 and 5 wt% water in NMP. It will be indicated as membrane A. Besides these lab-made membranes also commercially available membranes were used: Celgard X10 400 was kindly supplied by Hoechst; NTU(3250) and NTU(3050) were kindly supplied by NITTO and GR51PP was purchased from DOW/DDS. An overview of these membranes is given in table 1.

*Table 1. Overview of the membranes used for the characterization measurements.*

| Membrane type | material | configuration | skin layer | characteristic* |
|---|---|---|---|---|
| Celgard X10 400 | polypropylene | hollow fiber | no skin | pore size 50x150 $nm^2$ |
| NTU 3050 | polysulfone | hollow fiber | inside | MWCO 20,000 |
| NTU 3250 | polysulfone | hollow fiber | inside | MWCO 20,000 |
| GR 51 PP | polysulfone | flat sheet | - | MWCO 50,000 |
| Membrane A | PES/PVP | hollow fiber | outside | Retention (BSA) 98% |

* data as obtained from the suppliers.

### *5.3.3 Determination of PVP content in the membranes*

The PVP concentrations in the films were measured using micro element analysis (MEA)[24]. For this method the polymer is completely oxidised at 1800 °C. By gas chromatographic analysis of the reaction products the amount of C, H, N and S can be determined. The PVP content is expressed as weight percentage of the total amount of polymer and was calculated as follows:

$$[PVP](\text{in the film}) = \frac{[N](\text{mol}\%)*Mw(\text{PVP monomer})}{[N](\text{mol}\%)*Mw(\text{PVP monomer}) + [S](\text{mol}\%)*Mw(\text{PES monomer})} * 100\% \ [\text{wt}\%]$$

The concentration of PVP at the surface was measured using XPS[25]. With this technique the specimen is irradiated by a source of monochromatic X-rays. This causes emission of element specific photoelectrons that can be detected. In this way the concentration of N, O, C and S in the surface layer (2 to 10 atoms thick) can be determined. The ratio between the number of nitrogen groups in the surface of the membrane and the number of nitrogen groups in a PVP film was taken as the PVP concentration in the membrane surface:

$$[PVP]\ (\text{in the surface}) = \frac{[N]\ (wt\%)\ \text{in the surface of PES/PVP membrane}}{[N]\ (wt\%)\ \text{in the surface of PVP film}} * 100\%\ [wt\%]$$

Glass transition temperatures were measured using a DSC (Perkin Elmer 4). The scanning rate was 20 °C/min and the temperature interval was 75 - 250 °C. $T_g$ was determined in the second scan.

### *5.3.4 Microscopic techniques*

The SEM (JEOL JSM-T220A) was operated with an electron gun voltage of 15 kV. In chapter 4 it is shown that damage of the porous structure may occur due to capillary forces during drying. To avoid this damage, membranes before air drying were liquid exchanged by the sequence water, ethanol and hexane. For the preparation of cross-sections the membranes filled with ethanol were broken in liquid nitrogen. After breaking ethanol was exchanged with hexane and membranes were dried in air. With an argon sputter coater (Balzers Union SCD 040) a thin gold layer was placed on top of the membranes. The sputter time was 90 seconds, at a current of 15 mA, and the pressure was 0.05 mbar. The FESEM (Hitachi) was operated at 5 kV. For the examination with FESEM the membranes were coated with a 40 - 50 Å thick carbon layer.

For the cryo-preparation technique an Emscope (sp 2000A) was used. Water filled membranes were frozen in a nitrogen slush. After breaking with a knife the water was sublimated at 193 K for 30 min. Next the specimen was sputtered using argon at 7 Pa and an electron current of 20 mA. After 10 minutes a thin, blue coloured gold layer was present at the membranes. The exact thickness of this gold layer is not known but the blue colour indicates that it is about 10 nm. The sample was transferred under vacuum to the SEM (JEOL JSM-T220A). The specimen chamber of the SEM was also cooled down to 113 K.

In order to prepare samples for the TEM the membranes were embedded with an epoxy resin (Epon®). The embedding procedure is described elsewhere[28]. Staining of the samples seemed to be impossible because the staining material clustered at the surface. Thin (50 nm) sections were cut with a Histo Diatome diamond knife. The microscope (Akashi 002A) was operated at 60 kV.

The atomic force microscope was a Nanoscope II[27]. A V-shaped cantilever with a length of 200 μm, a $Si_3N_4$ pyramidal tip and a spring constant of 0.06 N/m was used. Surfaces were imaged at a constant force of 5 nN. Dry membranes were cleaned in hexane to remove any dust particles present.

### *5.3.5 Liquid displacement*

*Materials*

Isobutanol (Merck, pro analysi) and distilled water were mixed and kept for one night to remove any air bubbles present and to obtain two saturated immiscible phases. The interfacial tension is 1.85 mN/m at 22 °C[3]. One hollow fiber was glued at both sides in metal tubes to obtain a module with a length of 10 cm and a membrane surface of $7*10^{-4}$ $m^2$. To remove the glycerol used for storing the membranes the modules were flushed with water at a pressure of 2 bars for 30 minutes. After this they were syringed with the most wettable liquid and then placed in the wettable liquid overnight.

To determine the phase that most readily wetted the membrane a piece of membrane was placed in the water phase and a droplet of the isobutanol phase was placed at the surface. This was also done for a water droplet at the surface of a membrane placed in isobutanol. The droplet that showed the smallest contact angle with the membrane surface has the highest wetting power and was taken as the stagnant phase. Since the permeability of the membrane may be altered due to swelling of the membrane matrix the dimensions of the fiber were measured in the dry and the wet state. Assuming that the swelling of the porous structure is completely isotropic a comparison of the diameters of the fiber was taken as a rough indication of the swelling.

*Displacement set-up*

For the measurements the set-up developed by Munari and co workers[5] has been used. Instead of increasing the pressure and measuring the flux through the membrane which would be obvious, in this set-up the flux is chosen as the independent variable while the pressure needed to obtain this flux is registered. A schematic representation of the set-up is shown in figure 2. A HPLC pump (Waters 590) is used to enforce a certain flow through the membrane. This will cause a pressure difference across the membrane. The high pressure side is in the bore of the hollow fiber. The pressure is measured using two sensors (Cerabar, 0-1 bar and 0-10 bar). The accuracy of the sensors is 0.5%.

Before the measurement can start the stagnant liquid in the bore of the fiber has to be replaced by the displacing liquid. To prevent any pressure build up that might give liquid displacement already in some large pores the three-way valve is turned to 'open' and a very low flow rate is used. After this the valve is closed and the measurement can start. When, after the displacement measurement, in all pores the stagnant liquid has been displaced the pump is stopped and the pressure difference reduces to zero. Then the flux of the

membrane for the displacing liquid is measured at different pressures in order to verify whether the permeability is independent of the pressure.

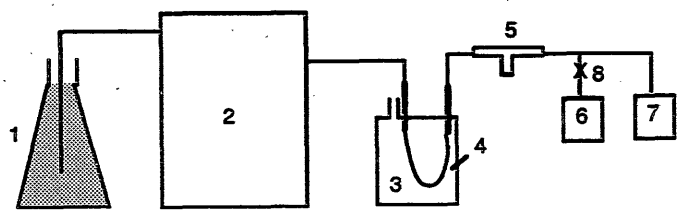


*Figure 2. Schematic drawing of the liquid displacement set-up. The container and the measuring cell were placed in a thermostatic bath.*

### *5.3.6 Flux and retention measurements*

The distilled water used for the flux and retention measurements was prefiltered by a reverse osmosis membrane. Bovine Serum Albumin (No A2153, fraction V, 96-99% albumin) was purchased from Sigma Chemical Company. Solutions of BSA (1 g/l) were prepared in a phosphate buffer of pH 7.4 containing 0.1 M NaCl. The BSA solutions were prefiltered using a 0.2 µm filter (Millipore). The concentrations of the BSA solutions were measured spectrophotometrically (Philips PU 8720 UV/VIS) at 280 nm. The crossflow velocity in the filtration set-up was 3 m/s, measurements were performed at 20°C. The high pressure was always at the side of the membrane skin layer. For the pure water flux measurement water was on-line prefiltered using a 0.2 µm filter (Gelman TDC).

For measurements which are necessary to determine the fouling resistance and the osmotic pressure two identical cross-flow filtration set-ups were used. One set-up was used for the filtration of pure water, the other for the filtration of the BSA solution. Both of them are recirculation systems. After the pure water flux was measured the fibers were removed from the set-up and placed into the second filtration set-up to measure the flux for the BSA solution. Then the fibers were replaced in the first set-up to determine the pure water flux again. During the first minute of the last filtration step the feed stream which had passed through the module was removed to prevent pollution of the pure water by BSA.

### *5.3.7 Adsorption of BSA*

BSA solutions were prepared as described before. Buffers of pH 4.6 and 6 were made by adding citric acid to the phosphate buffer. Sodium azide (0.002 g/l) was added to all BSA solutions. Water fluxes were measured in the cross-flow filtration set-up. The trans-membrane pressure was 2 bars. The flux was measured after 30 minutes of filtration, by then it was practically constant. After this the membranes were removed from the set-up and placed in the BSA solution at 20 °C. For the hollow fibers having the selective toplayer at the outside the bore was filled with water so that adsorption took place only from the outside. After the adsorption time the membranes were replaced in the cross-flow set-up. The water flux was measured after 10 minutes of filtration. To prevent accumulation of BSA in the set-up the feed stream which had passed through the module was removed during the first minute of filtration.

## 5.4 Results and discussion

### *5.4.1 PVP content of the PES/PVP membranes*

The PVP content of flat sheet asymmetric membranes as was measured with XPS and MEA are listed in table 2. The most striking result is that at the surface of the membranes the concentrations of PVP are much higher than the mean concentration over the total membrane thickness. It can also be seen in table 2 that the residual amount of PVP in the membrane is higher if, for the same molecular weight, the casting solution contained more PVP or if the molecular weight of PVP used is higher. For the membranes treated with hypochlorite the results are not very consistent anymore but it is clear that hypochlorite preferentially removes PVP in the membrane. This was is shown in chapter 4.

The data indicate that the PVP content in the ultimate membrane depends on the diffusion behavior of PVP during membrane formation. If the diffusion coefficient of PVP is low, as it is for K90, only a few molecules will be able to diffuse out of the polymer (PES) rich phase before solidification of this phase occurs. It is not possible to measure the time between the onset of phase separation and the solidification process but solidification will certainly be most rapid in the toplayer and that is the place were most of the PVP molecules are trapped.

*Table 2. PVP content of flat asymmetric membranes, expressed as weight percentage of the total polymer content. PES concentration was 20 wt% in all casting solutions. The solvent was NMP and the nonsolvent was water. The PVP content at the surface of the membranes was measured with XPS. The PVP content in the membrane is the mean concentration over the total membrane thickness and this was measured with MEA.*

| Mw PVP | PVP (PES+PVP) in the casting solution [wt%] | PVP(PVP/PES film) PVP(PVP film) at the surface of the membrane [wt%] | PVP (PES+PVP) in the total membrane [wt%] | PVP (PES+PVP) in the total membrane after NaOCl [wt%] |
|---|---|---|---|---|
| K30 | 20 | 15 | 2.2 | 2.4 |
| K30 | 33 | 14 | 3.4 | 2.7 |
| K30 | 43 | 14 | 3.5 | 3.2 |
| K30 | 50 | 18 | 4.6 | 2.6 |
| K15 | 33 | 12 | 3.4 | 2.8 |
| K60 | 33 | 17 | 4.5 | 2.9 |
| K90 | 33 | 33 | 12.5 | 4.7 |
| Membrane A: K30/K90 | 16.5/16.5 | | 4.6 | 1.7 |

It can be concluded that the amount of PVP in the membrane is mainly determined by diffusion of PVP from the polymer (PES) rich phase to the polymer (PES) lean phase during the time between the onset of phase separation and the solidification of the PES rich phase. The amount of PVP in the ultimate membrane is very low and is lowered even more by treating the membranes with hypochlorite.

The low total PVP concentrations are in agreement with the results found by Lafreniere et al.[8]. Roesink[9] measured the total amount of PVP in microfiltration membranes of poly(ether imide) (PEI) and PVP using NMR. Starting with a polymer casting solution containing 43 wt% PVP K90, 28 wt% PVP was found in the membranes before treatment with a hypochlorite solution. After this treatment the membranes still contained 8 wt% PVP. The higher PVP concentrations in PEI/PVP membranes probably result from a better interaction of PVP with PEI compared to the interaction between PVP and PES.

For the homogeneous films as well as for the asymmetric membranes glass transition temperatures were measured using the DSC equipment. For all samples only one glass transition temperature was found, indicating that the two polymers form a homogeneous blend. A correlation between $T_g$ and the composition of the blend could not be found. The glass transition temperatures of some homogeneous films were even lower than the $T_g$ of pure PVP. Although Painter et al.[28] ascribe such a behavior to strong hydrogen bonding between the two polymers the low $T_g$'s of these films are probably due to residual solvent or water.

### *5.4.2 Morphology of ultrafiltration membranes*

An important characteristic of the ultrafiltration membranes studied here is the nodular structure in the toplayer. The formation of these structures is discussed in chapter 6. These polymer spheres can be visualised with SEM if magnifications of x35,000 and higher are used. For a common SEM clear images at these high magnifications can only be realised with an acceleration voltage of 15-20 kV. The specimen are prevented from beam damage by coating them with a gold layer. The presence of the gold layer with a certain thickness ($t$) will enlarge the diameter of the polymer spheres from $d$ to $d+2t$. For a PES membrane this is illustrated in figure 3. The points are the diameters of the nodules estimated from SEM photographs after sputtering the specimen for different times. The interrupted line represents two times the thickness of the gold layer for the given sputter time as given by the supplier of the sputter coater machine. The dimension of the nodules is found by extrapolation to sputter time zero and for this membrane the mean diameter is estimated at 66 nm.

For a field emission microscope a much thinner carbon layer is sufficient to protect the polymeric materials from beam damage. Photographs of membrane A (the standard membrane) obtained with this technique can be seen in figure 4. The size of the nodules is 40 nm for this membrane.

Using the cryo-preparation technique it is in principle possible to obtain an image of the membrane structure in the wet state and study the effect of drying on the morphology. However high resolution studies appear to be impossible due to destruction of the polymer matrix by the high energy electrons (beam damage). It was not possible to obtain clear images at magnifications above x10,000 which means that the toplayers could not be seen properly. For the *sublayer* the influence of the drying process is shown in figure 5. Photograph 5a was taken after cryo-preparation of the membrane. Most water has been removed by sublimation at 193 K but bound water is still present. For the photograph in figure 5b a second sublimation step inside the microscope at 213 K was performed. During this step almost immediately the

bound water is removed and a structure comparable with a non-cryo prepared membrane structure is obtained.

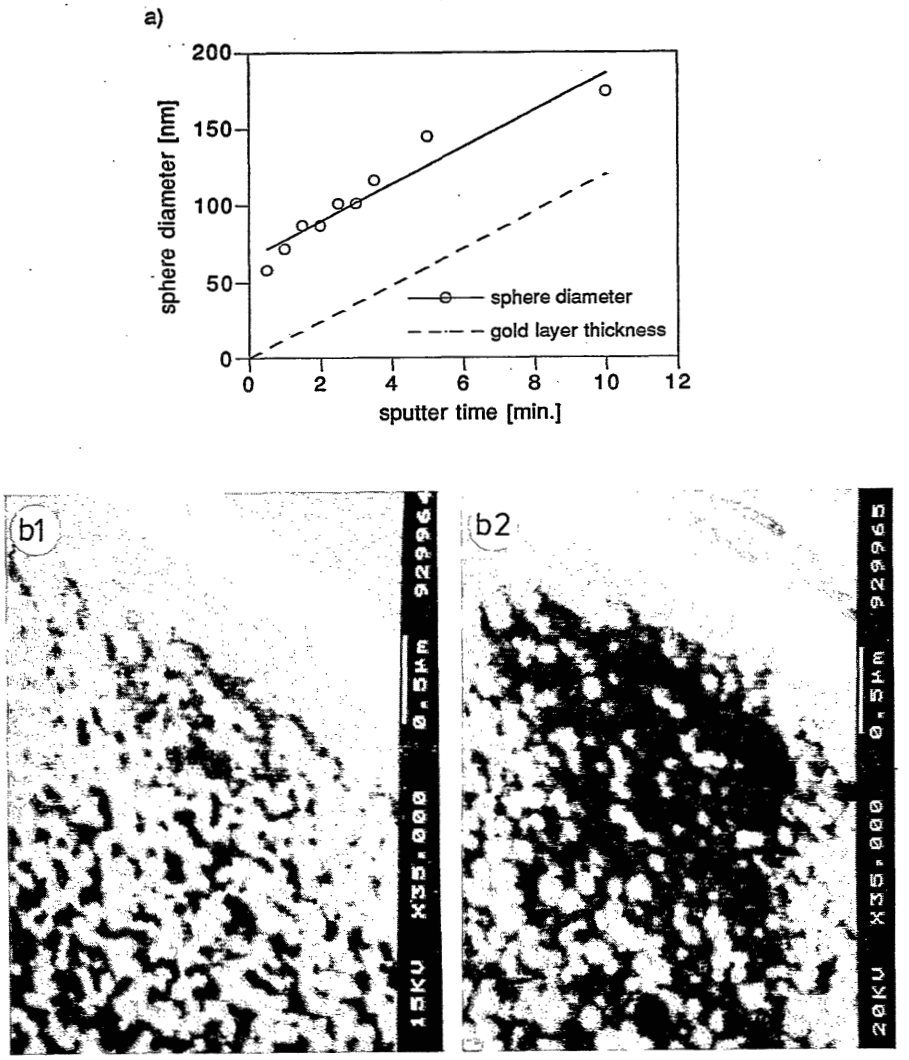


*Figure 3. The effect of the gold coating layer on the apparent nodule size in scanning electron microscopy: a) experimentally obtained diameter of the spheres versus the sputter time. b) photographs of the cross section of the toplayer for sputter times 2 (b1) and 5 (b2) minutes.*

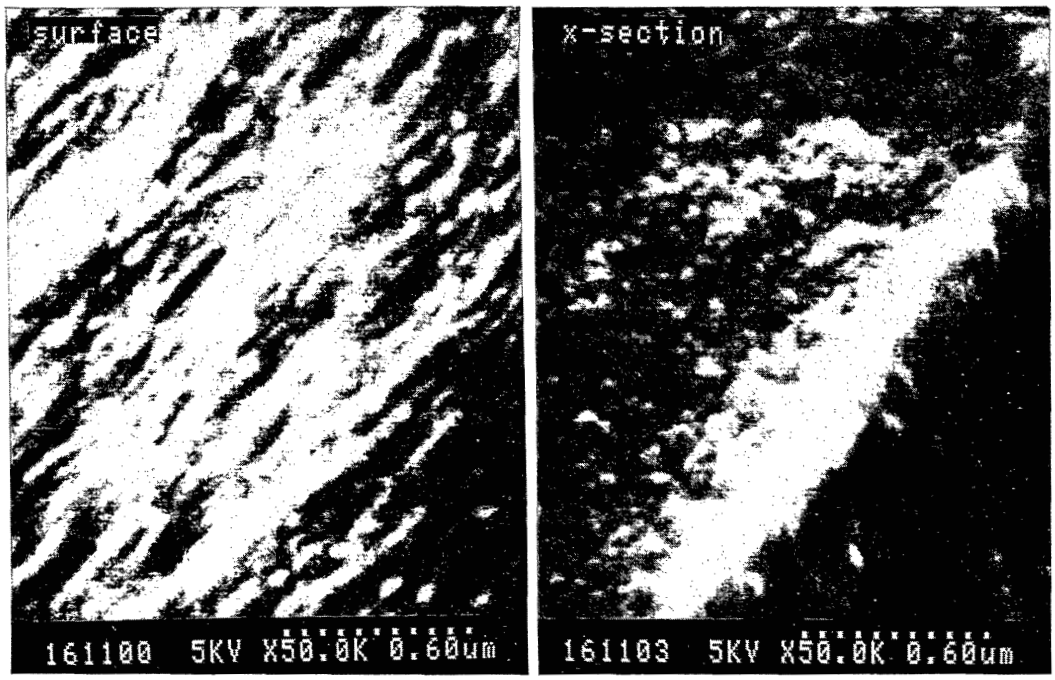


*Figure 4. Topview and cross section of the toplayer of membrane A. Images from the field emission electron microscope.*

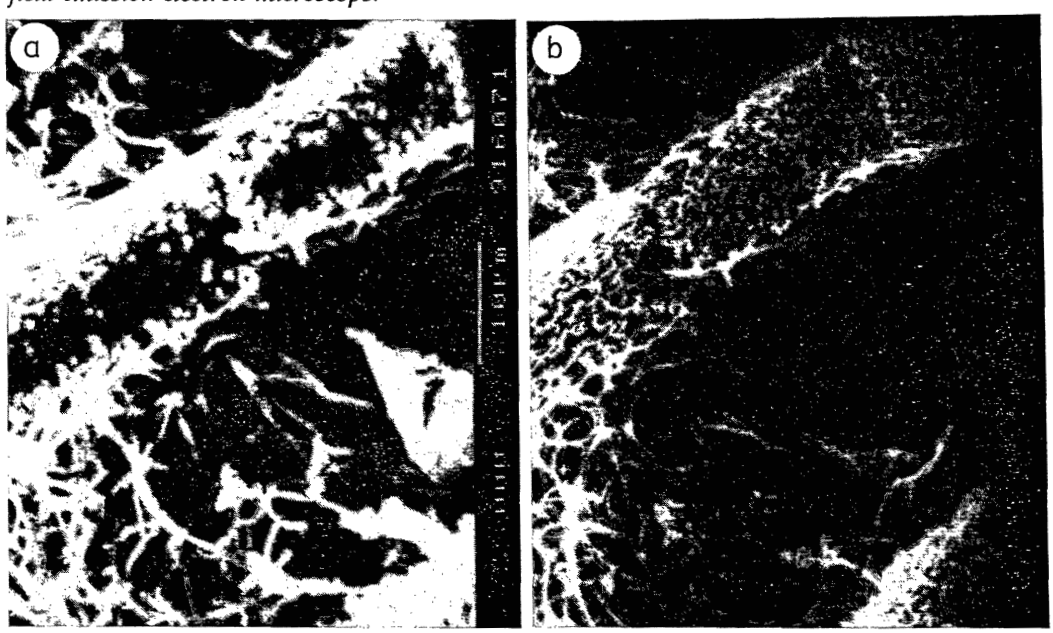


*Figure 5. SEM images of a PES/PVP membrane after applying the cryo-preparation technique. a) photograph taken after sublimation of free water at 193 K. b) photograph taken after a second sublimation step; sublimation of bound water at 213 K.*

With the transmission electron microscope a good contrast between the membrane material (dark) and the embedding material (light) could be obtained even without staining. Three images at different magnifications can be seen in figure 6. In the toplayer the nodular structure is visible. The porosity of the toplayer as found with TEM seems much higher than the porosity on SEM images. The large white spots in the toplayer (best visible in figure 6b) are possibly artifacts: small cracks in the thin membrane slices were formed in the cutting process. The formation of the cracks may be *i)* due to differences in hardness of the polymer material and the resin or *ii)* caused by unfilled pores in the membrane because of insufficient diffusion of the viscous embedding material into the finely porous structure.

For the atomic force microscope a special treatment of the membrane sample is not necessary. Images of a flat sheet PES membrane are shown in figures 7a and 7b. If the operating forces are too high (20nN) damage of the polymer surface structure may occur as can be seen in figure 7c. Here the central section was scanned with a probing force of 20 nN. The remainder of the picture was scanned with a probing force of 5 nN. It is obvious that the irregularity of the central section is caused by the high probing force. Another difficulty arises if the features to be investigated are of the same dimensions as the tip size (10-20 nm). Then the line scan gives a profile of the shape of the tip instead of the shape of the sample irregularity. So especially the interpretation of nodular structures has to be done with care.

A disadvantage of the AFM technique is that the surface roughness should not be too high (not larger than 2 μm). This makes the study of cross sections impossible since the brittle crack usually has a very rough surface.

To sum up these results it can be said that especially at high magnifications all microscopic techniques give a more or less deformed image of the real membrane morphology. However despite their draw-backs microscopic techniques are indispensable for the characterization of membranes. As for the membrane structure all pictures shown of the toplayer of ultrafiltration membranes of PES or PES/PVP indicate that this layer consists of polymer nodules. Estimation of the size of the nodules is quite difficult. The formation of such a polymer structure is discussed in chapter 6.

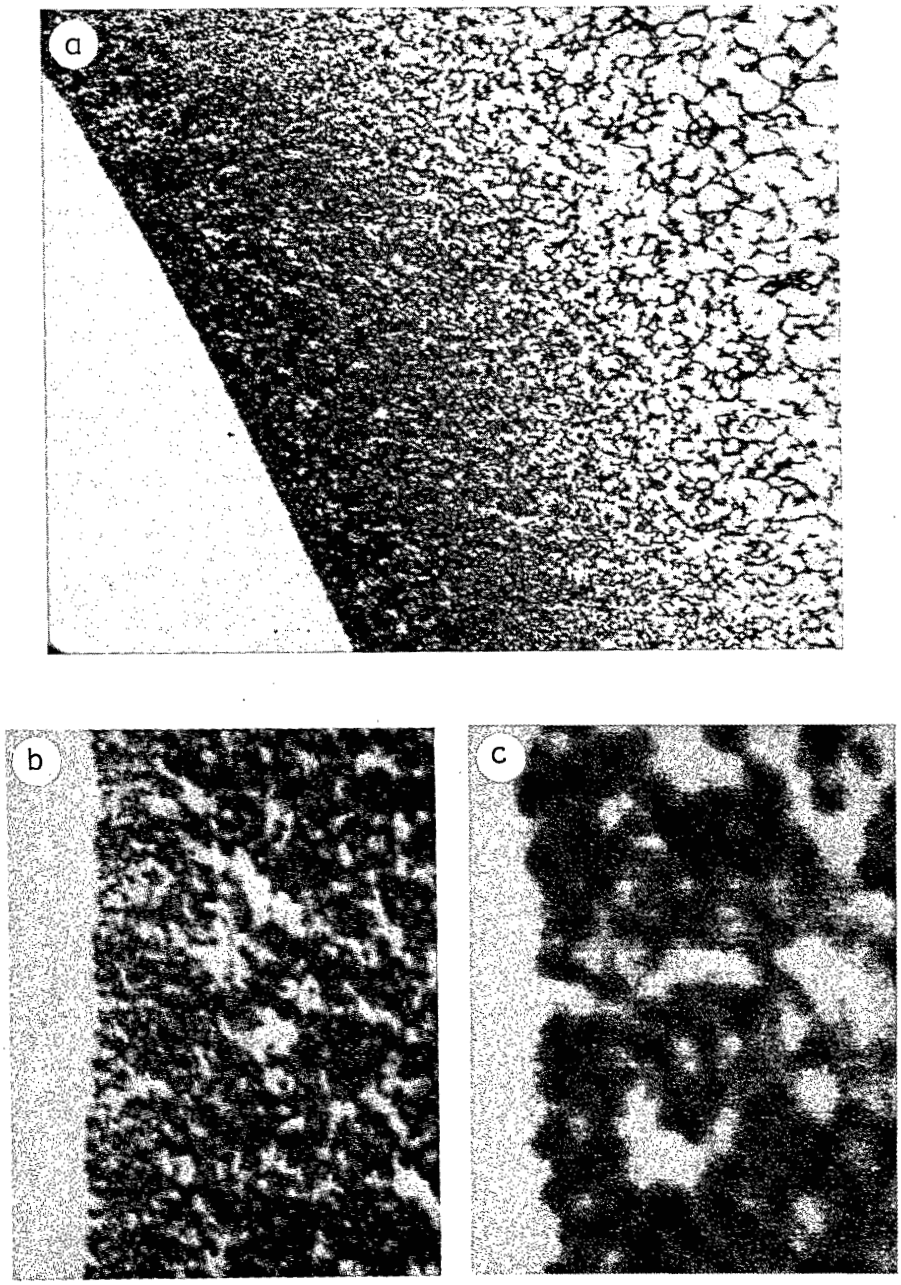


*Figure 6. Photographs of the toplayer of a PES/PVP ultrafiltration membrane as obtained with a transmission electron microscope. Three magnifications: a) x4,685, b) x21,000 and c) x100,000.*

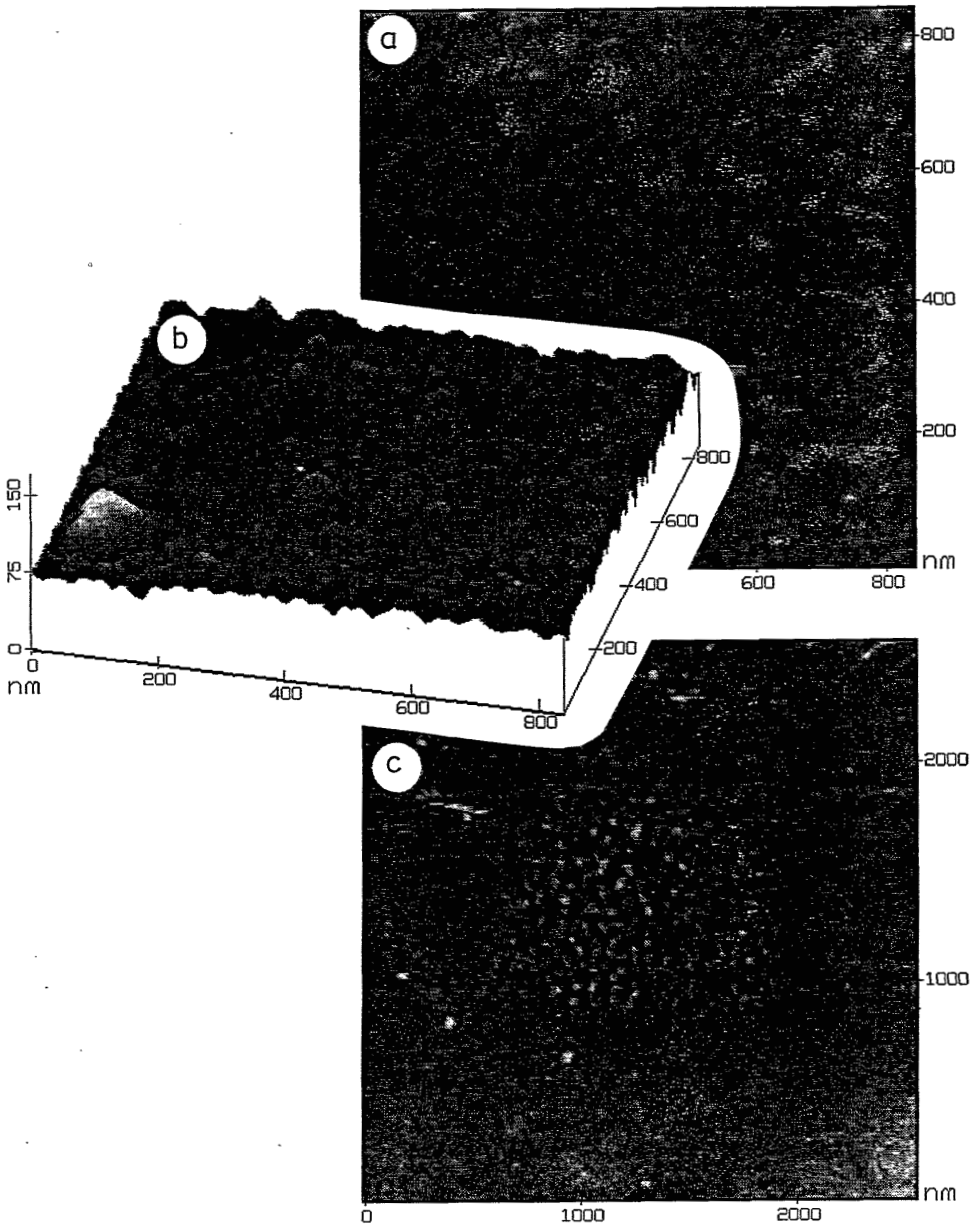


*Figure 7. AFM images of the morphology at the surface of a PES ultrafiltration membrane. a) Top view of the nodular structure of the toplayer, b) Same scan as figure a) now a tilted view, c) Change of the membrane morphology due to interaction of the polymer material with the tip of the AFM. The central section was scanned with a probing force of 20 nN. The remainder of the picture was scanned with a probing force of 5 nN. (a) and b) were also scanned at 5 nN)*

### 5.4.3 Liquid displacement

Two types of hollow fiber membranes have been measured with this technique, a lab-made PES/PVP membrane (the standard membrane A) and a Celgard poly-propylene membrane. For reliable measurements the lowest pressure that could be applied accurately was 0.1 bar. Measurements were stopped at a maximum of 5 bars to prevent the fiber from breaking. Using the mutual saturated liquid pair isobutanol/water (interfacial tension 1.85 mN/m)[3] it means that pores with radii between 370 nm (0.1 bar) and 7 nm (5 bar) can be measured.

*Measuring PES/PVP hollow fiber*

For the PES/PVP membrane water saturated with isobutanol was found to be the best wetting phase and it was used as the stagnant liquid. The permeabilities of the membrane for pure water and for pure isobutanol have first been measured. After correction for the viscosities the water permeability was 85% of the isobutanol permeability. The difference is probably caused by a higher degree of swelling of the membrane in water. However when the diameter of the dry fiber is compared with the diameters of the fibers swollen in the two saturated liquids the swelling is 7% for both liquids. Thus although the sorption of water is probably higher than the sorption of isobutanol, this does not result in a difference in swelling behavior of the membrane in either of the two mutually saturated phases. Based on these experiments it will be assumed that the swelling of the membrane structure does not change during the measurement.

Performing the displacement measurements it appeared that each stepwise increase of the liquid flow through the membrane was immediately followed by an increase of the pressure ($P_{max}$) in the bore of the fiber. Next the pressure decreased until it became constant after a few minutes ($P_{end}$). This behavior is illustrated in figure 8 where both pressures are plotted as a function of the flux through the membrane. To calculate the *permeability* belonging to this pressure the flow (J) was divided by $P_{end}$ because this indicates the equilibrium pressure. However for a few moments the pressure in the membrane has been higher than $P_{end}$ and smaller pores (related to $P_{max}$) have already responded. Therefore $P_{max}$ was used to calculate the *pore size distribution* of the membrane. After determination of the permeability using $P_{end}$ the indicated pressure will always be $P_{max}$. The difference between $P_{max}$ and $P_{end}$ was not always the same but about 0.2 bar. This effect can be diminished by a more gradual increase of flow.

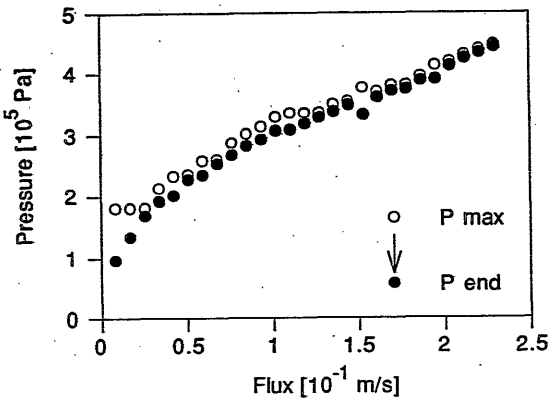


*Figure 8. Results of a displacement measurement of membrane A. For each stepwise increase of the flux through the membrane (by an increase of the flow of the HPLC pump) pressure first increases to $P_{max}$ and then reaches the equilibrium pressure $P_{end}$.*

The cumulative permeability is plotted versus the pressure in figure 9. The unfilled circles shown in figure 9 are the data of the displacement measurement. The straight line represents the isobutanol permeability of the membrane when it is completely filled with the isobutanol phase. For an ideal situation this permeability must be independent of the pressure and the line should be horizontal.

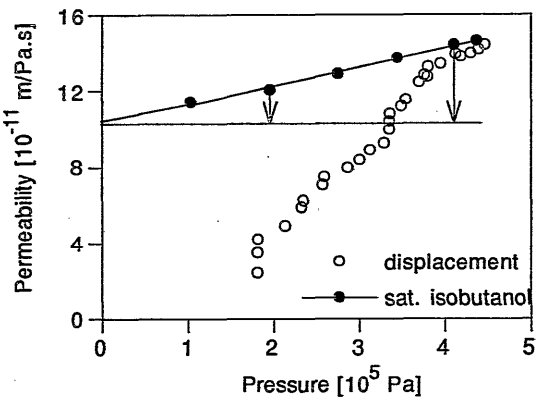


*Figure 9. Permeabilities of the displacement measurement (lower curve) and of the fully liquid displaced membrane (upper curve) for saturated isobutanol. The arrows indicate the correction for the pressure dependency of the permeability.*

From the results it can be seen that the permeability increases with increasing pressure. This can be caused by expansion of the fiber since the high pressure side of the pressure difference is inside the fiber whereas the layer with the smallest pores is at the outer surface of the fiber. The permeability at zero pressure is found by extrapolation. For the membrane shown in figure 9 this permeability is $1*10^{-10}$ m/Pa.s.

To correct the data of the displacement measurement for the influence of the pressure each value of the permeability is diminished with the pressure times the slope of the upper line. In figure 10 the corrected cumulative permeability is plotted versus the pressure. The increase of the permeability upon an increase of pressure is due to displacement of the liquids in pores with a radius related to the pressure by equation 1. The differential permeability and the pore size distribution can be found by fitting the experimental data with an exponential function and plotting its derivative to the pressure versus the pore radius (obtained from $P_{max}$ through equation 1).

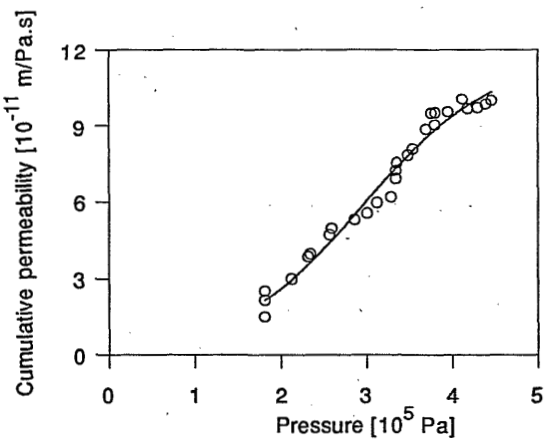


*Figure 10. Corrected cumulative permeability. The full line represents a fit with an exponential function of the experimental points.*

In figure 11 also the pore size distribution as calculated from equation 2' is plotted. To determine the thickness of the toplayer of asymmetric membranes SEM pictures can be used. However the pore size gradient of PES/PVP membranes is very gradual and a transition from toplayer to sublayer can not be seen clearly. Cuperus et al.[6] used a gold-sol-method and for polysulfone membranes a toplayer thickness of 0.2 µm was found which value has also been used here. The tortuosity was chosen to be 1. For the viscosity of saturated isobutanol the value of pure iso-butanol was used ($3.5 *10^{-3}$ Pa.s).

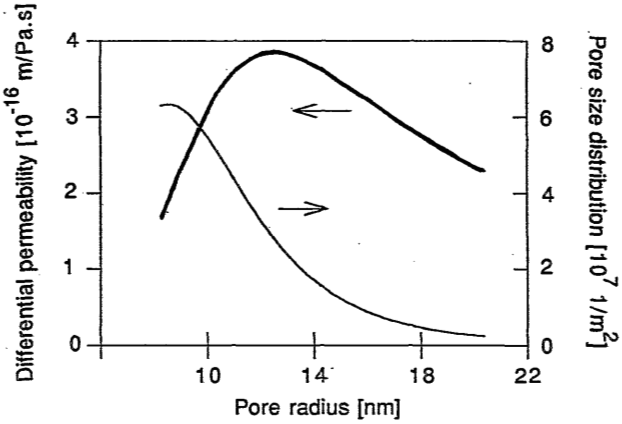


*Figure 11. Permeability distribution and differential pore size distribution of membrane A.*

The difference between this value and that of isobutanol saturated with water is expected to be negligible. In figure 11 it can be seen that the number of small pores (~10 nm) is very large. The contribution of these pores to the total permeability however is not very important because the resistance towards liquid flow is very large (the resistance is proportional to $1/r^2$).

After the measurement the module was removed from the set-up, syringed with the water phase and kept in the water phase. When the same module was measured a second time very different characteristics were found. In figure 12 the corrected cumulative permeability for a module of membrane A in three successive measurements is given. The pore size distribution curves resulting from these measurements are shown in figure 13. In the second run the total permeability of the membrane is 2.5 times as high as in the first run which is caused by the appearance of larger pores. For the first measurement the maximum of the pore size distribution curve is at a pore radius smaller than 10 nm. In the second run this is shifted to a pore radius of 25 nm. The difference between the second and third run is not very profound. In figure 12 it can be seen that in the second and third run the curves bend upwards at $5*10^5$ Pa. This means that also pores equal to or smaller than 10 nm are present. However the data have been fitted assuming a pore size distribution with one maximum. In figure 13 the second peak at small radius is not found by fitting the data but the maximum pore radius is found by simply applying equation 1. Bimodal pore size distributions in membranes have also been measured by Munari and co-workers[5].

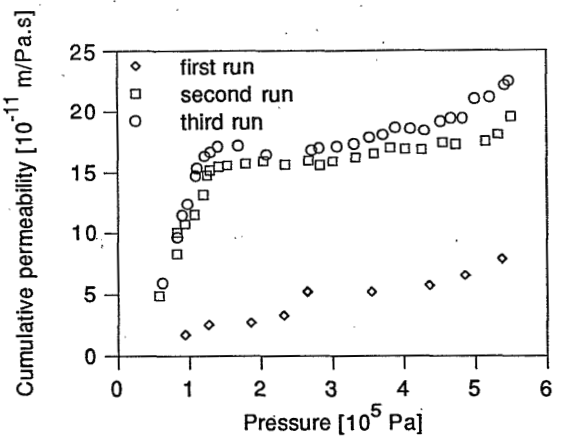


*Figure 12. Corrected cumulative permeability versus the applied pressure for three successive measurements of the same module (membrane A).*

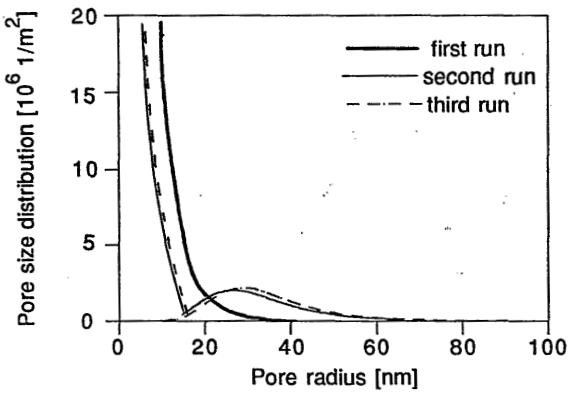


*Figure 13. Pore size distribution of membrane A after fitting the data presented in figure 12 with an exponential function assuming a pore size distribution with one maximum. In the second and the third run a bimodal pore size distribution is found: the second maximum at small pore radius is schematically drawn in this figure.*

The low permeability found in the first run is probably caused by traces of glycerol or incomplete filling of the pores by the stagnant liquid. The expansion of the fibers at increasing pressure is too little to cause such a strong increase in permeability. Also, the time between two measurements was usually 24 hours during which relaxation of the expansion would occur. The small difference between the second and third run could be a result of the expansion. Since it is not possible to measure pores larger than 370 nm with the pair of liquids chosen here, after the experiments the fibers were

measured with the bubble point technique (Coulter porometer) to verify whether any large holes were present. For this technique to be applicable the membranes must be dried and then filled with a fluor-hydrocarbon; in a displacement measurement the liquid is then replaced by air. No pores larger than 100 nm were found with the Coulter porometer.

The reproducibility of the measurements for different membrane samples is shown in figure 14 where the pore size distribution as found by the second run is given for two modules made from the same batch of fibers. The pore size distributions are not the same and also the permeabilities of the membranes differ quite a lot ($2*10^{-10}$ m/Pa.s and $1.4*10^{-10}$ m/Pa.s). Because the reproducibility of lab-made membrane fibers seems not very good more measurements have to be performed in order to draw reliable conclusions concerning the structure of the membranes. The reproducibility of the first run (not shown here) is very bad although it is always lower than the second run. This is also an indication that the first run is not very reliable.

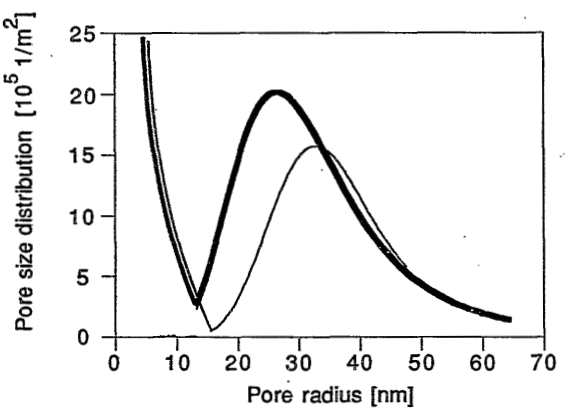


*Figure 14. Reproducibility for two samples of membrane A as measured with the liquid displacement method. The pore size distribution for the second run is shown for two modules of membrane A. At radii smaller than 10 nm the curve is schematically drawn.*

In figure 12 the total permeability in the second run is $1.5*10^{-10}$ m/Pa.s, thus the flux per bar for saturated iso-butanol is 54 $l.m^{-2}h^{-1}bar^{-1}$. After correction for the viscosity the water flux would be 189 $l.m^{-2}h^{-1}bar^{-1}$. If it is assumed that the water flux is 85% of the saturated iso-butanol flux as was found experimentally for water and pure isobutanol the flux becomes 161 $l.m^{-2}h^{-1}bar^{-1}$. The water flux of membrane A is about 100 $l.m^{-2}h^{-1}bar^{-1}$. Although assumptions have to be made to compare the fluxes they seem to be of the same order.

*Measuring Celgard membranes*

For the Celgard membrane saturated isobutanol was the best wetting phase and it was used as the stagnant liquid. An increase of the diameter after placing the membranes in the saturated liquids for three days could not be measured. The pores in Celgard membranes are not cylindrical but ellipsoidal. According to the supplier the pore size was 50x150 $nm^2$ which was determined using electron microscopy. This means that $r_2=3*r_1$ and with $\cos\theta = 1$ equation (1) becomes:

$$\Delta P=\frac{4}{3}\frac{\gamma}{r} \qquad (1')$$

with r the smallest pore radius of the ellipsoidal cross section.

The pore size distribution of the first and the second run are shown in figure 15. For this membrane the pore sizes have decreased in the second run. This could be due to swelling although any difference in fiber dimensions could not be measured. Another reason for this effect might be the compressibility of the fiber during the first measurement. It was found that for this membrane, in contradiction to the PES/PVP membrane, permeability decreases with increasing pressure. Fouling of the membrane during the first measurement could also be the reason for the smaller pore sizes found.

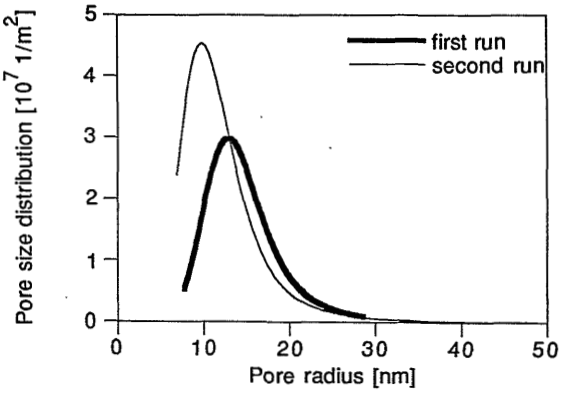


*Figure 15. Pore size distribution of the Celgard membrane as determined in the first and second run.*

The mean pore radius for the first run is 13 nm, thus the pore diameter is 26 nm. This is half of the value as given by the supplier. It has to be mentioned here that the pore sizes found using the liquid displacement technique are the sizes at the narrowest spots of the pore channels. The SEM pictures are

made at the surface of the membrane and this is not necessarily the most narrow passage of the pores. If cylindrical pores are assumed instead of ellipsoidal shapes the calculated maximum of the pore size distribution lies at a diameter of 39 nm.

### *5.4.4 Flux and retention*

Presumed compressibility of membrane A during filtration has been determined by measuring the water flux of one module using a sequence of pressures in the cross-flow set-up. The permeate side always was at atmospheric pressure. The results are shown in figure 16 and it can be seen that the flux per unit of pressure (the permeability) is almost constant. The membrane fibers are only slightly compressible in the pressure range 0.5 bar to 2.5 bars and the compressibility is reversible. In figure 16 there also is a curve giving the water flux as a function of time measured at a trans-membrane pressure of 2 bars. Over 2 hours there is only a small decrease in flux. Apart from compressibility, fouling of the membrane due to impurity of the 'pure' water may play a role in this long term flux decrease.

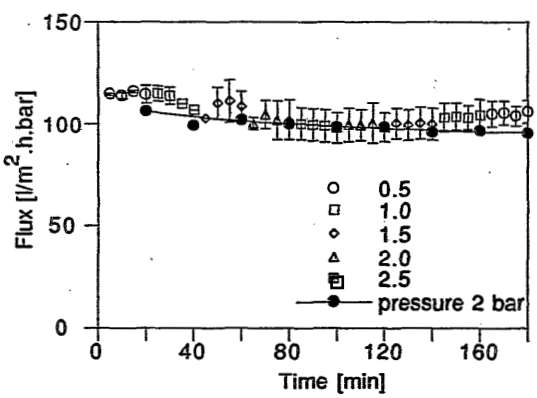


*Figure 16. The water flux per unit of pressure of membrane A measured as a function of time. For one experiment the trans-membrane pressure was kept at 2 bars for 3 hours. For the other experiments trans-membrane pressure was changed every 20 minutes.*

The effect of concentration polarization and fouling phenomena during the retention measurements has been studied by successively measuring the water flux, the permeate flux of a (0.1 wt%) BSA solution and the water flux again. The results are plotted in figure 17. It can be seen that the flux is decreased drastically when a BSA solution is applied. The flux recovery after removal of the BSA solution (after 20 minutes) is only small. Using equation 3 the membrane resistance was calculated to be $R_m=4.0*10^{12}$ $m^{-1}$. The

resistance caused by the BSA due to pore plugging and/or the formation of a cake layer is of the same magnitude as the membrane resistance: $R_f=3.8*10^{12}$ $m^{-1}$. After replacing the protein solution by water the flux increases only slightly indicating that the osmotic pressure caused by concentration polarization of the proteins is not very large ($\Delta\Pi=0.4*10^5$ Pa).

It is also possible that the difference of pure water flux before and after filtration of the BSA solution is caused by adsorption of protein on the walls of the pores. The thickness of the adsorbed layer can then be calculated using equation 5 and the result is $\Delta r_{pore} / r_{pore} = 0.16$. The mean pore radius as found by the liquid displacement method is 25 nm. Thus the thickness of the adsorbed layer is 4 nm which means a side-on adsorbed monolayer of BSA molecules.

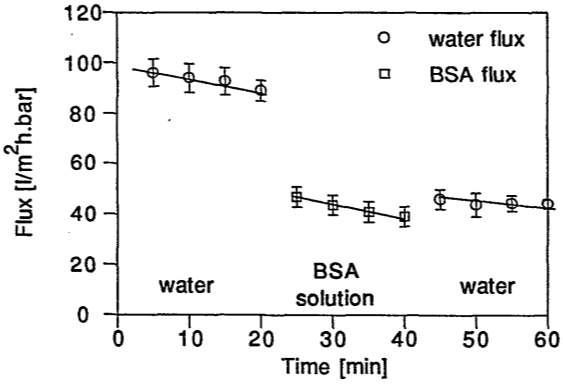


*Figure 17. The flux per unit of pressure through membrane A as a function of time. The first 20 minutes the feed solution was water. Then a 1 g/l BSA solution was applied at the feed side. After 20 minutes again water was the feed solution. The trans-membrane pressure was 2 bars and the cross-flow velocity was 3 m/s.*

The BSA retention was measured every five minutes and appeared to be constant during the 20 minutes of filtration of the BSA solution; the retention was 98%. Estimation of the retention according to Ferry 's equation (equation 4) using the pore size of the membrane (diameter 50 nm) gives R=23%. If the thickness of the adsorbed layer is taken into account the calculated retention is R=31%. Thus the experimental retention is much higher than could be expected from the pore radius of the membrane. This implies that the flux reduction during retention measurements is caused by the formation of a cake layer at the surface. The BSA concentration in the permeate is to a large extent determined by the retention of the cake layer.

Another possibility is that the large pores in the membrane are rapidly plugged by BSA molecules. It was shown that a rapid flux decline occurs during the first minutes of filtration of the BSA solution. This flux decline will be strongest for the larger pores. Through these large pores there will initially be a large convective flow. This flow will drag along the protein molecules resulting in a fast agglomeration followed by aggregation of the protein molecules at the pore entrance. This effect was also found by Kim et al.[29] who examined the nature of fouling deposits for high and low flux ultrafiltration membranes. For high flux membranes flux reduction was mainly caused by pore plugging. When in the experiments presented here after 5 minutes the retention of the membranes is measured all large pores are possibly blocked by aggregates of BSA and the retention is much higher than would be expected from the pore size distribution of the membrane. Based on the smaller average pore size of the non-plugged pores the flux would be 25 $l.m^{-2}h^{-1}bar^{-1}$ since the contribution of the small pores to the total permeability is 25 % as can be seen in figure 12.

The experiments were also performed at trans-membrane pressures of 0.5 and 1 bar. The resistance of the fouling layer was $R_f=1.7*10^{12}\ m^{-1}$ for 0.5 bar and $R_f=3.0*10^{12}\ m^{-1}$ for 1 bar. These results are in agreement with expectations since at a lower trans-membrane pressure the compaction of the cake-layer at the membrane surface is less and its resistance is lower. The retention was not influenced by the trans-membrane pressure and was 98% in all three cases.

The membranes used by Pellegrino and co-workers[15] showed a higher membrane resistance ($R_m>1.7*10^{13}\ m^{-1}$) compared to the membrane resistance found for membrane A. For their polycarbonate membrane (surface treated with PVP) the fouling resistance was larger than the membrane resistance while for the cellulose membrane the fouling resistance was smaller. For the polycarbonate membrane they found that the flux reduction due to concentration polarization was much smaller than the reduction due to fouling which is also the case for membrane A. A quantitative comparison of the results as presented here and those found by Pellegrino and co-workers is not possible because the BSA concentrations of the feed solutions were not the same. However the same trend was found for membrane A as for the PVP treated polycarbonate membrane of Pellegrino and co-workers.

### *5.4.5 Adsorption of BSA*

The adsorption behavior of hollow fiber membranes prepared from spinning solutions which differed in concentration and in molecular weight of PVP has been measured and compared with commercially available polysulfone

membranes. Membrane A was used to determine the adsorption time and the BSA concentration necessary to obtain a plateau value of the flux reduction.

The time dependency of the adsorption process was determined using a solution that contained 5 g/l BSA. In figure 18 the relative flux reduction (1-$RF_W$) is plotted versus the adsorption time. It can be seen that after 24 hours the plateau value is practically reached. For all other experiments the adsorption time used was 24 hours.

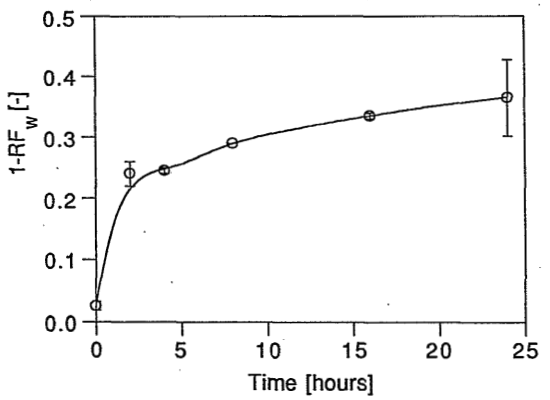


*Figure 18. The relative flux reduction of membrane A after different contact times for adsorption from a 5 g/l BSA solution at pH 7.4.*

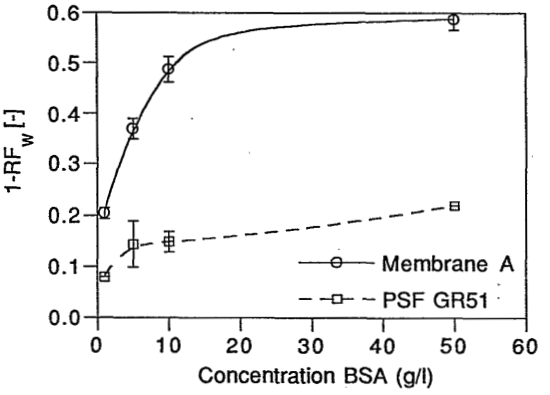


*Figure 19. The relative flux reduction of membrane A and GR51 after contact with BSA solutions which differed in BSA concentration at pH 7.4 for 24 hours.*

The concentration dependency of the adsorption process for membrane A and for a flat polysulfone membrane (GR51PP) are represented in figure 19. For the polysulfone membrane the plateau value is reached at a lower BSA concentration. Also the relative flux reduction is much lower than for membrane A. The adsorption behavior of membrane A as it is shown in the figures 18 and 19 is comparable with the hypochlorite treated PEI/PVP microfiltration membranes measured by Roesink et al.[22]. For the following experiments a BSA solution containing 10 g/l BSA was used.

In table 3 hollow fiber membranes (and one flat sheet membrane) of commercial origin are compared with fibers spun in our laboratory. The effect of amount and molecular weight of PVP added in the spinning dope is investigated.

*Table 3. Water flux and relative flux reduction for a number of membranes. The relative flux reduction was determined after contacting the fibers for 24 hours with a 10 g/l BSA solution at pH 7.4. The numbers indicate the polymer concentrations in the spinning solutions. All membranes containing PES are lab-made hollow fibers with the selective toplayer at the outer surface. These membranes were treated with hypochlorite before the flux measurement was performed.*

| Membrane (wt%/wt%) | water flux ($J_0$) [$l.m^{-2}h^{-1}bar^{-1}$] | ($1-RF_W$) [-] |
|---|---|---|
| NTU(3250)* | 63 | 0.25 |
| NTU(3050)* | 100 | 0.28 |
| Psf (GR51)** | 50 | 0.15 |
| PES 20 | 3 | 0.20 |
| PES/PVP(K15) 20/10 | 87 | 0.42 |
| PES/PVP(K60) 20/10 | 75 | 0.37 |
| PES/PVP(K90) 20/10 | 172 | 0.34 |
| PES/PVP(K90) 20/7.5 | 200 | 0.54 |
| PES/PVP(K90) 20/12.5 | 118 | 0.30 |
| membrane A: PES/PVP 20/5(K90)/5(K30) | 100 | 0.49 |

* Hollow fiber with selective toplayer at the bore side
** Flat sheet membrane

The flux reduction is less severe if in the spinning solution the concentration of PVP was larger or the molecular weight was higher, thus for a higher PVP content of the membranes.

The results show that the adsorption of BSA causes a more severe reduction of the water fluxes for the membranes containing PVP compared to PES or polysulfone membranes. One should be very careful when drawing conclusions from these measurements because the configuration is not the same for all membranes (flat sheets and hollow fibers). Also the fluxes are different meaning that the morphological structures of the membranes are not the same. Due to differences in morphology it can not be concluded definitely that at the outer surface and the pore wall surfaces of the PVP containing membranes more protein molecules have adsorbed.

As has been done for the retention measurements the flux decrease due to adsorption can be used to calculate the decrease in pore size by adsorption of BSA on the pore wall using equation 5. For membrane A the flux reduction is 49% which is equal to the flux reduction for the retention measurement (see paragraph 5.4.4). Therefore $\Delta r_{pore} / r_{pore} = 0.16$ and with a mean pore radius of 25 nm the thickness of the adsorbed layer is 4 nm. Thus during the adsorption time a monolayer of BSA molecules on the pore walls is formed assuming that the pore structure of the membrane can be described by parallel cylindrical pores. The formation of a cake-layer on top of the membrane is not likely to occur in these experiments since no pressure gradient was used to force the proteins towards the membrane.

The influence of pH of the BSA solution has also been investigated. The iso-electric point of BSA is at pH 4.7. Because the protein structure is very compact at this pH the amount of protein adsorbed is expected to be high. At pH further away from this point the adsorption is usually lower. However in figure 20 it can be seen that both membrane A and the GR51 membrane show a different behavior. For membrane A the flux reduction at pH 6 is about the same as for the polysulfone membrane but the flux reduction increases drastically at higher pH.

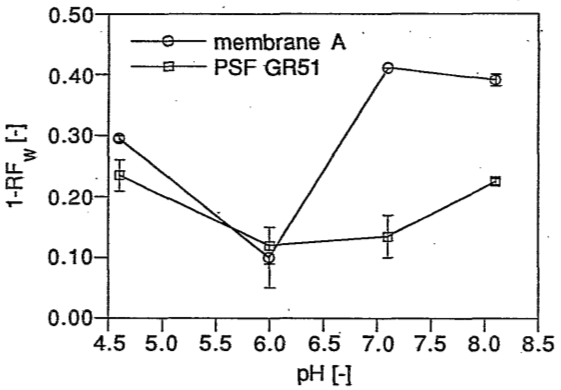


*Figure 20. The relative flux reduction of membrane A and GR51 after contact with a 10 g/l BSA solution at different pH for 24 hours.*

A comparable dependency of the flux reduction on pH for hypochlorite treated membranes was found by Roesink et al.[22]. Based only on these experiments it is not possible to find an explanation for this behavior. A hypothesis is that the reaction of hypochlorite with the polymeric membrane material induces (positively) charged groups on the membrane surface that have a specific interaction with BSA at high pH. A study on the mechanism of the reaction of PVP with hypochlorite as is presented in chapter 4 indicates that a small amount of carboxylic groups and amino groups are formed upon reaction. It is not known whether these groups can have special interaction with BSA. The flux reduction for the polysulfone membrane also increases for BSA solutions at pH higher than pH 6 although the effect is not as strong as for membrane A. An explanation for this behavior could not be found.

## 5.5 Final remarks

The characterization methods used in this chapter are combined by discussing the characteristics of one type of membrane (membrane A) that was studied with these methods. Membrane A was prepared by the dry-wet spinning technique from a polymer solution containing 20 wt% PES, 5 wt% PVP K90, 5 wt% PVP K30 and 5 wt% water in NMP. The selective toplayer of the asymmetric membrane was at the outer surface of the hollow fiber.

The PVP content of the membrane is very low compared with the PVP content of the casting solution though the concentration at the surface is higher than the mean concentration in the film. The amount of PVP is

reduced even further by the hypochlorite treatment. Since PVP is a hydrophilic polymer the amount of PVP determines the hydrophilicity of the membrane material. It is generally assumed that hydrophilic surfaces are less susceptible to protein adsorption. The adsorption study showed that for membranes having a higher PVP content the flux reduction after adsorption of BSA is less severe.

The flux reduction for membrane A (and other membranes containing PVP) is higher than the reduction for membranes without PVP. It is very likely that due to a different morphology of the membranes containing PVP the adsorption of proteins has a more profound effect on the water flux. It would therefore be better to measure the amount of protein adsorbed on non-porous films by labelling methods. Based on the assumptions that *i)* the flux through membrane A can be described by the Poiseuille equation and *ii)* the mean pore diameter of the membrane is 50 nm, the contact of the membrane with the BSA solution results in a mono-layer adsorption of protein on the surface of the pores.

Using different microscopic techniques it was shown that the selective toplayer of the ultrafiltration membranes consists of a nodular structure. For membrane A the mean nodule size is estimated from FESEM photographs and the diameter is 40 nm. A specific toplayer thickness can not be derived from these pictures since the structural changes towards larger pores in the sublayer is very gradual. In the toplayer of membrane A no pores can be seen. This means that either the pores are smaller than about 40 nm or the pores are not visible because *i)* the pore structure has collapsed upon drying the membrane or *ii)* the pores have been covered by the gold or carbon coating layer.

The pore size distribution of membrane A as has been determined with the liquid displacement method has a maximum in the differential pore size distribution at a pore diameter of 50 nm. Another maximum is present at a smaller pore size (diameter smaller than 20 nm). However the contribution of these pores to the total permeability of the membrane is only small.

The pores in membrane A having a diameter larger than 50 nm should appear on photographs made with the FESEM technique. Even after drying the membrane and coating it with a carbon layer pores as large as 50 nm should be visible. The number of pores larger than 50 nm is very small though ($25*10^6$ $1/m^2$) and the probability that one of these pores appears on a photograph is 0.02 %.

The retention of membrane A for BSA is 98%, the flux of the BSA solution is half the flux of pure water. Since the hydrodynamic dimensions of BSA are smaller than 14 nm one would expect that a considerable amount of this protein can pass through the membrane. Since this is not the case the reduction of the permeability is more likely to be caused by pore plugging or by the formation of a cake layer than by adsorption of proteins on the pore walls.

## 5.6 Conclusions

The PVP content of membranes prepared from a polymer solution containing PES and PVP can be measured. The amount of PVP in the ultimate membrane is related to the concentration and molecular weight of PVP in the polymer solution and to the time between demixing and solidification of the nascent membrane.

Using electron microscopy the nodular structure of PES/PVP ultrafiltration membranes can be visualised. Determination of pore sizes and toplayer thickness of these membranes is not possible by any of the microscopic techniques.

The liquid displacement method indicates that the pore sizes of PES/PVP membranes can be described by a bimodal distribution curve. Two maxima are found: at pore diameters of 50 nm and 15-20 nm respectively.

The flux of the membrane for a BSA solution is much lower than the pure water flux. The retention for BSA is 98%. These results are consistent with the pore size distribution found by the liquid displacement method if it is assumed that during filtration a cake layer is formed on top of the membrane or if pore plugging of the large pores occurs.

The flux reduction of PES/PVP membranes after adsorption of BSA is smaller for membranes having a higher PVP content. Comparison of these membranes with membranes without PVP is not possible due to large differences in morphology.

**Acknowledgement**
The authors would like to thank J.M. Schakenraad (Univerisity of Groningen) for performing the TEM photographs, M.A. Smithers for the FESEM photographs, and S.S. Sheiko for the AFM photographs. A.H.J. van

den Berg performed the XPS measurements and A. Montanaro the MEA measurements. G. Capannelli and A. Bottino (University of Genoa) are acknowledged for the discussions on the liquid displacement technique, H. Teunis is thanked for the preparation of the membranes.

## 5.7 Literature

1. Chapter 3 of this thesis, A new spinning technique for hollow fiber ultrafiltration membranes, also published in J. Mem. Sci. **78** (1993) 93
2. W. Norde, Adsorption of proteins from solution at the solid-liquid interface, Adv. Coll. Int. Sci., **25** (1986) 267
3. H. Bechold, M. Schlesinger, K. Silbereisen, Porenweite von Ultrafiltern, Koll. Z. **55** (1931) 172
4. F. Erbe, Blockierungsphänomene bei Ultrafiltern, Koll. Z. **59** (1932) 195
5. *a)* G. Capannelli, F. Vigo, S. Munari, Ultrafiltration membranes - Characterization methods, J. Mem. Sci., **15** (1983) 289
   *b)* G. Capannelli, I. Becchi, A. Bottino, P. Moretti, S. Munari, Computer driven porosimeter for ultrafiltration membranes. In: Characterization of Porous Solids, K.K. Unger (editor), Elsevier, Amsterdam 1988, p 283
   *c)* S. Munari, A. Bottino, P. Moretti, G. Capannelli, I. Bechi, Permporometric study on UF membranes, J. Mem. Sci., **41** (1989) 69
6. F.P. Cuperus, C.A. Smolders, Characterization of UF membranes: Membrane characteristics and characterization techniques, Adv. Coll. Int. Sci., **34** (1991) 135
7. G.B. van den Berg, C.A. Smolders, Flux decline in ultrafiltration processes, Desalination, **77** (1990) 101
8. L. Y. Lafreniere, F.D.F. Talbot, T. Matsuura, S. Sourirajan, Effect of poly(vinyl pyrrolidone) additive on the performance of poly(ether sulfone) ultrafiltration membranes, Ind. Eng. Chem. Res. **26** (1987) 2385
9. H.D.W. Roesink, Microfiltration: Membrane development and module design, thesis University of Twente, Enschede, 1989
10. *a)* R.M. Boom, Th. van den Boomgaard, C.A. Smolders, Equilibrium thermodynamics of a quaternary membrane forming system with two polymers. 1. Theory; submitted for publication to Macromolecules
    *b)* R.M. Boom, H.W. Reinders, H.H.W. Rolevink, U. Cordilia, Th. van den Boomgaard, C.A. Smolders, Equilibrium thermodynamics of a quaternary membrane forming system with two polymers. 2. Experimental; submitted for publication to Macromolecules
11. I.M. Watt, The principles and practice of electron microscopy, Cambridge University Press, Cambridge, 1985
12. P. Echlin, Low temperature microscopy and analysis of plant material. In: Past, present and future of electron microscopy in agricultural research., A. Boekestein (ed.) Wageningen, 1991, p. 75

13. G. Binnig, C.F. Quate, Ch. Gerber, Atomic force microscope, Phys. Rev. Lett., **12** (1986) 930
14. P. Dietz, P.K. Hansma, K.H. Herrmann, O. Inacker, H.D. Lehmann, Atomic-force microscopy of synthetic ultrafiltration membranes in air and under water, Ultramicroscopy, **35** (1991) 155
15. *a)* A.P. Peskin, M.K. Ko, J.J. Pellegrino, Three layer membrane model for characterizing ultrafiltration membranes, J. Mem. Sci., **60** (1991) 195
*b)* M.K. Ko, J.J. Pellegrino, Determination of osmotic pressure and fouling resistances and their effects on performance of ultrafiltration membranes, J. Mem. Sci., **74** (1992) 141
16. J.D. Ferry, Ultrafilter membranes and ultrafiltration, Chem. Rev., **18** (3) (1936) 373
17. B.D. Fair, A.M. Jamieson, Studies of protein adsorption on polystyrene latex surfaces, J. Coll. Int. Sci., **77**(1980) 525
18. E. Matthiasson, The role of macromolecular adsorption in fouling of ultrafiltration membranes, J. Mem. Sci.,**16** (1983) 23
19. P. Aimar, S. Baklouti, V. Sanchez, Membrane-solute interactions: influence on pure solvent transfer during ultrafiltration, J. Mem. Sci., **29** (1986) 207
20. J.L. Nilsson, Fouling of an ultrafiltration membrane by a dissolved whey protein concentrate and some whey proteins, J. Mem. Sci., **36** (1988) 147
21. L.J. Zeman, Adsorption effects in rejection of macromolecules by ultrafiltration membranes, J. Mem. Sci., **15** (1983) 213
22. H.D.W. Roesink, M.A.M. Beerlage, W.Potman, Th. van den Boomgaard, M.H.V. Mulder, C.A. Smolders, Characterization of new membrane materials by means of fouling experiments. Adsorption of BSA on polyetherimide-polyvinylpyrrolidone membranes, Coll. Surf., **55** (1991) 231
23. J.H. Hanemaaijer, T. Robbertsen, Th. van den Boomgaard, J.W. Gunnik, Fouling of ultrafiltration membranes, the role of protein adsorption and salt precipitation, J. Mem. Sci., **40** (1989) 199
24. E. Pella, B. Colombo, Simultaneous C-H-N and S microdetermination by combustion and gas chromatography, Microchimica Acta, I, 1978, p 271
25. A.B. Christie, X-ray photoelectron spectroscopy, In: Methods of surface analysis, J.M. Walls (ed.), Cambridge university press, Cambridge, 1989, p 127
26. E.H. Blaauw, J.A. Oosterbaan, J.M. Schakenraad, An improved Epon embedding for biomaterials, Biomaterials, **10** (5), (1989), 356
27. H.G. Dikland, S.S. Sheiko, L. van de Does, M. Moller, A. Bantjes, An atomic force scanning microscopy study on the morphology of elastomer-coagent blends, accepted for publication in Polymer
28. P.C. Painter, J.F. Graf, M.M. Coleman, Effect of hydrogen bonding on the enthalpy of mixing and the composition dependence of the glass transition temperature in polymer blends, Macromolecules, **24** (1991) 5630
29. K.J. Kim, A.G. Fane, C.J.D. Fell, D.C. Joy, Fouling mechanisms of membranes during protein ultrafiltration, J. Mem. Sci., **68** (1992) 79

6

# The Formation of Nodular Structures in the Toplayer of Ultrafiltration Membranes

I.M. Wienk, Th. van den Boomgaard, C.A. Smolders

## Summary

In this chapter the formation of nodular structures in the toplayer of ultrafiltration membranes is considered. A critical review of mechanisms described in literature is given. Flat sheet poly(ether sulfone) membranes and hollow fiber poly(ether sulfone)/poly(vinyl pyrrolidone) membranes were made by coagulation of a polymer solution in a non-solvent medium under different circumstances. From these experiments a number of empirical rules are found to describe the resulting morphology of the toplayer. A new mechanism for the formation of a nodular structure is proposed. It is based on the small diffusion coefficient of the polymer molecules compared to the diffusion coefficient of solvent and non-solvent combined with a high degree of entanglement of the polymer network. For instable compositions phase separation will proceed by growth in amplitude of concentration fluctuations. The rapid diffusional exchange of solvent for non-solvent in the toplayer leads to vitrification of the maxima of the concentration fluctuations which form the nodules. Complete disentanglement of the polymer chains between the nodules is not reached which explains the small pores and the low porosity of ultrafiltration membranes.

## 6.1 Introduction

Asymmetric polymeric ultrafiltration membranes made by the phase inversion technique usually have a toplayer consisting of closely packed spheres or nodules. The pore sizes of these membranes are between 1 and 100 nm and the surface porosities are very low (typically between 2 en 7 %)[1]. The pore size distribution of ultrafiltration membranes often has two maxima as

is reported in literature[2-4] and is also shown in chapter 5. The presence of nodules is reported by many researchers[1,4-17], but an appropriate mechanism for the formation has not yet been found.

In our research on the development of hollow fiber ultrafiltration membranes from the blend poly(ether sulfone) (PES) and polyvinyl-pyrrolidone (PVP) as described in chapters 2 and 3[18] a lot of membranes have been spun showing a nodular structure in the toplayer. In addition to these results flat membranes were made from poly(ether sulfone). These results are thought to give a better insight in the formation of nodular structures.

## 6.2 Theory: a literature study on the mechanisms for the formation of nodular structures

Panar et al.[2] were among the first to report on non-crystalline spheres of about 60 nm in the toplayer of reverse osmosis membranes. The spheres were called micelles and were thought to be present already in the casting solution. Reverse osmosis cellulose acetate (CA) membranes have been investigated by Kesting[6]. Nodules of 50 to 100 nm were believed to be para-crystalline in nature. The nodules are thought to be present in the casting solution and are immobilised in the toplayer due to extremely rapid solvent exchange upon immersion into water. In a later stage, aggregation into larger units (300-700 nm) occurs until they have disappeared in the final gel stage. For CA para-crystallinity is likely to occur, however nodules are also found in membranes made from amorphous polymers such as PES as is shown in this chapter.

The idea that precursors of the entities seen in the membrane structure are initially present in the casting solution is also used by other authors. Inhomogeneity of a polymer solution of cellulose acetate close to the binodal was shown by Kunst et al.[7,8]. Using activation energies of viscous flow and light scattering measurements evidence was found for a supermolecular structure in the polymer solution. The structure was more profound in case of high CA concentrations and for compositions close to the binodal. More structure in the polymer solution resulted in membranes with smaller pores from which Kunst concluded that a network was formed instead of small particles that would aggregate. Other researchers like Boom et al.[19] conclude from light scattering measurements of polymer solutions with a composition close to the binodal composition that large concentration fluctuations are present in the solution. Miyano et al.[9] defined a hydrodynamic radius of the polymer in the casting solution. They found a relation between this radius and the average pore size at the membrane surface. However the

hydrodynamic radii were about 30 Å whereas the pore sizes were ten times as large. Therefore these authors assumed the pores to be solvent filled spaces or spaces generated between aggregates of polymer molecules.

Kamide et al.[10] describe aggregation of primary polymer particles of 20 nm as a step in the membrane formation process. According to this theory the primary particles are not present in the casting solution but they are formed by nucleation of a polymer rich phase. Furthermore the aggregation process is very slow as it depends on the mobility of primary particles and on the surface free energy. The cellulose membranes studied by Kamide et al. were made from a casting solution containing 3-10 wt% cellulose. Phase separation was induced either by evaporation of the solvent when a non-solvent was present in the casting solution, or by immersion in a coagulation bath containing 30% solvent. For these conditions phase separation takes place at the low polymer concentration side of the critical point. For this system the mechanism as proposed by these authors (nucleation of the polymer rich phase) is correct; however other researchers referred to nucleation of a polymer rich phase to explain structures formed from more concentrated solutions (definitely beyond the critical point) and under much faster precipitation conditions.

Recently Kesting[4] introduced four tiers of structures in membranes: macromolecules, nodules (20 nm), nodular aggregates (40-100 nm) and supernodular aggregates. With this concept Kesting explains membrane formation as an aggregation process stopped at different stages without taking into account the casting conditions and the type of polymer. In this model the ultrafiltration membranes consist of nodular aggregates and the pores are the spaces between incompletely coalesced nodule aggregates.

Broens et al.[11] found nodules in the toplayers of poly(dimethyl phenylene-oxide) (PPO) membranes. PPO is a crystalline polymer. Nodules were described as structural units in the skin layer formed under conditions of fast diffusion processes and originating from gelation or crystallization. According to Ray et al.[12] nodules result from perturbations at the interface of polymer solution and coagulation bath. The perturbations are formed due to concentration and temperature fluctuations (Marangoni effect). Normally they decay but strong interactions between the coagulation medium and the solvent in the polymer solution can lead to stabilization and growth of these perturbations. But if such a surface phenomenon would cause nodule formation it would not be possible to explain several layers of nodules in the toplayer.

In the membrane formation mechanism as described by Kimmerle et al.[13] the

structure obtained after phase inversion of a polymer solution is dependent on the ratio of the polymer rich and the polymer lean phase at the moment of phase separation. In the phase diagram this ratio is determined by the position of the polymer composition at the tie-line. Nodular structures are formed in the toplayer of a membrane if strong non-solvents are used. A strong non-solvent is a liquid showing a high interaction with the solvent and a low interaction with the polymer. The use of a strong non-solvent means that upon immersion in a coagulation bath the diffusion processes are very rapid. Kimmerle et al. state that the composition of the polymer solution deeply enters the immiscibility gap in such a way that the volume of the polymer rich phase is very small. Phase separation then would result in a discontinuous polymer rich phase consisting of spheres. However calculations using mass transfer models as used by Reuvers et al.[20] show that immersion of a polymer solution into a bath of a strong non-solvent causes an increase of the polymer concentration in the toplayer.

Pinnau et al.[14] prepared polysulfone gas separation membranes from a solution containing a volatile solvent and a non-volatile non-solvent. After evaporation of the solvent the polymer solution was quenched in a non-solvent bath. In these gas-tight membranes the toplayer consisted of nodules. The nodular structure was said to be formed by spinodal demixing. In a later stage collapse of the nodules occured due to capillary forces. Spinodal demixing of the polymer solution resulting in a nodular structure in the toplayer of ultrafiltration membranes is also shown in the appendix to this thesis[15]. In normal diffusion processes spinodal demixing is not possible because diffusion coefficients become zero as the composition reaches the spinodal curve. In the apppendix[15] it is shown that the composition path is able to cross the spinodal curve due to the relatively small mobility of the polymer molecules compared to that of the components solvent and non-solvent. Later Boom et al.[21] found strong indications that for membrane systems with a polymeric additive such as PVP spinodal demixing occurs resulting in a bicontinuous structure. For these membranes the sub-structure is bicontinuous with a large pore volume but in the toplayer a dense nodular structure is found.

Recent developments in microscopic techniques can give better insight in the fine structures of ultrafiltration toplayers[16,17] as is also shown in chapter 5. Commercial polysulfone and poly(ether sulfone) membranes have been studied by Dietz et al.[1] using atomic force microscopy. No information was given on the preparation conditions of the membranes. However from the pictures shown it can be concluded that differences in packing modes of nodules of equal size can lead to membranes that differ in pore structure and

performance.

## 6.3 Experimental

Poly(ether sulfone) (PES) was purchased from ICI (Victrex 5200P, $M_w$ 44,000 g/mole). Two kinds of poly(vinyl pyrrolidone) (PVP) from Janssen Chimica were used, K90 ($M_w$ 507,000 g/mole) and K30 ($M_w$ 18,000 g/mole). The weight average molecular weights of the polymers were determined using GPC. The solvent used was 1-methyl-2-pyrrolidone (NMP). The non-solvents were water and 1-pentanol. NMP and 1-pentanol were purchased from Merck (analysis grade).

Flat membranes were made by casting a polymer solution on a glass plate followed by immersion in a water bath of 25°C. Hollow fibers were spun using a dry-wet-spinning technique as described in chapter 2 or a wet spinning technique with a triple orifice spinneret as is shown in chapter 3[18].

The membrane morphology was studied using a scanning electron microscope (SEM) (JEOL, JSM T220A). The water in the pores was replaced in a sequence of ethanol and hexane; after this the membranes were dried in air. For the cross-sections the membranes were broken in liquid nitrogen. For the SEM a thin (30 nm) gold layer was sputtered on the membranes using a sputter apparatus (Balzers Union SCD 040). Details on the use of microscopy for the characterization of membrane structures are discussed in chapter 5.

## 6.4 Results and discussion

First, some qualitative relations for the formation of nodular structures are derived. In chapter 5 it is shown that the nodules as they are imaged with the SEM appear to be larger than their realistic size due to the thickness of the gold coating layer. Direct estimations of the nodule sizes from SEM photographs are therefore not accurate and can only be used for qualitative mutual comparison.

### *6.4.1 Flat sheet PES membranes*

*The polymer concentration in the casting solution*

Flat sheet membranes were cast from solutions containing 10, 20, 30 or 40 wt% PES in NMP and coagulated in water. From the 10 wt% PES solution only a very thin film could be obtained since most of the polymer was dispersed in the coagulation bath. Photographs of the toplayer of these membranes are shown in figure 1. The more concentrated polymer solution

results in a membrane with a thicker toplayer. However the nodule sizes appear to be the same for all three membranes.

*Addition of non-solvent to the casting solution*
Homogeneous (transparent) solutions could be made containing 20 wt% PES in NMP and 3, 6 or 9 wt% water. Membranes made from these solutions are shown in figure 2. It can be seen that the nodule sizes are smaller for the membrane cast from the 9 wt% water solution. This indicates that nodules do not arise from aggregates present in the polymer solution because these aggregates would be larger if the composition of the solution lies closer to the binodal.

*Change in viscosity of the coagulation bath*
Thin films of a solution containing 25 wt% PES in NMP were coagulated in different water baths. The viscosity of the coagulation baths was increased by the addition of different amounts of PVP(K90). It was assumed that the only effect of PVP on the phase separation process is a change in viscosity (i.e. in kinetics), not a change in thermodynamics. The addition of PVP to the coagulation bath slows down the diffusion of both solvent and non-solvent. Photographs of the toplayers of these membranes are given in figure 3. It is clear that the nodular structure is not present in case the phase separation process is slow.

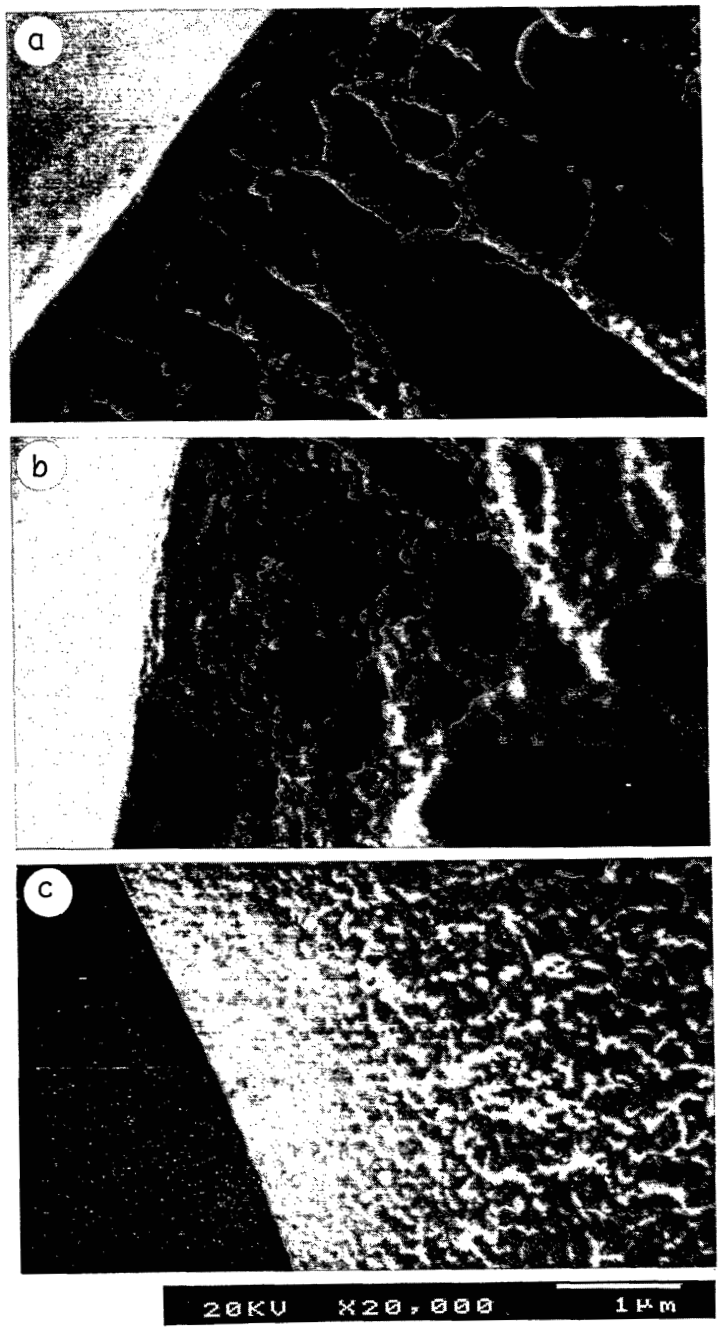


*Figure 1. Cross-sections (SEM) of the toplayers of PES membranes cast from solutions with different polymer concentrations: a) 20 wt%, b) 30 wt% and c) 40 wt%. Membranes were coagulated in a water bath at room temperature.*

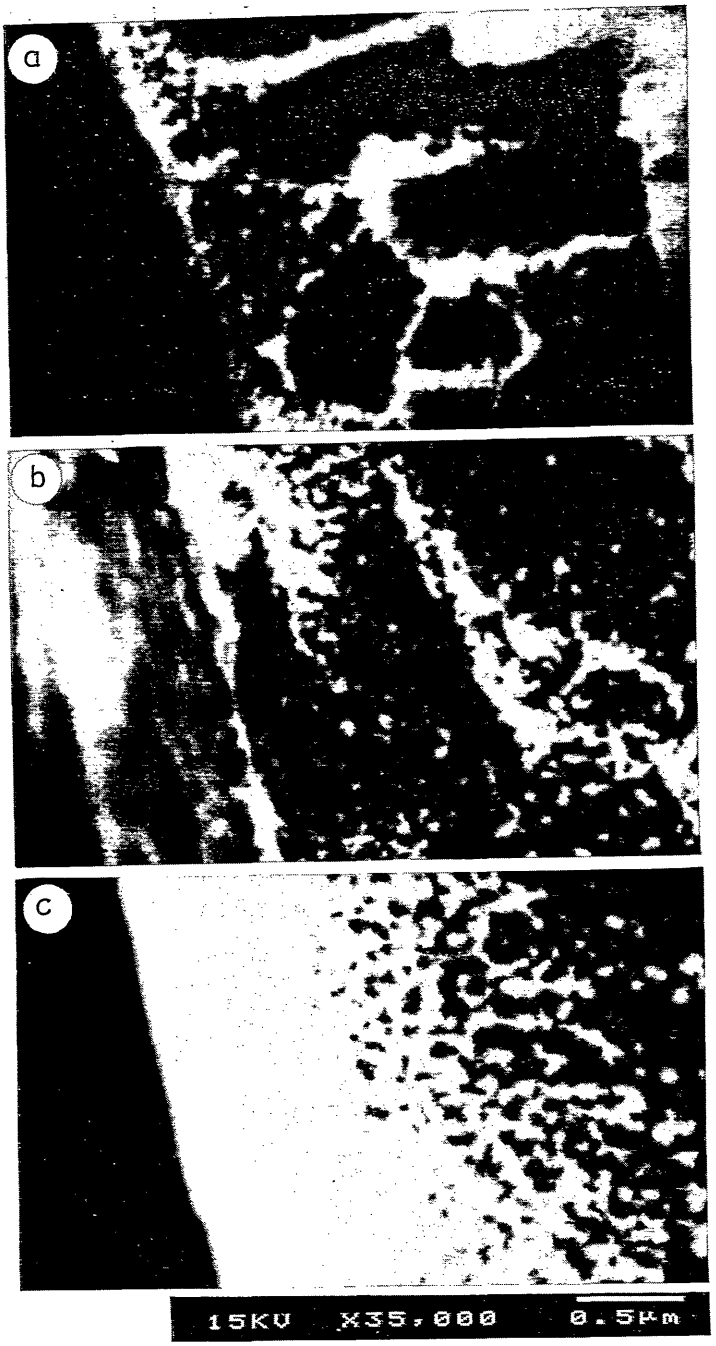


*Figure 2. Cross-sections of the toplayers of PES membranes cast from 20 wt% polymer solutions containing different concentrations of water: a) 3 wt%, b) 6 wt% and c) 9 wt%. The membranes were coagulated in a water bath at room temperature.*

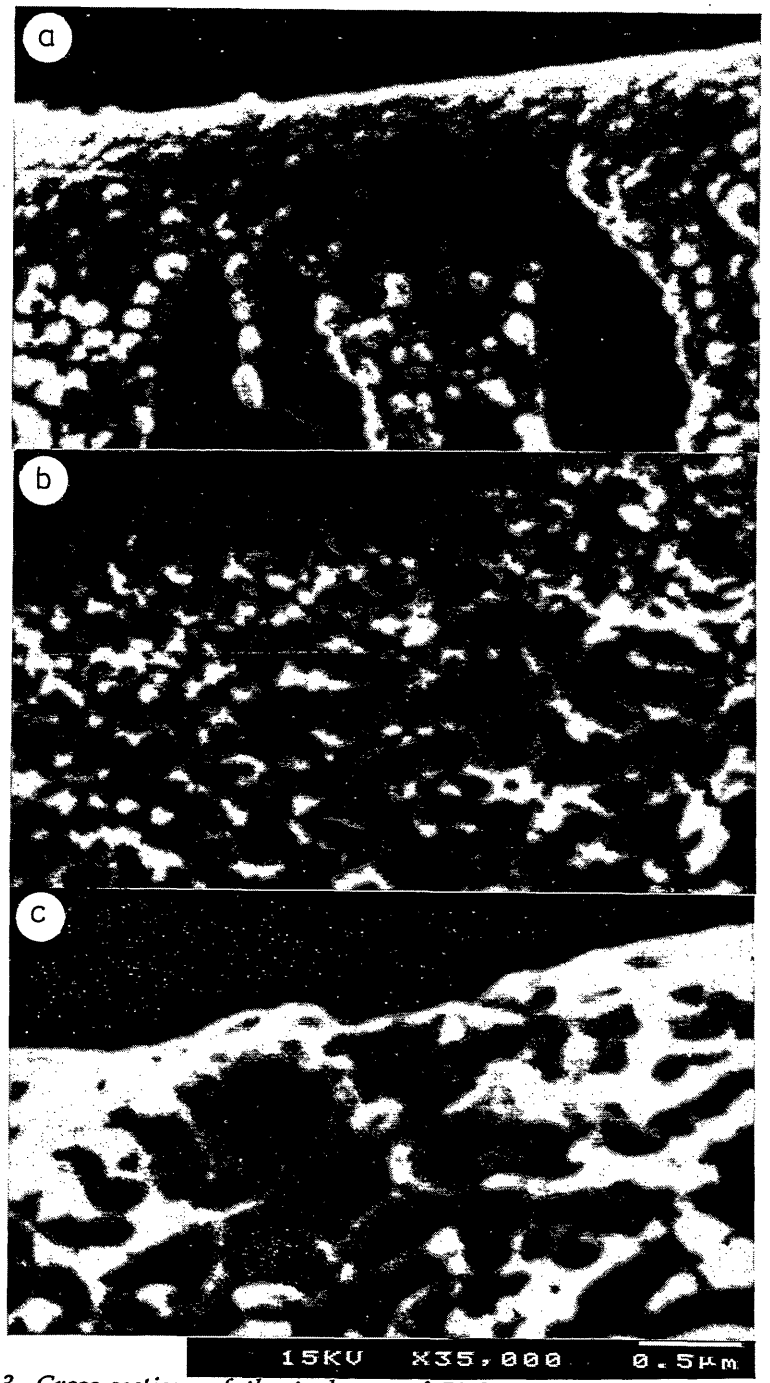


*Figure 3. Cross-sections of the toplayers of PES membranes (25 wt% polymer solution) coagulated in water with different amounts of PVP resulting in different viscosities: a) low viscosity (0.3 Pa.s), b) medium viscosity (1.1 Pa.s) and c) high viscosity (5 Pa.s).*

### *6.4.2 Hollow fiber PES/PVP membranes*

During the dry-wet-spinning of a polymer solution containing PES and PVP as described in chapter 2 the nascent membranes pass an airgap after which they enter a water bath of 20°C. The humidity in the airgap has been varied by applying a mixture of a dry and a water saturated nitrogen stream. The surface structure of the membranes obtained can be seen in figure 4. It is clear from these pictures that pore sizes at the surface are larger if more water vapor has been applied in the airgap. The polymer material surrounding the pores possesses a nodular structure. The sizes of the nodules are larger when the partial pressure of the water vapor in the airgap is higher but at the highest vapor pressure the membrane does not show a nodular structure.

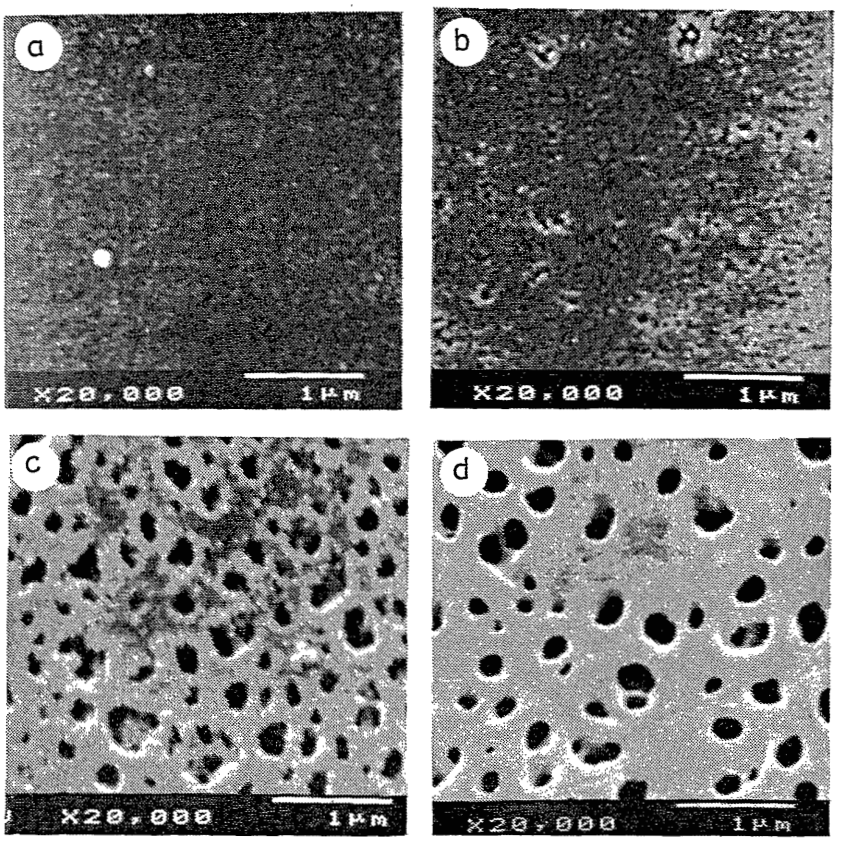


*Figure 4. Morphology of the surface of hollow fiber PES/PVP membranes spun with the dry-wet technique for different humidities of the airgap: a) 0.036 bar, b) 0.062 bar, c) 0.101 bar, d) 0.114 bar. After a residence time of 2.2 seconds in the airgap the fibers entered a water bath of 20 °C. The polymer solution used for spinning contained 20 wt% PES, 12.5 wt% PVP (K90), and 5 wt% water in NMP.*

Two more examples of the formation of a nodular structure in PES/PVP membranes will be mentioned here. In these cases the coagulation media used were not so strong a non-solvent for PES as in the case of water. The membrane shown in figure 5a was formed by applying a coagulation medium consisting of 60 wt% solvent (NMP) in water. In this situation the driving force for the outdiffusion of solvent (which is dependent on the concentration difference) is reduced. The membrane shown in figure 5b was made using a two bath system in which 1-pentanol was the first coagulation medium and water the second. The membrane formation for this type of spinning technique is discussed in chapter 3[18]. In the 1-pentanol medium the indiffusion of non-solvent is small so there the outdiffusion of solvent is in excess. Before the nascent membrane reaches the water bath, indiffusion of non-solvent can not occur. Still the presence of PVP causes demixing of the polymer solution already in the 1-pentanol medium as is shown in chapter 3[18].

For the two membranes shown in figure 5 the diffusion processes of solvent and non-solvent upon immersion of the polymer solution in the coagulation medium were slow when compared to the diffusion processes upon coagulation in a water bath. If a polymer solution consists of PES only, the slow diffusion processes does not cause the formation of a nodular structure as was shown in figure 3c. However the presence of PVP leads to a nodular structure even under conditions of slow diffusion of solvent and non-solvent. The two photographs in figure 5 also show that the nodule sizes are the smallest at the surface and increase further into the film.

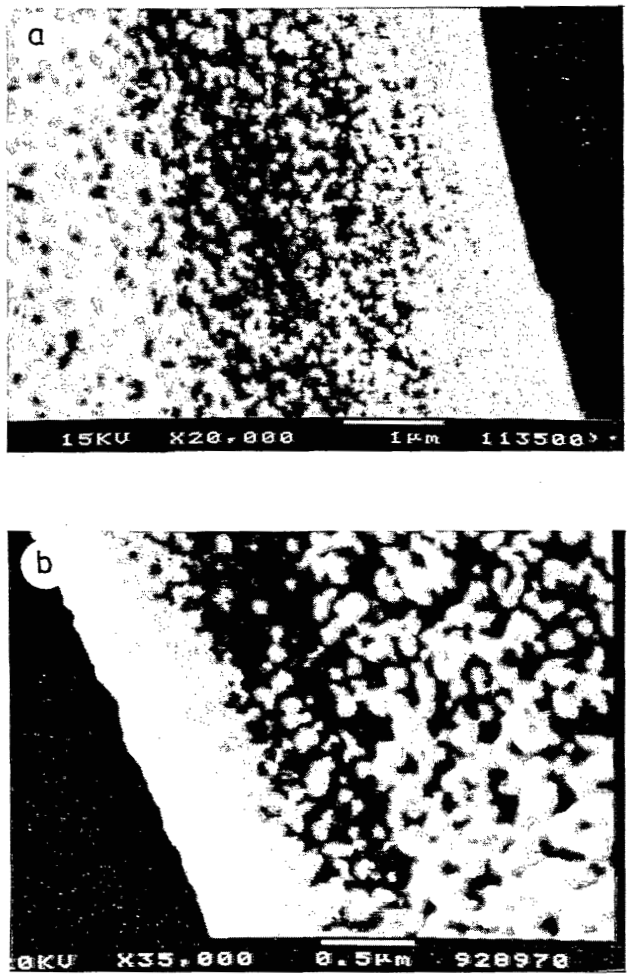


*Figure 5. Cross sections of the morphology of the toplayer of hollow fiber PES/PVP membranes. The polymer solution contained 20 wt% PES and 10 wt% PVP. Coagulation media were: a) bore side;, internal coagulation medium was 60 wt% NMP in water, b) outer surface;, spun with triple layer spinneret, external coagulation medium was 1-pentanol. After 0.5 seconds contact time with the first medium the fibers entered a water bath of 20 °C.*

From the experiments the following conclusions can be drawn:
- nodules are polymer spheres, present in the toplayers of asymmetric ultrafiltration membranes
- the diameter of nodules is difficult to estimate but it is in the order of 50 nm
- nodules are formed in a phase separation process under conditions of fast outdiffusion of solvent and fast indiffusion of non-solvent
- since PES is an amorphous polymer nodule formation is not caused by (partial) crystallization
- the size of the nodules is the smallest at the surface and increases deeper into the film until it gradually transforms into a porous structure
- the size of the nodules is smaller if the composition of the original polymer solution is lying closer to the binodal composition
- the size of the nodules is independent of the polymer concentration of the casting solution
- there is no indication that nodules are agglomerates of smaller spheres
- if PVP is present in the polymer solution the nodules are also formed at less rapid coagulation conditions
- a nodular structure can also be formed in a second coagulation step during spinning
- the size of the nodules is not directly linked to a certain pore size (this is also clear from the work of Dietz et al.[1]).

## 6.5 A new mechanism for the formation of nodular structures

### *6.5.1 Membranes prepared from a solution containing one polymer*

In the first moments upon immersion of a polymer solution in a coagulation bath of a strong non-solvent, fast diffusion processes of solvent and non-solvent take place in the toplayer. Since in the toplayer excess out-diffusion of solvent occurs the polymer concentration is increased and the diffusion processes are rapidly followed by vitrification of the polymer matrix. In this section it is discussed how this can result in a nodular structure.

Due to the large differences in molecular weight the transport of small components (solvent and non-solvent) in the system is much faster compared to the mobility of the polymer molecules. Using the nomenclature of de Gennes[22] the *cooperative* diffusion describes the transport of solvent and non-solvent in a polymer matrix. The mobility of a polymer molecule relative to other polymer molecules is called *reptation* (or tracer) diffusion. For a solution of 30 wt% PES in NMP the cooperative diffusion coefficient is $6.6*10^{-11}$ $m^2/s$ and the tracer diffusion is $7.5*10^{-16}$ $m^2/s$ as measured by Tkacik[23]. This means that during a short period of time the mobility of the

polymer molecules is restricted to short distances and a large scale rearrangement of the polymer network is impossible.

In the appendix to this thesis[15] it is suggested that the difference in mobility of the low molecular weight components compared to the high molecular weight polymer can lead to a large supersaturation of the polymer solution. Therefore the composition of the solution can become instable (spinodal composition) before phase separation by nucleation has taken place in the meta-stable (binodal) region. Using the spinodal demixing theory as described by Cahn[24] and Van Aartsen[25] and Smolders et al.[26], it was shown that the dimensions of the nodules found in the ultimate membrane coincide with the fastest growing wavelength of the concentration fluctuations. With this mechanism of growth of concentration fluctuations it can be explained that the nodule sizes are smaller in cases where the original composition is closer to the binodal and that they are smaller at the surface than deeper in the toplayer. Both loci with a composition initially close to the binodal as well as loci at the surface will deeply enter the immiscibility gap upon immersion. In these cases the composition will become highly instable before demixing starts and the wavelength of the concentration fluctuations is smaller.

Due to the difference between diffusion of solvent and non-solvent on the one hand and the relaxation behavior of the polymer on the other spinodal demixing is possible. However it is not yet clear how spinodal decomposition results in a nodular structure since mostly a co-continuous structure is formed. The formation of a nodular structure will be visualised on a molecular level.

The rapid out-diffusion of the solvent combined with the indiffusion of the non-solvent confronts the polymer molecules with a non-compatible environment. The reaction of the polymer molecules on this sudden change of state is an attempt to surround themselves with other polymer segments. In solutions of very low polymer concentration it is a well known phenomenon that a polymer coil collapses if the solubility strength of the environment is reduced for instance by a temperature quench[27]. In the systems discussed here the situation is more complicated. Due to the high polymer concentration the polymer molecules are not extended chains but highly entangled coils. The collapse of one polymer molecule in a polymer network is a tracer diffusion process and therefore it is rather slow. However the polymer molecules can diminish their interactions with the non-solvent by clustering of polymer segments into groups. The polymer clusters may consist of polymer segments of different molecules, adjacent clusters are connected by entanglements or by sharing polymer molecules.

The clustering of polymer segments is an up-hill diffusion process just as spinodal demixing. The polymer maxima of the concentration fluctuations present in the polymer solution will form the centres of the clusters. In the beginning of this process the clusters are highly connected because some polymer molecules are entangled in two adjacent clusters. In a later stage disentanglement of polymer segments between the spheres can lead to the formation of pores. However excess out-diffusion of solvent will increase the polymer concentration of the toplayer and will very soon result in vitrification of the polymer matrix. In the centres of the cluster the polymer concentration will be highest and these loci are the first to reach the concentration at which vitrification occurs. Because of the short time between demixing and vitrification the disentanglement process will not be completed.

When the thermodynamic conditions of demixing are the same as described above but the kinetics of the process are retarded as was the case for the membrane shown in figure 3c no nodular structure is found. The retardation of the diffusion of solvent and non-solvent makes the time scale of these processes comparable to the diffusion of the polymer molecules. Large supersaturation of the polymer solution will not occur and demixing takes place by nucleation and nucleus growth of a polymer lean phase.

*6.5.2 Membranes prepared from a solution containing two polymers*

For polymer solutions that contain the hydrophilic macromolecular additive PVP, nodules are also formed under circumstances where the diffusion processes of solvent and non-solvent are not particularly fast. This is due to the influence of PVP on the phase separation process as is described in chapters 2 and 3[18] based on the theory of Boom et al.[21,28,29]. If PVP is present in the polymer solution the demixing process starts as soon as the polymer solution contacts the coagulation medium even for conditions where, without PVP, a significant delay time for demixing might be found. The rate determining process for the demixing of such a solution is the diffusion of PVP relative to the other polymer PES[29]. Thus although the demixing process starts immediately the ability of the polymer solution to respond to the changes in composition depends on the diffusion of the two polymers with respect to each other and this is even more restricted than for a polymer solution without additive.

Boom[21,29] showed that under these circumstances the co-continuous sub-structure of the membrane (below the toplayer) is formed by spinodal demixing. In the toplayer of a membrane the diffusion processes (solvent/non-solvent exchange) are faster than in the sublayer and the

compositions of loci in the toplayer are deeper into the demixing region. Thus if the sublayer is formed by spinodal decomposition in the toplayer also spinodal demixing must have occurred. This is another strong indication that nodular structures are formed by a spinodal demixing mechanism. The fact that spinodal demixing results in a nodular structure in the toplayer and a co-continuous structure in the sublayer has two causes:
- in the toplayer the polymer concentration is higher due to loss of solvent (diffusion of solvent into the coagulation bath)
- in the toplayer the time available for demixing is short as demixing is rapidly followed by solidification of the polymer matrix.

The formation of a membrane matrix consisting of nodules in the toplayer surrounding pores with sizes in the microfiltration range can also be explained with the spinodal demixing mechanism. These kinds of membrane structures are shown in figure 4 and they were obtained by dry-wet spinning of a polymer solution containing PES and PVP. In the airgap water vapor diffuses into the polymer solution whereas out-diffusion of the non-volatile solvent is hardly possible. If the water concentration in the polymer solution has reached a certain value, phase separation occurs. As said before the determining process for phase separation is the diffusion and phase separation of PVP and PES and spinodal demixing occurs according to the theory of Boom[21,88,29]. Two phases arise: a PES rich and a PES lean phase. Both solvent and PVP diffuse from the PES rich phase towards the PES lean phase. This PVP phase forms the large pores in the ultimate membrane. Since the diffusion of solvent is faster than the diffusion of PVP the polymer concentration of the PES rich phase is enhanced.

At the moment that the nascent membrane enters the water bath it still consists of two liquid phases since no solvent was able to leave the polymer solution by diffusion into the coagulation medium. The PES rich phase (still containing a reasonable amount of PVP) can now be regarded as a small scale polymer solution coagulated in a water bath. Once immersed in the water bath the solvent can diffuse from the PES phase to the water bath. At the same time the diffusion of non-solvent which was only slow from the vapor phase is increased. For the PES rich phase this causes a new impulse for demixing between PES and PVP. Again a nodular structure is formed by spinodal decomposition rapidly followed by vitrification due to an excess outdiffusion of solvent.

When going from membrane a) to d) (see figure 4), the water vapor concentration is increased while the residence time of the nascent membrane in the airgap is constant, more water vapor diffuses into the polymer

solution. For the low vapor concentration (membrane a) the composition of the polymer solution as it enters the water bath is almost equal to the initial composition. Demixing of this solution does not start before it has entered the water bath. In the water bath spinodal demixing results in a nodular structure. For the higher vapor concentrations (membranes c and d) the demixing starts shortly after the polymer solution enters the airgap. By the time this nascent membrane enters the coagulation bath the phase separation has already proceeded so far that the polymer concentration in the PES phase has substantially increased and indeed in case 4d has almost reached the vitrification point. In case d the transition from airgap to water bath has no additional effect on the morphology. Medium vapor concentrations in the airgap result in the formation of a microporous membrane with a nodular structure as described above.

### *6.5.3 Pores in a nodular structure*

The SEM images of nodular structures show a packing of spheres that are more or less interconnected. Because this structure is formed by spinodal demixing as proposed in this chapter a continuous pore phase is expected to be present. The porous phase is not visible at SEM pictures but the nodular structures form the toplayers of ultrafiltration membranes and as such are permeable to a fair amount of water. This implies that a continuous network of pores has to be present among the spheres. The active pore size distribution of ultrafiltration membranes often shows two maxima[2-4]; which was also found for the PES/PVP membranes using the liquid displacement method (chapter 5). One maximum is at a pore size of about 50 nm and the second at a pore size smaller than 10 nm. According to the mechanism proposed here the large pores are found at loci were the disentanglement of polymer chains between the nodules was completed before vitrification occurred. As soon as at certain loci in the toplayer the disentanglement of polymer chains is completed and vitrification has not occurred yet the polymer lean phase can grow more easily to form larger pores of about 50 nm. At other places the nodules are still connected to each other by entangled polymer chains. The polymer concentration between the nodules is much lower than the concentration in the nodule itself. Spaces in the low concentration regions are the pores smaller than 10 nm. The time for demixing is only very short since the outdiffusion of solvent rapidly leads to vitrification. Thus, the disentanglement process is stopped in an early stage. The polymer concentration in the toplayer is also high which explains the low porosity of ultrafiltration membranes.

## 6.6 Conclusions

A new mechanism for the formation of nodular structures has been presented. The nodules are polymer spheres of about 50 nm present in the toplayers of ultrafiltration membranes. A nodular structure is formed by spinodal demixing of the polymer solution, rapidly followed by vitrification of the polymer matrix. Spinodal conditions are obtained when phase separation of a polymer solution is induced by fast diffusion of solvent and non-solvent. A low diffusion coefficient of the polymer molecules combined with a high degree of entanglement in the polymer network make the growth of concentration fluctuations a plausible mechanism for demixing. Due to excess out-diffusion of solvent the polymer concentration increases and the vitrification point is reached shortly after the beginning of demixing. The disentanglement process that separates the nodules from each other is not completed during demixing time. This is the reason for the small pores and the low porosity that are characteristic for ultrafiltration membranes. It was shown that if a hydrophilic polymeric additive is used the nodular structure is also formed in cases of slower diffusion of solvent and non-solvent. This result can be explained on the basis of theoretical views on phase separation in polymeric blends.

### Acknowledgement

The authors wish to express their gratitude to R.M. Boom, W.J. Briels and D.M. Koenhen (X-flow BV) for the enlightening discussions on the subject.

## 6.7 Literature

1. P. Dietz, P.K. Hansma, O. Inacker, H.D. Lehmann, K.H. Herrmann, Surface pore structures of micro- and ultrafiltration membranes imaged with the atomic force microscope, J. Mem. Sci., 65 (1992) 101
2. F.P. Cuperus, C. A. Smolders, Characterization of UF membranes: Membrane characteristics and characterization techniques, Adv. Coll. Int. Sci., 34 (1991) 135
3. S. Munari, A. Bottino, P. Moretti, G. Capannelli, I. Bechi, Permporometric study on UF membranes, J. Mem. Sci., 41 (1989) 69
4. R.E. Kesting, The four ties of structure in integrally skinned phase inversion membranes and their relevance to the various separation regimes, J. Appl. Pol. Sci., 41 (1990) 2739
5. M. Panar, H.H. Hoehn, R.R. Hebert, The nature of asymmetry in reverse osmosis membranes, Macromolecules, 6 (1973) 777
6. R.E. Kesting, Concerning the microstructure of dry-RO membranes, J. Appl. Pol. Sci., 17 (1973) 1771

7. B. Kunst, Z. Vajnaht, On the structure of concentrated cellulose acetate solutions, J. Appl. Pol. Sci., **21** (1977) 2505
8. B. Kunst, D. Skevin, G. Dezelic, A light-scattering and membrane formation study on concentrated cellulose acetate solutions, J. Appl. Pol. Sci., **20** (1976) 1339
9. T. Miyano, T. Matsuura, S. Sourirajan, Effect of polymer molecular weight, solvent and casting solution composition on the pore size and the pore size distribution of polyethersulfone (Victrex) membrane, Chem. Eng. Comm., **95** (1990) 11
10. K. Kamide, S.I. Manabe, Role of microphase separation phenomena in the formation of porous polymeric membranes, In: Material science of synthetic membranes, D.R. Lloyd (ed.), p. 197, ACS Symposium Series 269, Am. Chem. Soc., Washington, DC, 1985
11. L. Broens, F.W. Altena, C.A. Smolders, D.M. Koenhen, Asymmetric membrane structures as a result of phase separation phenomena, Desalination, **32** (1980) 33
12. R.J. Ray, W.B. Krantz, R.L. Sani, Linear stability theory model for finger formation in asymmetric membranes, J. Mem. Sci., **23** (1985) 155
13. K. Kimmerle, H. Strathmann, Analysis of the structure-determining process of phase inversion membranes, Desalination, **79** (1990) 283
14. I. Pinnau, W. Koros, Skin formation of integral-asymmetric gas separation membranes made by dry/wet phase inversion, Thesis University of Texas, Austin, 1991
15. Appendix to this thesis: R.M. Boom, I.M. Wienk, Th. v.d. Boomgaard, C.A. Smolders, Microstructures in phase inversion membranes. II. The role of a polymeric additive, published in J. Mem. Sci. **73** (1992) 277
16. A.K. Fritzsche, A.R. Arevalo, A.F. Connolly, M.D. Moore, V. Elings, C.M. Wu, The structure and morphology of the skin of polyethersulfone ultrafiltration membranes: a comparative atomic force microscope and scanning electron microscope study, J. Appl. Pol. Sci., **45** (1992) 1945
17. K.J. Kim, A.G. Fane, C.J.D. Fell, T. Suzuki, M.R. Dickson, Quantitative microscopic study of surface characteristics of ultrafiltration membranes, J. Mem. Sci. **54** (1990) 89
18. Chapter 3 of this thesis, A new spinning technique for hollow fiber ultrafiltration membranes, published in J. Mem. Sci. **78** (1993) 93
19. *a)* R.M. Boom, Th. v.d. Boomgaard, C.A. Smolders, Metastable demixing phenomena by thermal quench experiments. 1. Theory, submitted for publication to J. Appl. Pol. Sci.
    *b)* R.M. Boom, S. Rekveld, U. Cordilia, Th. v.d. Boomgaard, C.A. Smolders, Metastable demixing phenomena by thermal quench experiments. 2. The systems PES-NMP-water and PES-PVP-NMP-water, submitted for publication to J. Appl. Pol. Sci.
20. *a)* A.J. Reuvers, J.W.A. v.d. Berg, C.A. Smolders, Formation of membranes by means of immersion precipitation. I. A model to describe mass transfer during immersion precipitation, J. Mem. Sci., **34** (1987) 45
    *b)* A.J. Reuvers, C.A. Smolders, Formation of membranes by means of immersion precipitation. II. The mechanism of formation of membranes prepared from the system cellulose acetate-acetone-water, J. Mem. Sci., **34** (1987) 6729.
    *c)* R.M. Boom, Th. v. d. Boomgaard, C.A. Smolders, Mass transfer and thermodynamics during immersion precipitation for a two-polymer system, evaluation with the system PES-PVP-NMP-water, submitted for publication to J. Mem. Sci.

21. R.M. Boom, H.H.W. Rolevink, Th. v.d. Boomgaard, C.A. Smolders, Membranes prepared from PES and PS; Comparison with the PES-PVP system, to be submitted for publication to J. Mem. Sci.
22. P.G. de Gennes, Scaling concepts in polymer physics, Cornell Univ. Press, New York, 1989
23. *a)* G. Tkacik, L. Zeman, Component mobility analysis in the membrane forming system water/ N-methyl-2-pyrrolidone/polyethersulfone, J. Mem. Sci., **31** (1987) 273
*b)* L. Zeman, G. Tkacik, Thermodynamic analysis of a membrane forming system. Water/ N-methyl-2-pyrrolidone/polyethersulfone, J. Mem. Sci., **36** (1988) 119
24. J.W. Cahn, Phase separation by spinodal decomposition in isotropic systems, J. Chem. Phys., **42** (1965) 93
25. J.J. van Aartsen, C.A. Smolders, Light scattering of polymer solutions during liquid-liquid phase separation, Eur. Pol. J., **6** (1970) 1105
26. C.A. Smolders, J.J. van Aartsen, A. Steenbergen, Liquid-liquid phase separation in concentrated solutions of non-crystallizable polymers by spinodal decomposition, Koll. Z. u. Z. Pol., **243** (1971) 14
27. *a)* N.K. Ailawadi, J. Naghizadeh, Collapse transition in polymers, Mol. Cryst. Liq. Cryst., **38** (1977) 171
*b)* P.G. de Gennes, Kinetics of collapse for a flexible coil, J. Physique. Lett. **46** (1985) L639
*c)* J. Yu, Z. Wang, B. Chu, Kinetic study of coil-to-globule transition, Macromolecules, **25** (1992) 1618
28. *a)* R.M. Boom, Th. v.d. Boomgaard, C.A. Smolders, Equilibrium thermodynamics of a quaternary membrane forming system with two polymers. 1. Theory, submitted for publication to Macromolecules
*b)* R.M. Boom, H.W. Reinders, H.H.W. Rolevink, U. Cordilis, Th. v.d. Boomgaard, C.A. Smolders, Equilibrium thermodynamics of a quaternary membrane forming system with two polymers. 2. Experimental, submitted for publication to Macromolecules

## Appendix to this thesis

# Microstructures in Phase Inversion Membranes
### The Role of a Polymeric Additive

R.M. Boom, I.M. Wienk, Th. van den Boomgaard, C.A. Smolders

---


## Summary

Membranes were prepared from a casting solution of a water-soluble polymer, poly(vinyl pyrrolidone) (PVP), and a membrane forming polymer, poly(ether sulfone), in 1-methyl-2-pyrrolidone (NMP) as solvent, by immersing them in mixtures of water and NMP. It was found that the addition of PVP to the ternary system suppresses the formation of macrovoids in the sublayer, while the ultrafiltration-type toplayer consists of a closely packed layer of nodules. Using a model for mass transfer in this quaternary system, it is possible to explain the effects of the additive on macrovoid formation. Strong indications are found that the appearance of a nodular structure in the toplayer follows a mechanism of spinodal decomposition during the very early stages of the immersion step.


## 1 Introduction

Phase inversion is the most important process to prepare symmetric or asymmetric membranes. Because of the significance of immersion precipitation (phase inversion), the mechanism of formation of these membranes has been the subject of extensive investigation[1,2].

In recent years, Reuvers et al.[1] developed a model for the description of mass transfer during the immersion step. Two types of demixing occurring during immersion precipitation followed from this model: instantaneous demixing and delayed demixing. Taking this model of mass transfer in combination with liquid-liquid phase separation, effects of variations in the composition of the casting solution and the coagulation bath could be explained.

On the basis of the distinction between delayed and instantaneous demixing, Reuvers et al. proposed a mechanism for the formation of large fingerlike cavities (macrovoids), often occurring in the sublayer of immersion precipitation membranes[3].

Although this model is strictly valid only for ternary systems consisting of a membrane forming polymer, a solvent and a non-solvent for the polymer, some effects of the addition of a fourth component to the system can be explained with it.

In order to obtain an optimal membrane structure, an additive (a fourth component) is frequently used. Usually, the additive is a weak non-solvent for the polymer, e.g. glycerol in a system consisting of polysulfone, DMAc and water, or maleic acid in a system of cellulose acetate, dioxane and water.

Such an additive to the casting solution brings the initial composition of the casting solution nearer to the binodal. According to the mechanism proposed by Reuvers, this decreases the tendency of the solution to form macrovoids.

In other systems, polymeric additives are used. Well-known is the addition of poly (vinyl pyrrolidone) to a system consisting of polysulfone, and a solvent such as DMAc[4]. The most important effects of this type of additive are suppression of macrovoids, improved interconnectivity of the pores and higher porosities in the toplayer and in the sublayer. Further more, it appears that the toplayers of these membranes have a nodular structure.

Reuvers' model can not account for the effects of this type of additive. In this paper we will show some of the effects of the addition of poly(vinyl pyrrolidone) to the system consisting of poly(ether sulfone) and 1-methyl-2-pyrrolidone, coagulated with water.

In part A of this paper the mechanism underlying macrovoid formation will be discussed. We will present a model to describe mass transfer in a quaternary system consisting of two miscible polymers in a common solvent precipitated by a non-solvent for one of the polymers. On the basis of this model, we will come to a mechanism that can explain some of the effects of the polymeric additive.

In part B, the occurence of nodular structures in UF-type toplayers will be discussed. Experimental evidence will be given for a possible spinodal mechanism of formation of these nodular structures in toplayers.

## A. Macrovoid formation in systems with a macromolecular additive

### 2 Theoretical considerations

The system we want to investigate consists of four components:
- a non-solvent for the polymer, initially present in the coagulation bath (component 1).
- a solvent for the polymer, initially present in the polymer solution, and in some cases in the coagulation bath (component 2)
- the membrane forming polymer (component 3), present only in the polymer solution and in the final membrane
- the macromolecular additive used (component 4)

We assume that the additive is miscible with all components present.
A typical model system for this is the system used in our experiments: water (1) - 1-methyl-2-pyrrolidone (2) - poly(ether sulfone) (3) - poly(vinyl pyrrolidone) (4).

#### *2.1 Thermodynamics*

We have in our system two macromolecular components, both present at high concentrations in the same solution. Typical concentrations in casting solutions are 15 to 20 weight percent membrane forming polymer and 10 to 15 weight percent additive. The two polymers both are far above their overlap concentrations and form entangled, intertwined coils, since we know that the two polymers are well miscible. This implies that we assume that the Flory-Huggins interaction parameter between the additive and the membrane forming polymer is low. In the case of poly(ether sulfone) and poly(vinyl pyrrolidone) this interaction parameter has been determined (with high-pressure osmometry) to be lower than zero, which indicates that the two polymers form homogeneous blends at all concentrations.

Phase separation in such a system involves the demixing of the intertwined polymers. In equilibrium, the polymeric additive has moved to the membrane forming polymer lean phase. This process is considerably slower than the exchange processes of solvent and non-solvent between the casting solution and the coagulation bath occurring directly upon immersion, because the separation of the two polymers involves the movement of one polymer with respect to the other.

It is therefore convenient to distinguish two time scales for the first moments of the immersion step.
1. The shorter time scale is valid for the process of exchange of solvent and non-solvent. On this time scale, the two polymers, effectively behave as one

component. Transport of the low-molecular weight components through the polymeric network is possible; transport of the polymers with respect to each other is not possible.
2. The longer time scale is the time scale at which the two polymers can move relative to each other: the polymeric additive moves into the polymer lean phase.

These time scales have different thermodynamic regimes to which they respond. Therefore, the phase diagrams of both time scales should be evaluated. From a thermodynamic point of view, the short time scale is characterized by the absence of any polymer in the polymer lean phase. It only contains solvent and non-solvent. This characteristic feature will be used to determine the thermodynamics on the short time scale. During the longer time scale, the macromolecular additive is allowed to be present in the membrane forming polymer lean phase.

### *2.2 Equilibrium calculations*

The basis of the calculations is the Flory-Huggins expression for the chemical potential of mixing in a quaternary systems:

$$\frac{\Delta G_m}{RT} = n_1 \ln\varphi_1 + n_2 \ln\varphi_2 + n_3 \ln\varphi_3 + n_4 \ln\varphi_4 + g_{12}n_1\varphi_2 + \chi_{13}n_1\varphi_3 + g_{14}n_1\varphi_4 + g_{23}n_2\varphi_3 + g_{24}n_2\varphi_4 + g_{34}n_3\varphi_4 \quad (1)$$

All ternary and quaternary interaction parameters are neglected. This means that the phase diagrams calculated should only be used in a semi-quantitative way.

The derivatives of the free enthalpy of mixing with respect to the number of moles of each component are the chemical potentials of mixing. Phase equilibria are calculated by using the algorithm proposed by Altena et al.[5]. The following objective function F is minimized:

$$F = \sum_{i=1}^{4} \left( \frac{\mu_i^a - \mu_i^b}{RT} \right)^2 \quad (2)$$

in which the index $^a$ belongs to the concentrated phase while the index $^b$ is for the diluted phase, and $\varphi_i$ and $\mu_i$ denote the volume fraction and the chemical potential of component i, respectively. T is the temperature, and R is the gas constant.

As discussed before, it is assumed that in the diluted phase no polymer is present. In this case, the relations for the chemical potentials collapse to those

for a binary system, and the objective function F in equation 2 consists only of two terms (i = 1,2), those for the chemical potentials of the nonsolvent 1 and the solvent 2.

*2.3 Modelling of mass transfer*

To describe mass transfer in the polymer solution and in the coagulation bath, we expand the model developed by Reuvers et al.[1]. We will summarize the most important points from this model.

The continuity equations are in our case the same as the ones Reuvers used:

$$\frac{\partial}{\partial t}\left(\frac{\varphi_i}{\varphi_3}\right) = \sum_{\substack{j=1 \\ j\neq i}}^{4} \left\{ \frac{\partial}{\partial m}\left( v_i \varphi_3 L_{ij} \frac{\partial \mu_j}{\partial m} \right) \right\} \qquad (3)$$

while the binary diffusion in the coagulation bath is described by:

$$\frac{\partial \varphi_i}{\partial t} = \frac{\partial}{\partial y}\left( D_{ij} \frac{\partial \varphi_i}{\partial y} \right) - \frac{\partial \varphi_i}{\partial y}\left( J_1^{y=0} + J_2^{y=0} \right) \qquad (4)$$

$J_i^{y=0}$ means here the flux ($ms^{-1}$) of component i through the boundary layer between polymer solution and coagulation bath.

The spatial coordinate m in equation 3 is described by:

$$m = \int_{\xi=0}^{\xi=x} \varphi_3 d\xi \qquad (5)$$

in which x is the distance from the moving interface (between the polymer solution and the coagulation bath) into the polymer solution. The spatial coordinate y into the coagulation bath is taken from the (moving) interface. It is assumed that both the coagulation bath and the polymer solution are semi-infinite.

The mobility coefficients $L_{ij}$ can be found with the Stefan-Maxwell approach, which relates the driving forces (the chemical potential gradients) to the velocities $\bar{v}_i$ of the components.

$$\frac{\partial \mu_i}{\partial x} = \sum_{j=1}^{4} c_j R_{ij} (\bar{v}_j - \bar{v}_i) \qquad i = 1,2,3,44 \qquad (6)$$

Here, $R_{ij}$ is the so-called friction coefficient between component i and j; $c_i$ stands for the concentration of component i. For a detailed description of how the mobility coefficients are related to the Stefan-Maxwell friction coefficients $R_{ij}$ we refer to Reuvers et al.[1], who describe this for a ternary system.

Our calculations are aimed only at the short time scale. It is assumed that the two polymers cannot move with respect to each other. In formula:

$$\bar{v}_3 - \bar{v}_4 = 0 \tag{7}$$

The Stefan-Maxwell equations now simplify to a semi-ternary problem.

$$\frac{\partial \mu_i}{\partial x} = c_1 R_{i1}(\bar{v}_1 - \bar{v}_i) + c_2 R_{i2}(\bar{v}_2 - \bar{v}_i) + (c_3 R_{i3} + c_4 R_{i4})(\bar{v}_3 - \bar{v}_i) \qquad i = 1,2 \tag{8}$$

Equations 8 are used in combination with the continuity equations (equations 3 and 4) to calculate the composition profiles as a function of time. We assume that the concentrations at the interface between the casting solution and the coagulation bath are constant. This is a reasonable suggestion for the first moments of immersion. Reuvers[1] showed that in this case, the composition profile is only dependent on the variable (a partial Fourier number):

$$l = \frac{m}{\sqrt{t}} \tag{9}$$

This indicates that the composition profile calculated not only represents the initial composition profile in the toplayer, but also the dependence on time of the compositions at each position in the polymer solution.

The composition profiles were calculated in double precision, with the D04PGF routine from the NAG-library. Calculations were performed according to the following scheme:

1. Equilibrium conditions are assumed at the interface; the polymer concentration at the interface is estimated as a first guess.
2. Composition profiles are calculated both in the polymer solution and in the coagulation bath.
3. The fluxes at both sides of the interface, found from the calculated composition profiles, are compared.
4. The steps 1 to 3 are repeated with varying polymer concentration at the interface, until the flux through the interface of each component is equal at both sides of the interface.

## 3 Experimental set up

### *3.1 Materials*

The membrane forming polymer poly(ether sulfone) (Victrex 5200P) was supplied by ICI. Molecular weight was 43,800 g/mole as determined by GPC measurements. The additive poly(vinyl pyrrolidone) (PVP) was purchased from Janssen Chimica. Different types of PVP were used indicated by a K-number, K15 ($M_w$ 10,000 g/mole), K30 ($M_w$ 18,000 g/mole), K60 ($M_w$ 228,000 g/mole) and K90 ($M_w$ 507,000 g/mole). 1-Methyl-2-pyrrolidone (Merck, synthetic grade) was used as solvent, while the non-solvent used was water.

### *3.2 The spinning process*

Hollow fibers were spun by the dry-wet spinning technique (described in chapter 2) or by a two bath system (described in chapter 3). The filtered and degassed polymer solution was pumped through a spinneret. In the dry-wet technique the solution leaving the spinneret passes an airgap (the first stage) after which it enters into a coagulation bath (the second stage). On the bore side an internal coagulation bath was pumped. In case of the two bath system the first and second stage were two different outer coagulation baths. The first bath and the internal coagulation bath were NMP-water mixtures at ambient temperatures. The second stage always was a water bath and its temperature could be varied. After spinning, residual solvent was removed by flushing with water for two days.

### *3.3 Electron Microscopy*

Morphology of the membranes was studied with an electron microscope (SEM, JEOL JSM T220A). Sample preparation was done as follows. After displacement of water by ethanol and ethanol by hexane the membranes were dried in air. In a sputtering apparatus (Balzers Union SCD 040) a thin gold-layer was deposited on the membranes.

## 4 Results

### *4.1 Experimental*

The effects of a polymeric additive on the membrane morphology obtained is shown in figure 1, which gives cross sections through membranes made with varying concentrations of polymeric additive and varying molecular weights of the additive.

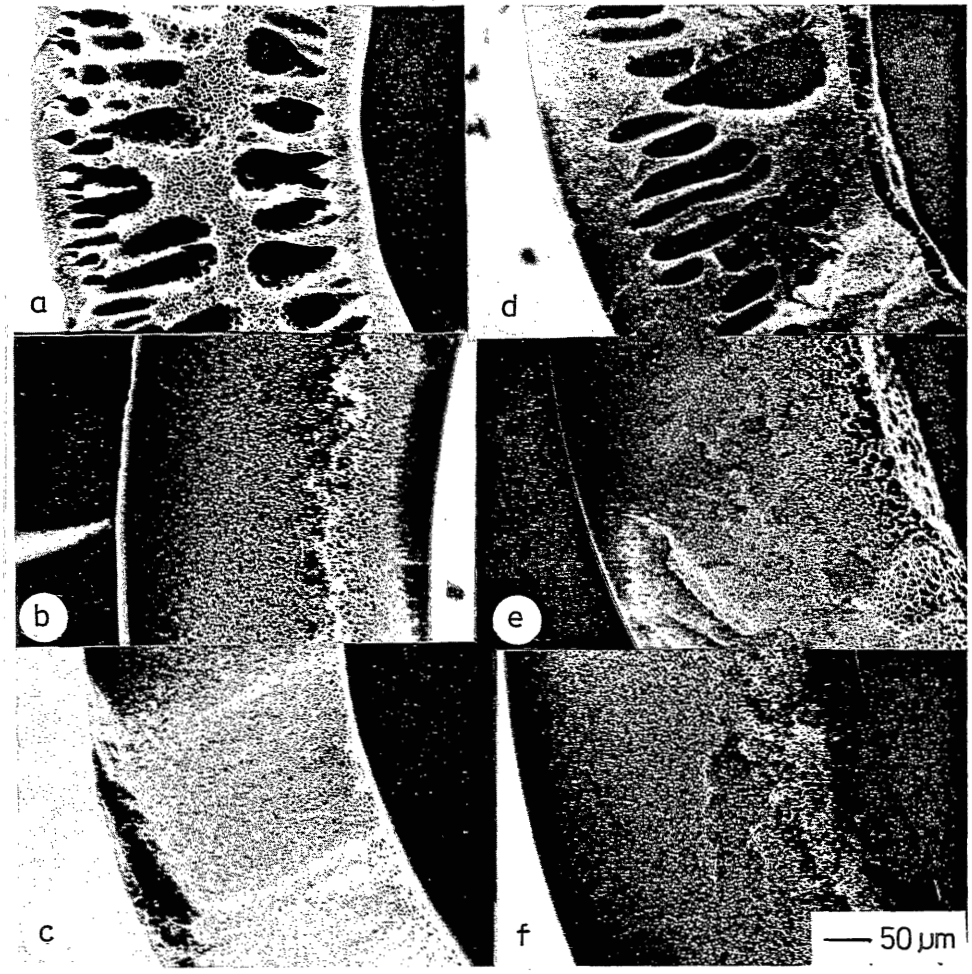


*Figure 1. SEM pictures of cross sections through hollow fibers. Concentration of poly(ether sulfone) was 20 wt%; 5 wt% water was added to the casting solution. In case of A,B and C the indicated coagulation bath is the bore liquid. At the outside an airgap of 5 cm was applied after this the fibers entered a water bath of 73 °C. For D,E and F the indicated coagulation bath is the first external stage of the bath, the second stage was a water bath of 24 °C. The bore liquid was 80 wt% NMP in water.*

| No. | Casting Solution wt% PVP (K number) | Coagulation bath (wt% NMP) | No. | Casting Solution wt% PVP (K number) | Coagulation bath (wt% NMP) |
|---|---|---|---|---|---|
| A | 5 (K90) | 40 | D | 10 (K30) | 20 |
| B | 7.5 (K90) | 40 | E | 10 (K60) | 20 |
| C | 10 (K90) | 40 | F | 10 (K90) | 20 |

It appears that the molecular weight of the polymeric additive is an important parameter. Addition of a polymeric additive of a certain minimum molecular weight results in the absence of macrovoids in the membrane structure. It further appears that a certain minimum concentration of polymeric additive is needed to suppress macrovoid formation.

*4.2 Equilibrium calculations*

Phase equilibria were calculated according to the conditions discussed in the theoretical section. The ratio of weight percentages of components 3 and 4 was varied. The resulting phase diagrams are shown in figure 2.

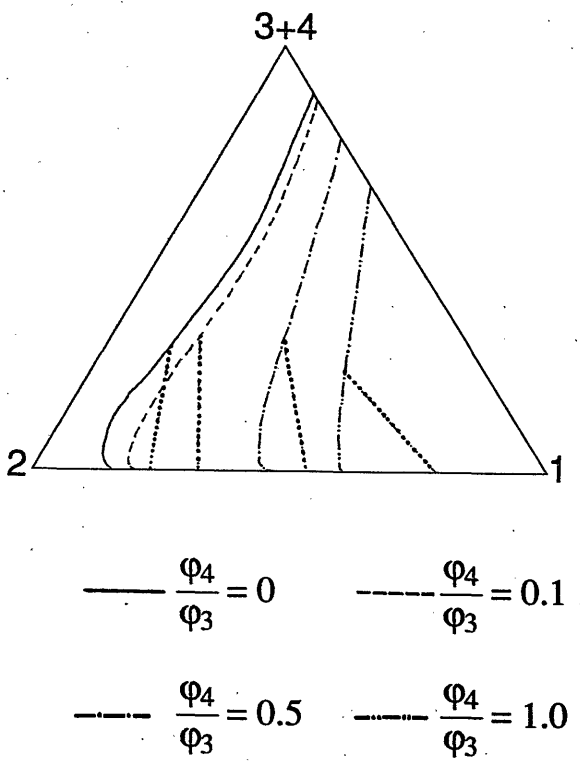


*Figure 2. Phase diagrams for the short time scale in systems with a macromolecular additive.*

*Parameters used[6]:*

$g_{12} = 1.0; g_{23} = 0.5; c_{13} = 1.5; g_{14} = 0.4; g_{24} = 0.5; g_{34} = -1.0.$

*Molecular weights:*

*1) water, 18 g mole$^{-1}$; 2) NMP, 99 g mole$^{-1}$; 3) PES, 18 kg mole$^{-1}$; 4) PVP, 40 kg mole$^{-1}$.*

Parameters used are based on measurements for the system poly(ether sulfone) - 1-methyl-2-pyrrolidone - water, by Tkacik et al.[6], and measurements performed in our own laboratory. These measurements were done with high-pressure osmometry: a PES-NMP solution was brought into contact with NMP via a Cuprophan™ membrane, that swells only slightly in NMP. The polymer was found not to permeate through the membrane measurably over a period of at least one week. By determining the equilibrium osmotic pressure in the solution cell, the interaction parameters could be determined.

It appears from the computations that with increasing content of component 4 (the additive), the binodal shifts to the non-solvent corner. These phase diagrams are only valid as long as the two polymers cannot move relative to each other, i.e. as long as polymeric additive is absent in the polymer lean phase.

*4.3 Mass transfer*

Initial composition profiles were calculated for a system in which the ratio of the weight fractions of the polymeric components is unity. It was assumed that the diffusivity of component 4 was equal to the diffusivity of component 3. In our model system consisting of poly(ether sulfone) (3) - poly(vinyl pyrrolidone) (4) - 1-methyl-2-pyrrolidone (2), measurements of diffusion coefficients of both polymeric components (3,4) in the solvent (2) justify this assumption. These measurements were performed in our laboratory with an analytical ultracentrifuge by following a small imposed gradient in the polymer concentration by means of a Schlieren optical system.

A typical composition profile calculated is shown in figure 3. This profile is only valid for the first instances after immersion. The influence of the concentration of solvent in the coagulation bath has been considered, resulting in the curves in figure 4.

For higher solvent concentrations in the coagulation bath, there is no composition jump at the interface anymore, because the initial composition profile does not reach a binodal composition. A gradual transition from the casting solution to the coagulation bath is obtained. When a polymeric solution with a composition as discussed is coagulated in a coagulation bath with a high concentration of solvent, the coagulation bath turns slightly turbid, indicating dissolution of some polymer in the coagulation bath. This is in agreement with the calculated results.

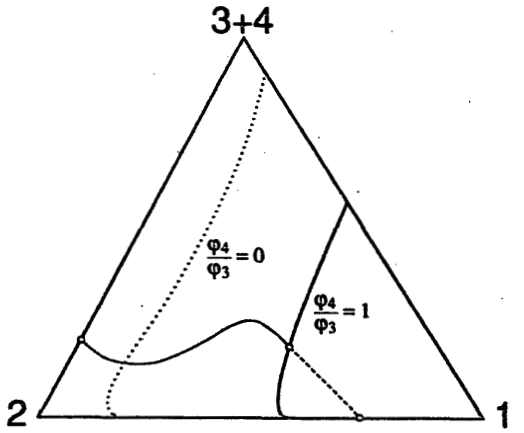


*Figure 3. Composition profile for $\varphi_4/\varphi_3$ = 1.0. Thermodynamic parameters are as in figure 2. Kinetic parameters are valid for the experimental system water - 1-methyl-2-pyrrolidone - poly(ether sulfone) - poly(vinyl pyrrolidone):*

$$\frac{v_i RT}{M_j R_{ji}} = A\ 10^{-9-B\varphi_i}\ \frac{m^2}{s}$$

$$R_{1k}=\frac{v_1}{v_2}R_{2k} \quad \text{for } k = 3,4$$

i = 1, j = 2: A = 0.6; B = 0.0;

i = 3 or 4, j = 2: A = 18.0; B = -4.386

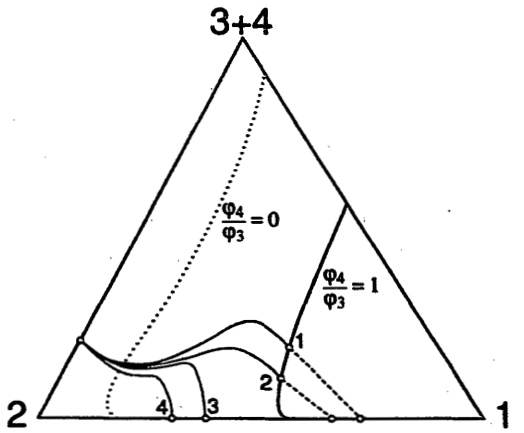


*Figure 4. Composition profiles calculated with the same parameters as in figure 3. The concentration of solvent in the coagulation bath is increasing from 0 to 65 volume%.*

## 5 Discussion

Experiments showed that only an additive of a certain minimum molecular weight and present at a certain minimum concentration is effective to prevent macrovoid formation. We will now discuss how the calculated results may explain these facts.

Calculations showed that at all concentrations of solvent in the coagulation bath, delay of demixing is obtained with respect to the phase diagram for the short time scale. After some moments of immersion however, the longer time scale, in which polymer-polymer movement is possible, is gaining importance. When the polymeric additive is able to diffuse into the membrane forming polymer lean phase, the 'real' binodal close to the polymer-solvent axis is gaining importance again. The area of the demixing gap thereby increases dramatically, and the compositions already created in the toplayer appear to be very unstable. Hence, demixing, once started, will be relatively fast in the toplayer.

Complete equilibrium calculations (i.e. without any assumptions concerning concentrations) show that the polymeric additive (4) usually is almost exclusively present in the polymer (3) lean phase. The binodal in this case shifts to lower water concentrations in the polymer (3) rich phase than when no additive (4) would have been present in the system. Therefore, as an indication for this situation, the binodal valid for a system without any additive present in the system can be used (see figure 4).

The change from the 'virtual' binodal for the short time scale to the 'real' binodal that represents real phase equilibria in the phase diagram implies that for solutions containing a polymeric additive, delay of demixing as described by Reuvers[1] cannot occur at all. Even at high concentrations of solvent in the coagulation bath (where a solution without the additive would exhibit delay of demixing), compositions which are unstable in the long time scale are created in the toplayer during the short time scale. From figure II.4, one might even say, that in the toplayer conditions for spinodal demixing are created. We will expand on this topic in part B.

The measurement of light transmission through precipitating membranes indeed indicates that addition of a polymeric additive induces a certain instantaneous demixing process, at conditions that would give delay of demixing without the additive. This can be related to the effects the additive has on macrovoid formation, as will be explained in the next paragraph.

*5.1 Macrovoid formation*

Reuvers proposed a mechanism of formation of macrovoids in ternary systems consisting of non-solvent, solvent and membrane forming polymer[3]. The mechanism is summarized in short here.

A casting solution, demixing according to an instantaneous mechanism, obtains higher and higher solvent concentrations in the nuclei of the polymer lean phase present in the proceeding coagulation front. At a certain point, these solvent concentrations become so high locally, that conditions become favorable for delay of demixing. Delay of demixing is characterized, due to loss of solvent which is larger than the influx of non-solvent, by a shrinkage of the polymer solution, and, consequently, an increasing volume of the coagulation bath. In this case a nucleus in the neighborhood is serving as a coagulation bath. The nucleus will therefore grow. As long as the conditions of delayed demixing remain the same, i.e. as long as the solvent concentration in the nucleus remains high enough, the growth of the nucleus continues.

We return to the quaternary system with a polymeric additive. As we have seen, in a system with a polymeric additive, delay of demixing does not take place, as long as the two time scales can be operative. Local conditions for delay of demixing cannot take place. Growth of a nucleus is effectively blocked by the creation of new nuclei. Apparently, the addition of a polymeric additive hinders macrovoid formation.

This effect can only take place when enough additive is present: at lower concentrations the demixing gap does not shift enough to the right in the phase diagram to induce any significant effect during the short time scale. On the other hand, the diffusion of the two polymers with respect to each other should be slow compared to the diffusion of solvent and non-solvent in the polymer solution. Otherwise, it is not possible to distinguish a short time scale from the longer one. Delay of demixing will then still be possible. To avoid this, a certain minimum molecular weight of both polymers in the system is required. Since in most cases the molecular weight of the membrane forming polymer is fixed, this means that the molecular weight of the additive should have a certain minimum value. This is in agreement with the facts found in the experimental section.

## B. Nodular structures in ultrafiltration membranes

### 6 Theoretical considerations

Open pore structures in membranes are formed by nucleation and growth of the polymer lean phase in the metastable region between the binodal and the spinodal curve. However the toplayer of ultrafiltration membranes often does not show an open pore structure nor a completely homogeneous gel layer. It consists of closely packed spheres of polymeric material with a diameter of about 50-200 nm. and is often referred to as a nodular structure[7].

The formation of a nodular structure can not be explained by nucleation of the polymer lean phase. It is also not very likely that nucleation of the polymer concentrated phase occurs because this only happens at initially low polymer concentrations, below the critical point. A possible explanation for the formation of a nodular structure could be that it is a result of spinodal demixing.

#### *6.1 Spinodal demixing*

In the spinodal region the homogeneous system is unstable. A nucleus of one of the binodal phases is not necessary to initiate phase separation. A theory of spinodal decomposition has been developed by Cahn[8]. Very small concentration fluctuations with a wavelength above a critical value will grow. Due to negative diffusion coefficients 'up-hill' diffusion takes place. This means that the amplitude of the wave grows whereas the wavelength remains constant. Van Aartsen[9] showed that spinodal demixing can also occur in polymer solutions when quenched to a temperature below the spinodal temperature. Combining Cahn's theory of spinodal demixing and Debije's theory describing random concentration fluctuations in polymer solutions an expression for the fastest growing wavelength ($D_m$) was found:

$$D_m = 2\pi l \,/\, [3\,(1-T/T_s)]^{0.5} \qquad (10)$$

The wavelength ($D_m$) is linearly related to the radius of gyration (l) of the polymer and is therefore dependent on molecular weight as well as on the thermodynamic interaction between polymer and solvent. The wavelength decreases if the quenching temperature (T) is lowered, i.e. if the polymer solution is brought deeper inside the spinodal region. The spinodal temperature is dependent on the polymer concentration and is indicated by $T_s$. Smolders et al.[10] determined $D_m$ for a 15 weight percent poly-2,6-dimethyl-1,4-phenylene oxide (PPO) solution in caprolactam. The radius of gyration is of the order of 20 nm. At an undercooling of 30°C below the

spinodal temperature the calculated wavelength is $D_m$=260 nm.

According to Smolders et al.[10] the fast spinodal demixing process is followed by a slower phenomenon to reach the final equilibrium phases. At high quenching temperatures this could be measured using dilatometry and electron microscopy. By dilatometric measurements it was found that a large change in volume occurring upon quenching is followed by a second volume effect on a longer time scale. Electron microscopy showed droplets of the polymer concentrated phase increasing in size with time. The ultimate structure is fairly uniform with a characteristic distance between the polymer rich regions.

## 7 Results

Hollow fibers were spun as described in the experimental setup of part A of this paper. The membrane morphology of the toplayer is shown in figure 5. The surface top view (figure 5A) shows a bi-continuous structure which is typical for spinodal decomposition. Nodule size is estimated at about 50 nm. In the cross section (figure 5B) the structure at the surface is not very well visible. Nodular size increases from 50 nm (at 0.5 μm distance from the surface) to 100 nm (5 μm below the surface). Below the toplayers which are shown, the membranes have an open pore structure (not shown in this picture).

In figure 6 the cross section of a toplayer for moderate coagulation conditions is shown. The coagulation bath contained 60% of the solvent in the non-solvent. Therefore the non-solvent concentration gradient in the toplayer was much smaller. For this membrane nodule size is almost equal over the toplayer thickness. At the surface the nodules are more closely packed.

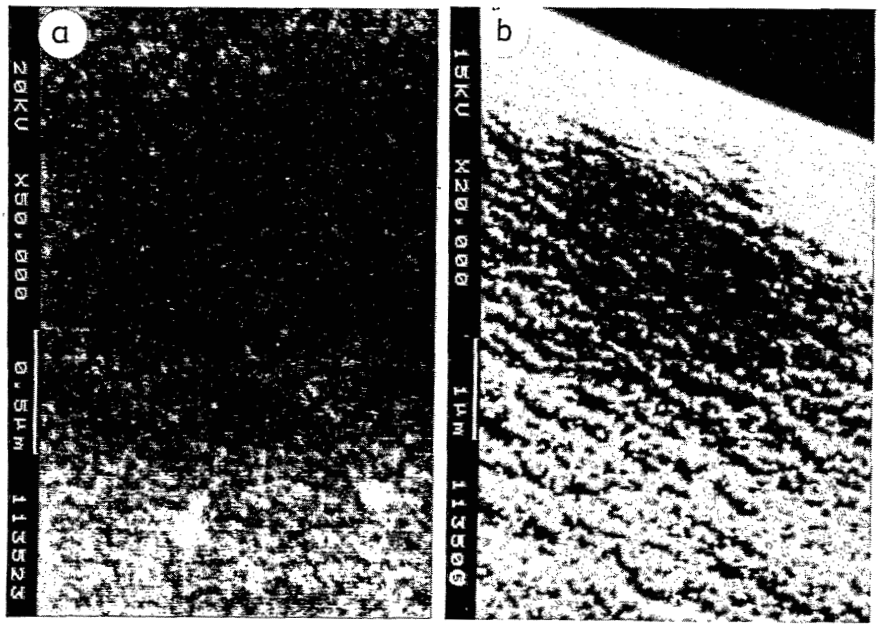


*Figure 5. Scanning electron microscopic pictures of hollow fibers. A: surface view, B: cross section at the* outside *toplayer region. Concentration of poly(ether sulfone) was 17 wt%, concentration of poly(vinyl pyrrolidone) (K90) was 13 wt%. After an airgap of 1.5 cm. the fiber was coagulated in a pure water bath of 26 °C.*

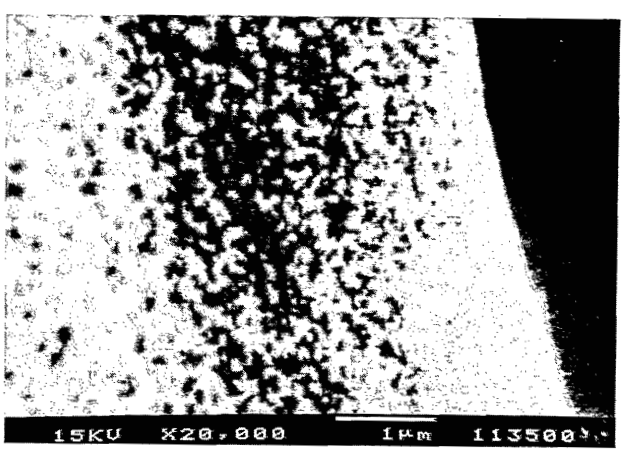


*Figure 6. Scanning electron microscopic picture of hollow fibers; cross section at the* bore side *toplayer. Concentration of poly(ether sulfone) was 17 wt%, concentration of poly(vinyl pyrrolidone) (K90) was 13 wt%. Internal coagulation bath was 60 wt% NMP in water.*

## 8 Discussion

The nodular structure in ultrafiltration membranes formed by immersion precipitation resembles the structure obtained by quenching a polymer solution. This makes spinodal decomposition a reasonable mechanism for nodule formation. However, spinodal demixing can not be related to the membrane formation model of Reuvers et al.[1] The calculated composition paths can never cross the spinodal curve, because at these compositions the chemical potential gradients and fluxes are all zero. If we assume that for the extremely fast formation of ultrafiltration toplayers the established theory based on equilibrium thermodynamics is not valid for the three (or four) component system, an alternative mechanism can be proposed.

### *8.1 Formation of ultrafiltration toplayers*

In an ultrafiltration membrane-forming system the interaction between solvent and non-solvent is very high. Upon immersion in the coagulation bath fast exchange of solvent and non-solvent takes place in the toplayer. Due to their high molecular weight the polymer molecules are not mobile enough in the initial stage, there is a certain relaxation time. Solvent and non-solvent molecules can diffuse through the polymer coils by movement of polymer chain segments while at the same time the polymer chains as a whole do not move at all. When the polymer concentration is kept constant the composition of the polymer solution rapidly crosses the metastable region without being able to demix according to a nucleation mechanism. During this diffusion process only polymer chain segments are moving. Therefore the spinodal curve, calculated for a system where polymer molecules as a whole can diffuse, is not valid. This means that the composition of the film can enter the region which is the spinodal region in equilibrium conditions.

Fast penetration into the binodal region without nucleation has also been reported by other authors. According to Kimmerle[11] a certain period is necessary for nucleation to start. This induction time becomes smaller according to Kimmerle as the composition changes towards the spinodal curve. So, if diffusion processes are very fast the composition deeply enters the binodal region before phase separation sets in. Cohen et al.[12] report that phase separation in viscous polymer solutions is relatively slow compared to the diffusional equilibration of solvent and non-solvent. According to them phase separation begins at compositions lying at the limit of metastability i.e. the spinodal curve.

Thus, until the relaxation time of the polymer in solution has elapsed the solution is still homogeneous while the composition has reached the spinodal region. When after a certain time the polymer molecules start to

diffuse, spinodal decomposition occurs rapidly.

A difference in mobility between polymer chain segments and polymer molecules as a whole was also distinguished by Tkacik and Zeman[6]. They applied quasi-elastic light scattering (QELS) to water/NMP/PES systems. For intertwined polymer solutions two clearly distinguishable relaxation times and diffusion coefficients were measured. Relaxation times of a 20 weight percent solution of PES in NMP were $1*10^{-4}$ seconds for the fast mode and 1 second for the slow mode. Binary diffusion coefficients of a 30 weight percent solution of PES in NMP were $6.6*10^{-11}$ $m^2/s$ for the fast mode and $7.5*10^{-16}$ $m^2$ /s for the slow mode, respectively.

With these values an estimation can be made of the part of the film which will be in the spinodal region at the moment the polymer molecules start to diffuse, 1 second after immersion. We use Fick's second law for infinite media[13]:

$$\frac{C_x - C_1}{C_0 - C_1} = \mathrm{erf}\frac{x}{2\sqrt{(Dt)}} \qquad (11)$$

and take the non-solvent concentration at the surface $C_0$=50%, the initial non-solvent concentration in the polymer solution $C_1$=0%, and its concentration at the spinodal $C_x$=20%. The fast mode binary diffusion coefficient for solvent and polymer as given by Tkacik[7] is used as the diffusion coefficient for non-solvent through the polymer network. The relaxation time of the network is t=1 s. Then the penetration depth can be calculated as x=6 μm. This means that a layer of 6 μm will be in the spinodal region and can give a nodular structure. This is in agreement with the experimental results.

The wavelength of the fastest growing wave is dependent on the penetration depth into the spinodal region. The composition at the surface is the first to cross the spinodal and therefore will have proceeded further into the spinodal region. Here the wavelength will be smaller. In figure 5 it can be seen that indeed the nodular size is smallest at the surface and becomes larger going deeper into the membrane toplayer.

### *8.2 Quaternary systems*

For a quaternary system with two high molecular weight components other conditions may also give rise to spinodal decomposition. In the previous part it has been described that the composition of the polymer solution can enter

the spinodal region as long as the relaxation time of the polymer molecules has not elapsed. But the model, proposed in part A, for demixing of quaternary systems can explain the occurrence of spinodal demixing even after the relaxation time has elapsed.

For moderate coagulation conditions, e.g. if the coagulation bath contains a considerable amount of solvent, the diffusion processes are slower. As stated in part A on the short time scale the two polymers can be regarded as one and the relevant binodal is situated on the right hand side of the phase diagram close to the nonsolvent corner. Before this binodal is reached the relaxation time has elapsed and the two polymers can diffuse but not with respect to each other. Once the two polymers can diffuse with respect to each other, the system gradually starts to react in agreement with the original quaternary binodal and spinodal curve situated more to the left in the phase diagram (see figure 3). From this moment on, the compositions in the toplayer lie in the unstable region and spinodal demixing occurs rapidly, finally resulting in a nodular structure.

In figure 6 a nodular structure was formed with a coagulation bath that contained 60% solvent. Due to the smaller concentration difference the coagulation velocity is smaller and normally an open pore structure would be formed. However due to the addition of a second polymer phase separation is faster and a nodular structure is formed.

## 9 Conclusions from A and B

### *9.1 Macrovoid formation*

It appears that the macromolecular nature of the additive is responsible for the suppression of formation of macrovoids. The reason is that the two polymers present in the same solution have to diffuse with respect to each other in order to phase separate. Since this process, for high enough molecular weight components, is much slower than low-molecular weight diffusion, two time scales are created.

The short time scale is responsible for the creation of a toplayer which has a high non-solvent content without demixing. These compositions are highly unstable in the longer time scale. Delay of demixing in such a system is not possible anymore. Because the formation of macrovoids is closely connected to the phenomenon of delayed demixing, macrovoid formation is effectively hindered.

*9.2 Nodular structures*

It has been shown that the nodular structure appearing in the toplayer of ultrafiltration membranes is probably a result of spinodal demixing. Although the phase separation process is diffusion controlled there are two ways in which the composition of the polymer solution can cross the spinodal curve.

*i)* In the first period of fast immersion processes solvent and non-solvent diffuse through a "fixed" polymer network. Thermodynamics based on equilibrium states are not valid for these first moments after immersion. Compositions are reached which appear to lie in the spinodal region when polymer molecules become mobile and thermodynamics are valid again.

*ii)* For systems with a high molecular weight additive, in the first moments after immersion, the binodal and spinodal curve are situated close to the non-solvent corner. Upon regaining the normal thermodynamic conditions (for the longer time scale) the compositions are found to lie definitely in the spinodal region of the real phase diagram.

## 10 List of Symbols

Units are between brackets.

| | |
|---|---|
| $C_x$ | Concentration at place x [kg $m^{-3}$] |
| $C_0$ | Concentration at the surface [kg $m^{-3}$] |
| $C_1$ | Initial concentration in the film [kg $m^{-3}$] |
| $c_i$ | Concentration of component i [kg $m^{-3}$] |
| $D_{ij}$ | Binary diffusion coefficient of components i and j [$m^2$] |
| $D_m$ | Perturbation wavelength [m] |
| $\Delta G_m$ | The enthalpy of mixing [J] |
| $g_{ij}$ | Concentration dependent Flory-Huggins interaction parameter between component i and j [-] |
| $L_{ij}$ | Diffusivity between components i and j; to be evaluated with the Stefan-Maxwell approach |
| l | Radius of gyration [m] |
| m | Modified spatial coordinate in the polymer solution; $m = \int_{\xi=0}^{\xi=x} \varphi_3 d\xi$ , [m] |
| $n_i$ | Number of moles of component i [moles] |
| R | Gas constant [J $mole^{-1}$ $K^{-1}$] |
| $R_{ij}$ | Stefan-Maxwell friction coefficient between components i and j, found from binary diffusion data[1] |
| T | Temperature [K] |

| | |
|---|---|
| $T_s$ | Spinodal temperature [K] |
| t | Time [s] |
| $v_i$ | Specific volume of component i [$m^3\ kg^{-1}$] |
| $\bar{v}_i$ | Velocity of component i [$m\ s^{-1}$] |
| x | Spatial coordinate originating from the interface, going into the polymer solution [m] |
| y | Spatial coordinate originating from the interface, going into the coagulation bath [m] |
| $m_i$ | Chemical potential of mixing of component i (equal to $\frac{\partial \Delta G_m}{\partial n_i}$) [J $mole^{-1}$] |
| $\varphi_i$ | Volume fraction of component i [-] |
| $c_{ij}$ | Concentration independent Flory-Huggins interaction parameter between component i and j [-] |

## 10 Literature


1. *a)* A.J. Reuvers, J.W.A. van den Berg, C.A. Smolders, Formation of membranes by means of immersion precipitation. Part I. A model to describe mass transfer during immersion precipitation, J. Mem. Sci., **34** (1987) 45
   *b)* A.J. Reuvers, C.A. Smolders, Formation of membranes by means of immersion precipitation. Part II The mechanism of formation of membranes prepared from the system cellulose acetate-acetone-water, J. Mem. Sci., **34** (1987) 67
2. L.Yilmaz, A.J. McHugh, Modelling of asymmetric membrane formation. I. Critique of evaporation models and development of a diffusion equation formalism for the quench period, J.Mem. Sci., **28** (1986) 287
3. C.A. Smolders, A.J. Reuvers, R.M. Boom, I.M. Wienk, Microstructures in phase inversion membranes. I. Formation of macrovoids, J. Mem. Sci., **73** (1992) 259
4. *a)* I. Cabasso, E. Klein, J.K. Smith, Polysulphone hollow fibers. II. Morphology, J. Appl. Pol. Sci., **21**(1977) 165
   *b)* P. Aptel, N. Abidine, F. Ivaldi, J.P. LaFaille, Effect of spinning conditions on ultrafiltration properties, J. Mem. Sci., **22** (1985) 199
   *c)* L.Y. Lafrenière, F.D.F. Talbot, T. Matsuura, S. Sourirajan, Effect of poly(vinyl pyrrolidone) additive on the performance of poly-ethersulphone ultrafiltration membranes, Ind. Eng. Chem. Res., **26** (1987) 2385
   *d)* T.A. Tweddle, O. Kutowy, W.L. Thayer, S. Sourirajan, Polysulphone ultrafiltration membranes, Ind. Eng. Chem. Prod. Res. Dev., **22** (1983) 320
5. F. Altena, C.A. Smolders, Calculation of liquid-liquid phase separation in a ternary system of a polymer in a mixture of a solvent and a non-solvent, Macromolecules, **15** (1982) 1491
6. *a)* L. Zeman, G. Tkacik, Thermodynamic analysis of a membrane forming system. water/N-methyl-2-pyrrolidone/poly(ether sulfone), J. Mem. Sci., **36** (1988) 119

*b)* G. Tkacik, L. Zeman, Component mobility analysis in the membrane forming system. water/N-methyl-2-pyrrolidone/poly(ether sulfone), J. Mem. Sci., **31** (1987) 273

7. L. Broens, F.W. Altena, C.A. Smolders, Asymmetric membrane formation as a result of phase separation phenomena, Desalination, **32** (1980) 33
8. J.W. Cahn, Phase separation by spinodal decomposition in isotropic systems, J. Chem. Phys., **42** (1965) 93
9. J.J. van Aartsen, Light scattering of polymer solutions during liquid-liquid phase separation, Eur. Pol. J., **6** (1970) 919
10. C.A. Smolders, J.J. van Aartsen, A. Steenbergen, Liquid-liquid phase separation in concentrated solutions of non-crystallizable polymers by means of spinodal decomposition, Koll. Z. u. Z. Pol., **243** (1971) 14
11. K. Kimmerle, Quantitative Betrachtung des Phaseninversionsprozesses bei der Herstellung von Membranen, PhD-theses Stuttgart 1988
12. C. Cohen, G.B. Tanny, S. Prager, Diffusion-controlled formation of porous structures in ternary polymer systems, J.Pol. Sci., **17** (1979) 477
13. J. Crank, The mathematics of diffusion. 2nd ed. Oxford 1975

# Summary

In this thesis the preparation and characterization of ultrafiltration membranes is presented. The membranes are prepared in a hollow fiber configuration by extrusion of a polymer solution through a spinneret. Contacting the polymer solution with a non-solvent for the polymer induces phase separation of the solution resulting in a porous polymer structure: the membrane. Apart from the membrane forming polymer (poly(ether sulfone), PES) a polymer additive (poly(vinyl pyrrolidone), PVP) is present in the solution. This additive is known to affect the membrane formation process and to improve the fouling properties of the ultimate membrane.

For the preparation of the hollow fibers two spinning techniques have been used. In the dry-wet spinning technique (chapter 2) water is used as the non-solvent coagulation medium. The nascent membrane passes an airgap with a certain humidity before it enters a water bath. The pore structure at the outer surface is mainly determined by the conditions in the airgap. It was found that in a series of experiments the results are in accordance with the theory on phase separation only if forces like gravity, shear forces and die-swell acting on the polymer spinning solution are constant. The pore structure at the inner surface of the hollow fiber can be influenced by changing the ratio of solvent and non-solvent of the internal coagulation medium.

The second spinning technique used is the dual bath method by means of a new type of spinneret (chapter 3). A coagulation medium is pumped through the outer opening of a triple orifice spinneret. After a certain time the nascent membrane enters a water bath where the first coagulation medium is replaced by water. This technique, which was originally developed for the formation of asymmetric membranes with a non-porous toplayer, is applied here for the preparation of asymmetric membranes with a porous toplayer. The presence of the polymer additive PVP appears to be essential to induce demixing in the first coagulation medium resulting in a porous structure with ultrafiltration characteristics.

Before the spun fibers are suitable for testing several post treatment steps

have to be performed. The influence of these treatments on the performance of the membranes has been investigated in chapter 4. The temperature of the rinsing bath, necessary to remove residual solvent, affects the pore size and the amount of PVP present in the membrane. Drying of the membranes is not possible because this causes collapse of the ultrafine porous structure. Therefore the best way to store the membranes is with glycerol in the pores. Swelling of tails of partially captured PVP molecules present in the pores of the membrane causes a low permeability. This can be diminished by treating the membranes with a hypochlorite solution which removes part of the PVP molecules. The mechanism of the chemical reaction of hypochlorite with PVP was investigated (appendix chapter 4). Strong indications have been found that the reaction involves chain scission of PVP according to a radical mechanism.

Attempts were made to prepare a non-fouling ultrafiltration membrane by incorporating a hydrogel at the pore walls of a microfiltration membrane (chapter 4). Preliminary experiments did not lead to satisfying results. Impregnation of a microfiltration membrane with PVP followed by a crosslinking reaction of PVP using persulfate resulted in a gel layer at the surface of the membrane.

For the characterization of the ultrafiltration membranes a number of techniques was critically studied (chapter 5). The characteristics of membranes can be divided in composition related parameters, morphology and pore size distribution parameters and performance related parameters. The PVP content of the membranes is measured using micro element analysis and XPS. The amount of PVP present in the membrane is low due to diffusion of PVP out of the membrane forming phase during the phase separation process. Several microscopic techniques often used to study membrane morphology are compared. Using these techniques the nodular structure present in the toplayer of the membranes can be visualised. Determination of pore sizes and toplayer thicknesses of these ultrafiltration membranes is not possible by any of the microscopic techniques. Pore size distributions of the membranes can be measured using the liquid displacement method. The characteristic pore size distribution has two maxima; one at a pore radius of 25 nm and one at a radius smaller than 10 nm.

When these membranes are used to filter a solution containing bovine serum albumin (BSA) the flux is half of the pure water flux of the membrane and the retention is about 98%. Using filtration models it can be shown that the low flux and high retention are the result of either a highly resistant cake layer build at the surface of the membrane or blocking of the large pores by

BSA molecules. An adsorption study on a time scale longer than used for the filtration measurements was performed using BSA solutions under non-convective flow conditions. For these experiments it was found that adsorption of BSA results in a decrease of membrane permeability. The permeability decrease is lower if the PVP content of the membrane is higher.

A striking characteristic of the morphology of many ultrafiltration membranes is that the toplayer consists of a nodular structure. A new mechanism for the formation of this structure is proposed (chapter 6). The mechanism is based on the small diffusion coefficient of the polymer molecules compared to the diffusion coefficient of solvent and non-solvent molecules combined with a high degree of entanglement of the polymer network. Demixing of the system takes place by growth of the amplitude of concentration fluctuations and is rapidly followed by vitrification at loci of concentration maxima of these fluctuations which initiates the nodule formation.

The appendix to this thesis contains the basic ideas on the theory of membrane formation by phase separation of a polymer solution containing two polymers which is used throughout this thesis. Also preliminary ideas concerning the formation of a nodular structure as described in chapter 6 are presented in the appendix.

## Samenvatting

In dit proefschrift is de vorming en karakterisering van ultrafiltratie membranen beschreven. De membranen worden gemaakt in de vorm van holle vezels door middel van extrusie van een polymeeroplossing door een spinkop. Als de polymeeroplossing in contact komt met een niet-oplosmiddel voor het polymeer zal ontmenging (fase scheiding) van de polymeeroplossing optreden. Hierdoor ontstaat een poreuze polymeer structuur: het membraan. In de polymeeroplossing bevindt zich behalve het membraanvormende polymeer (poly(ether sulfon), PES) een additief polymeer (poly(vinyl pyrrolidon), PVP). Het is bekend dat dit additief polymeer het membraan-vormings-proces beïnvloedt en bovendien de mate waarop het uiteindelijke membraan zal vervuilen vermindert.

Voor het maken van de holle vezels is gebruik gemaakt van twee spin technieken. Bij de droog-nat-spin techniek (hoofdstuk 2) is het niet-oplosmiddel water. De geëxtrudeerde polymeer oplossing passeert een luchttraject met een bepaalde vochtigheid waarna het in een waterbad komt. De poriestructuur aan het buitenoppervlak wordt voornamelijk bepaald door de condities in het luchttraject. De resultaten van de spinexperimenten kunnen worden verklaard met de theorie van fase-scheiding. Dit is echter alleen mogelijk indien krachten zoals de zwaartekracht, afschuifkrachten en de 'die-swell' die tijdens het spinnen op het zich vormende membraan werken bij een serie experimenten constant zijn. De poriestructruur aan het binnenoppervlak van de holle vezel kan worden beïnvloed door de verhouding oplosmiddel / niet-oplosmiddel van het interne precipitatie-medium te veranderen.

De tweede spintechniek is het twee-bad systeem dat gebruik maakt van een nieuw type spinkop (hoofdstuk 3). Een precipitatie medium (niet-oplosmiddel) wordt verpompt door de buitenste opening van een spinkop met drie concentrische openingen. Na een bepaalde tijd komt het zich vormende membraan in een waterbad waar het eerste precipitatiemedium wordt vervangen door water. Deze techniek, die is ontwikkeld voor de vorming van asymmetrische membranen met een niet-poreuze toplaag,

wordt hier toegepast voor de vorming van poreuze toplagen. Door de aanwezigheid van het additief polymeer PVP begint de ontmenging al in het eerste precipitatie medium, hetgeen essentieel is voor de vorming van een poreuze structuur met ultrafiltratie eigenschappen.

Voordat de membranen kunnen worden getest zijn er nog een aantal behandelingsstappen nodig. De invloed van deze behandelingen op de prestatie van de membranen is onderzocht in hoofdstuk 4. Sporen oplosmiddel worden verwijderd in een spoelbad. De temperatuur van dit waterbad heeft invloed op de poriegrootte en de hoeveelheid PVP in de membranen. Drogen van de membranen is niet mogelijk, omdat hierdoor de poreuze structuur in de toplaag zou inklappen. De membranen kunnen daarom het best worden bewaard met glycerol in de poriën. In eerste instantie is de doorlaatbaarheid van de membranen laag. Dit wordt veroorzaakt door de aanwezigheid van gezwollen staarten van vastzittende PVP moleculen in de poriën. Een behandeling van de membranen met een natrium-hypochloriet (chloorbleekloog) oplossing vergroot de doorlaatbaarheid. Een gedeelte van het PVP wordt bij deze behandeling verwijderd. Het mechanisme van de reactie van PVP met hypochloriet is onderzocht (appendix hoofdstuk 4). De resultaten van dit onderzoek geven aan dat ketenbreuk van PVP volgens een radicaal mechanisme plaatsvindt.

Er is geprobeerd een niet-vervuilend ultrafiltratie membraan te verkrijgen door een hydrogel aan te brengen aan de poriewanden van een microfiltratie membraan (hoofdstuk 4). Inleidende experimenten leidden echter niet tot goede resultaten. Een microfiltratie membraan werd geïmpregneert met PVP waarna dit polymeer met persulfaat werd vernet. Deze behandeling resulteerde in een hydrogel op het *oppervlak* van het membraan in plaats van aan de poriewand.

Om de ultrafiltratie membranen te karakteriseren werden een aantal karakteriserings-technieken kritisch bestudeerd (hoofdstuk 5). De eigenschappen van membranen kunnen in drie groepen worden verdeeld: de samenstelling van het membraan, de structuur en de poriegrootte verdeling en de filtratie eigenschappen. Om het PVP gehalte van de membranen te meten werd gebruik gemaakt van micro element analyse en XPS. De hoeveelheid PVP in de membranen is laag, omdat PVP tijdens het fase-scheidings-proces uit de membraanvormende fase diffundeert. De structuur van de membranen kan worden bestudeerd met electronen microscopie. Met deze techniek kan de nodulaire (bolletjes) structuur van de toplaag van de membranen worden gevisualiseerd. Het is niet mogelijk om met deze techniek de poriegrootte of de dikte van de toplaag te bepalen. De

poriegrootte van de membranen kan wel worden gemeten door gebruik te maken van de vloeistof-verdringings-methode. De karakteristieke poriegrootte verdeling heeft twee maxima: één bij een poriestraal van 25 nm. en één bij een straal kleiner dan 10 nm.

Met deze membranen kan een waterige oplossing met het eiwit Runder Serum Albumine (BSA) worden gefiltreerd. De flux (doorlaatbaarheid) tijdens filtratie van de eiwitoplossing is de helft van de flux voor zuiver water. De retentie van de membranen voor BSA is 98 %, hetgeen wil zeggen dat 98% van het eiwit door het membraan wordt tegengehouden. Met filtratie modellen kan worden aangetoond dat de lage flux en hoge retentie het gevolg zijn van ofwel de vorming van een koeklaag op het oppervlak van het membraan ofwel dat de grote poriën verstopt raken met eiwit. Een adsorptie studie met BSA oplossingen zonder convectieve stroming toont aan dat bij lange tijden adsorptie van het eiwit resulteert in een verlaagde doorlaatbaarheid. De afname van de doorlaatbaarheid is kleiner als het PVP gehalte van de membranen hoger is.

Een opvallend kenmerk van de structuur van veel ultrafiltratie membranen is de nodulaire structuur in de toplaag. Er is een nieuw mechanisme voorgesteld dat de vorming van deze structuur beschrijft (hoofdstuk 6). Het mechanisme is gebaseerd op de lage diffusie-coëfficiënt van het polymeer in vergelijking met de diffusie-coëfficiënten van oplosmiddel- en niet-oplosmiddel-moleculen in combinatie met een grote verstrengeling van het polymere netwerk. Ontmenging van dit systeem vindt plaats door de groei van de amplitude van concentratie-fluctuaties en wordt snel gevolgd door verglazing op plaatsen waar de amplitude van de concentratie-fluctuaties maximaal is, wat nodule vorming initiëert.

De appendix van het proefschrift bevat de grondbeginselen van de theorie over membraanvorming door fase-scheiding van een polymeer-oplossing die twee polymeren bevat. Deze theorie wordt door het hele proefschrift gebruikt. De appendix bevat ook de inleidende ideeën betreffende de vorming van nodulaire structuren zoals deze in hoofdstuk 6 zijn beschreven.

## Levensloop

Ingrid Wienk werd geboren op 1 maart 1965 te Oldenzaal. In 1983 behaalde zij het VWO diploma aan het Twents Carmellyceum aldaar. In datzelfde jaar begon zij met de studie Chemische Technologie aan de Universiteit Twente. De stageopdracht werd verricht bij DuPont in Dordrecht alwaar zij een fysisch transport model opstelde voor het drogen van polymeer pellets. De afstudeer opdracht "Holle vezel membranen voor microfiltratie" werd uitgevoerd in de onderzoeksgroep Membraantechnologie. In 1989 behaalde zij het ingenieursdiploma.

Van april 1989 tot april 1993 was Ingrid Wienk werkzaam als assistent in opleiding in de groep Membraantechnologie van professor Smolders, momenteel de groep van professor Strathmann, aan de Universiteit Twente. Het aldaar verrichtte onderzoek staat beschreven in het voorliggende proefschrift.